



New Madrid Seismic Zone Catastrophic Earthquake Response Planning Project



Impact of New Madrid Seismic Zone Earthquakes on the Central US

-- Volume II --

Detailed Methodology and Results

**MAE Center Report No. 09-03
October 2009**

The report “Impact of New Madrid Seismic Zone Earthquakes on the Central US” is comprised of two volumes. A summary of all methodology and results, conclusions and future work is included in Volume I. Volume II includes detailed explanations of all impact assessment methodology and model components. Additionally, comprehensive discussions of all impact assessment model results are included for direct damage, economic loss, social vulnerability, social impacts, response and commodities requirements, medical needs, transportation and utility network models, and uncertainty quantifications. Lastly, a comparison of the research team’s previous earthquake impact assessment of the Central US is provided. A table of contents for Volume II is included and is followed by the table of contents for the summary document, Volume I.

Table of Contents for Volume II

Appendix 1: Hazard.....	A1-1
Appendix 2: Inventory.....	A2-1
Appendix 3: Fragility Relationships.....	A3-1
Appendix 4: Threshold Values.....	A4-1
Appendix 5: Direct Damage and Economic Losses.....	A5-1
Appendix 6: Social Impact and Response Requirements.....	A6-1
Appendix 7: Maps for Direct Damage and Economic Loss.....	A7-1
Appendix 8: Flood Risk Modeling.....	A8-1
Appendix 9: Transportation Network Modeling.....	A9-1
Appendix 10: Utility Network Modeling.....	A10-1
Appendix 11: Uncertainty Characterization Method 1.....	A11-1
Appendix 12: Uncertainty Characterization Method 2.....	A12-1
Appendix 13: Comparison with Previous Study.....	A13-1

Table of Contents for Volume I

Contributions.....	ii
Scenario Disclaimer.....	v
Executive Summary.....	vi
Table of Contents.....	viii
List of Figures.....	ix
List of Tables.....	xi
Introduction.....	1
Model Overview and Component Characteristics.....	3
Regional Seismicity	3
Overview of HAZUS Modeling.....	4
Overview of MAEViz Modeling.....	6
Modeling Components and Characteristics.....	8
Social Impacts and Requirements Analysis.....	28
Overview of Results from Impact Assessment.....	44
Direct Damage to Infrastructure, Induced Damage, Casualties and Economic Loss.....	44
Flood Risk Analysis.....	82
Network Models.....	84
Uncertainty Analysis.....	89
Social Impacts and Requirements Analysis.....	92
Required Extensions of Earthquake Impact Modeling in the NMSZ.....	118
Improvements to Current Models.....	118
New Models and New Components.....	123
Applications Requiring Earthquake Impact Results.....	129
Conclusions.....	131
References.....	133

Appendix 1 - Hazard

Hazard is defined as any physical phenomenon associated with an earthquake that affects normal activities. Earthquake hazard defines ground shaking and ground deformation, and also includes ground failure, surface faulting, landslides, etc. There are several ways to define an earthquake hazard. The minimum requirements to define a hazard involve quantifying the level of shaking through peak ground motion parameters or peak spectral values. This appendix focuses on hazard definition and generation of shake maps. Initially, hazard definition requirements in HAZUS are explained. Subsequently, new soil classification and liquefaction susceptibility maps are discussed. The new ground shaking maps created for the scenario event employed in this study are also discussed.

Definition of Hazard in HAZUS

In HAZUS Technical Manual (FEMA, 2008), ground motion is characterized by: (1) spectral response, based on a standard spectrum shape, (2) peak ground acceleration, and (3) peak ground velocity. There are three options available to define ground motion in HAZUS:

- Deterministic ground motion analysis
- USGS probabilistic ground motion maps
- User-supplied probabilistic or deterministic ground motion maps

For the computation of ground shaking demand, the following inputs are required:

- **Scenario** - The user must select the basis for determining ground shaking demand from one of three options: (1) a deterministic calculation, (2) probabilistic maps, supplied with the program, or (3) user-supplied maps. For a deterministic calculation of ground shaking, the user specifies a scenario earthquake magnitude and location. In some cases, the user may also need to specify certain source attributes required by the attenuation relationships supplied with the methodology.
- **Attenuation Relationship** - For a deterministic calculation of ground shaking, the user selects an appropriate attenuation relationship (or suite of relationships) from those supplied with the program. Attenuation relationships are applicable to various geographic areas in the U.S. (Western United States vs. Central Eastern United States) as well as various fault types for WUS sources. Figure 1 shows the regional separation of WUS and CEUS locations as defined by USGS in the development of the National Seismic Hazard Maps.
- **Soil Map** - The user may supply a detailed soil map to account for local site conditions. This map must identify soil types using a scheme based on the site class definitions specified in the 1997 *NEHRP Provisions*. In the absence of a soil

map, HAZUS will amplify the ground motion demand assuming Site Class D throughout the region of interest. The user can also modify the assumed Site Class type for all sites by modifying the analysis parameters in HAZUS (i.e. change the Site Class from D to A, B, C, or E).

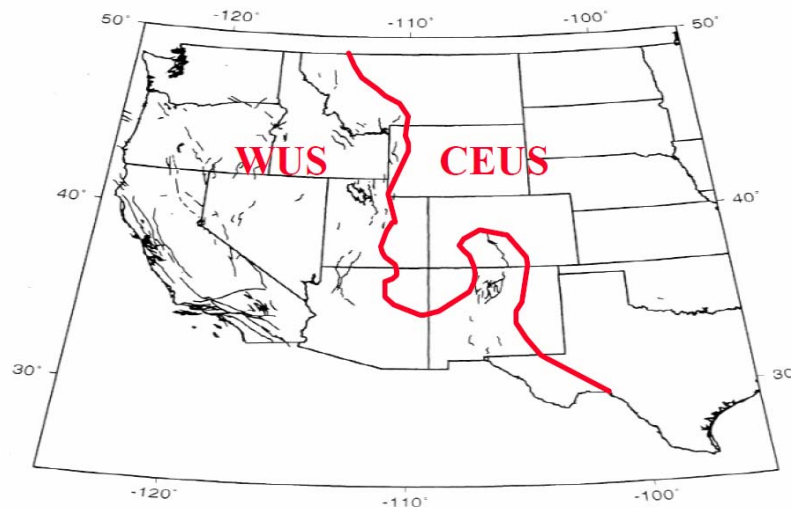


Figure 1: WUS and CEUS Region Boundaries (FEMA, 2008)

For a deterministic scenario event, the user specifies the location (e.g., epicenter) and magnitude of the scenario earthquake. There are three options available within the program to define the earthquake source: (1) specify an event from a database of WUS faults, (2) choose an historical earthquake event, or (3) use an arbitrary epicenter location.

In the case of the user-specified hazard, the user must supply peak ground acceleration (PGA), peak ground velocity (PGV), and spectral acceleration contour maps at 0.3 and 1.0 seconds. This option allows the user to develop a scenario event from various source models not available in HAZUS. Soil amplification is not applied to any user-supplied ground shaking maps, thus all soil amplification must be incorporated into the user-supplied ground shaking maps prior to their use in HAZUS.

As stated, hazard definition consists of ground motion and ground deformation. Ground motion definition was previously discussed, while ground deformation constitutes three types of ground failure: liquefaction, landslides, and surface fault rupture. Each of these types of ground failure is quantified by permanent ground deformation (PGD).

Liquefaction is a phenomenon that causes soils to lose their bearing capacity, or ability to carry load. During sustained ground shaking pore water pressure builds between soil particles effectively changing solid soil into a liquid with soil particle suspended in the liquid. This process commonly occurs in soft, loose soils such as sand. Liquefaction causes permanent ground deformations such as lateral spreading and vertical settlement, both of which increase the likelihood of damage to infrastructure located on these vulnerable soils.

The development of a liquefaction susceptibility map first requires the evaluation of soil/geologic conditions throughout the region of interest. Youd and Perkins (1978) addressed the susceptibility of various types of soil deposits by assigning a qualitative susceptibility rating based upon the general depositional environment and geologic age of deposits. The relative susceptibility ratings from Youd and Perkins (1978) are shown in Table 1. Based on the age, depositional environment, and possibly the material characteristics of each location a liquefaction susceptibility map is constructed with susceptibility levels ranging from 'None' to 'Very High'. These susceptibility levels are utilized in the program to determine permanent ground deformation resulting from both spreading and settlement.

Table 1: Liquefaction Susceptibility of Sedimentary Deposits (Youd and Perkins, 1978)

Type of Deposit	General Distribution of Cohesionless Sediments in Deposits	Likelihood that Cohesionless Sediments when Saturated would be Susceptible to Liquefaction (by Age of Deposit)			
		< 500 yr Modern	Holocene < 11 ka	Pleistocene 11 ka - 2 Ma	Pre-Pleistocene > 2 Ma
(a) Continental Deposits					
River channel	Locally variable	Very High	High	Low	Very Low
Flood plain	Locally variable	High	Moderate	Low	Very Low
Alluvial fan and plain	Widespread	Moderate	Low	Low	Very Low
Marine terraces and plains	Widespread	---	Low	Very Low	Very Low
Delta and fan-delta	Widespread	High	Moderate	Low	Very Low
Lacustrine and playa	Variable	High	Moderate	Low	Very Low
Colluvium	Variable	High	Moderate	Low	Very Low
Talus	Widespread	Low	Low	Very Low	Very Low
Dunes	Widespread	High	Moderate	Low	Very Low
Loess	Variable	High	High	High	Unknown
Glacial till	Variable	Low	Low	Very Low	Very Low
Tuff	Rare	Low	Low	Very Low	Very Low
Tephra	Widespread	High	High	?	?
Residual soils	Rare	Low	Low	Very Low	Very Low
Sebka	Locally variable	High	Moderate	Low	Very Low
(b) Coastal Zone					
Delta	Widespread	Very High	High	Low	Very Low
Esturine	Locally variable	High	Moderate	Low	Very Low
Beach					
High Wave Energy	Widespread	Moderate	Low	Very Low	Very Low
Low Wave Energy	Widespread	High	Moderate	Low	Very Low
Lagoonal	Locally variable	High	Moderate	Low	Very Low
Fore shore	Locally variable	High	Moderate	Low	Very Low
(c) Artificial					
Uncompacted Fill	Variable	Very High	---	---	---
Compacted Fill	Variable	Low	---	---	---

Generation of Ground Motion and Liquefaction Susceptibility Maps

Significant improvements to ground motion and liquefaction characterizations in this study build upon the progress of previous Central US earthquake impact assessments. New maps soil characterization maps were developed by the Central United States Earthquake Consortium (CUSEC) State Geologists. The CUSEC State Geologists provided new maps detailing the soil classification and liquefaction susceptibility of the entire eight-state study region in the Central US. The Geological Surveys in each state produced its own state map Soil Site Class and Liquefaction Susceptibility maps which were later combined to form two regional maps for use in HAZUS analysis.

Soil Site Class Maps

The procedures outlined in the NEHRP provisions (Building Seismic Safety Council, 2004) and the 2003 International Building Codes (International Code Council, 2002) were followed to produce the soil site class maps. Initially, soils are classified as either liquefiable soils, thick soft clay, or thin (or no) soil areas. Descriptions of each general soil type are as follows:

Liquefiable Soils (Soil Site Class F): The detection of liquefiable soils was conducted through identification of any of the four categories of Site Class F. If site soil profile characteristics correspond to any of these categories, the site is classified as Site Class F.

The four categories include:

1. Soils vulnerable to potential failure or collapse under seismic loading such as liquefiable soils, quick and highly sensitive clays, or collapsible weakly cemented soils.
2. Peats and/or highly organic clays ($H > 10$ feet of peat and/or highly organic clays where H is the thickness of soil)
3. Very high plasticity clays ($H > 25$ feet with plasticity index $PI > 75$)
4. Very thick soft/medium stiff clay ($H > 120$ feet)

Based on the above criteria, all eight states in the NMSZ impact assessment included some Site Class F soils, with the exception of Kentucky.

Thick Soft Soils (Soil Site Class E): Soil profiles were investigated for the existence of a total thickness of soft clay > 10 ft (3 m), where a soft clay layer is defined by moisture content $w \geq 40\%$ and plastic limit $PL > 20$. If these criteria are satisfied, the site is classified as Site Class E.

Thin Soils: International Building Codes exclude soils less than ten feet thick between the top of bedrock and building foundations for consideration in the soil site class maps. Therefore, areas with a soil thickness less than ten feet are classified according to the bedrock properties.

CUSEC State Geologists used the entire column of soils material down to bedrock and did not include any bedrock in the calculation of the average shear wave velocity for the column, since it is the soil column and the difference in shear wave velocity of the soils in comparison to the bedrock which influences much of the amplification. Using these procedures, along with the Fullerton et al. (2003) map, a soil site class map was produced for the eight NMSZ states (Figure 2).

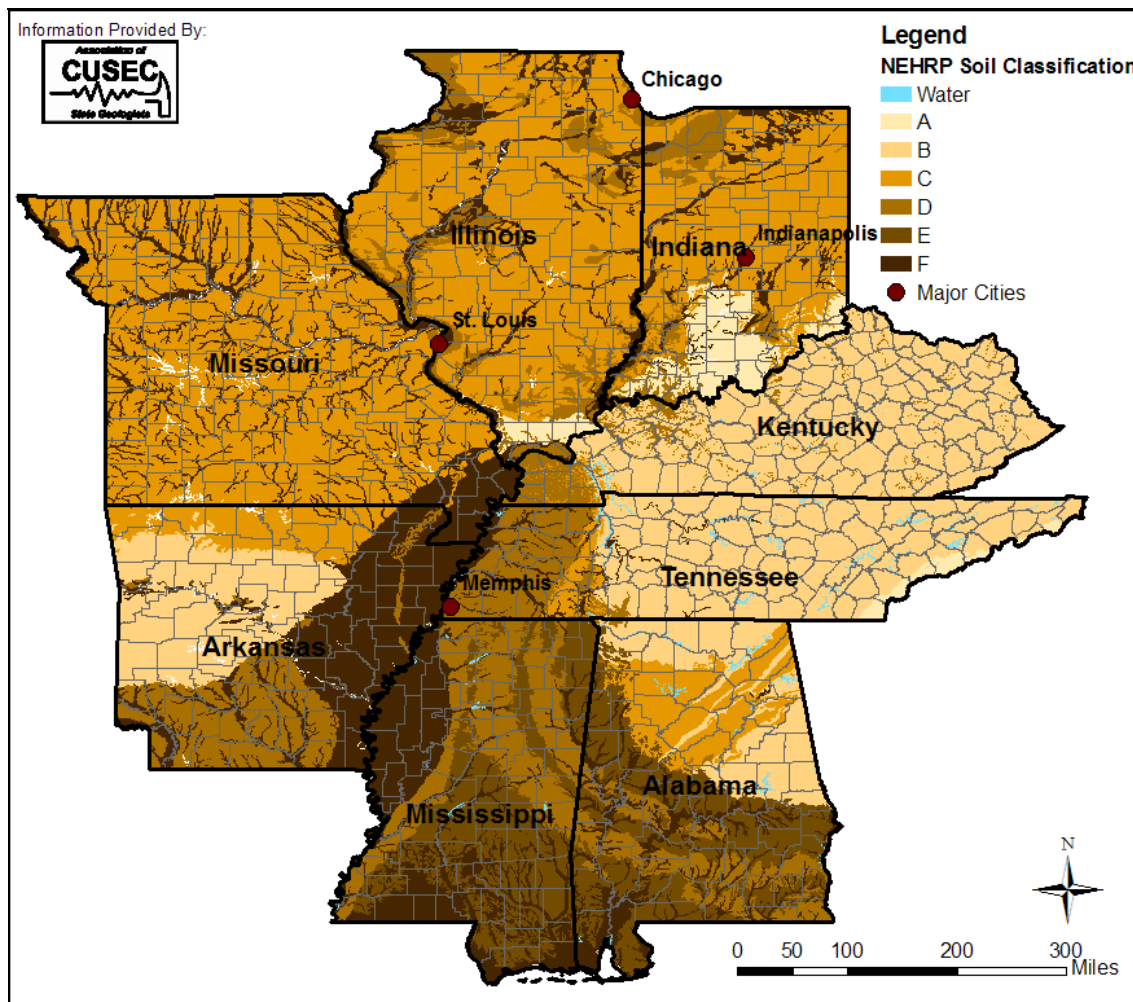


Figure 2: Soil Site Class Map (CUSEC, 2008)

Liquefaction Susceptibility Map

As mentioned previously the liquefaction susceptibility characterization utilized in HAZUS is based on the work of Youd and Perkins (1978) which is shown in Table 1. The regional map created by the State Geological Surveys was compared with the Fullerton et al. (2003) map as well as additional interpretations of the state geological surveys to produce the eight-state liquefaction susceptibility map illustrated in Figure 3.

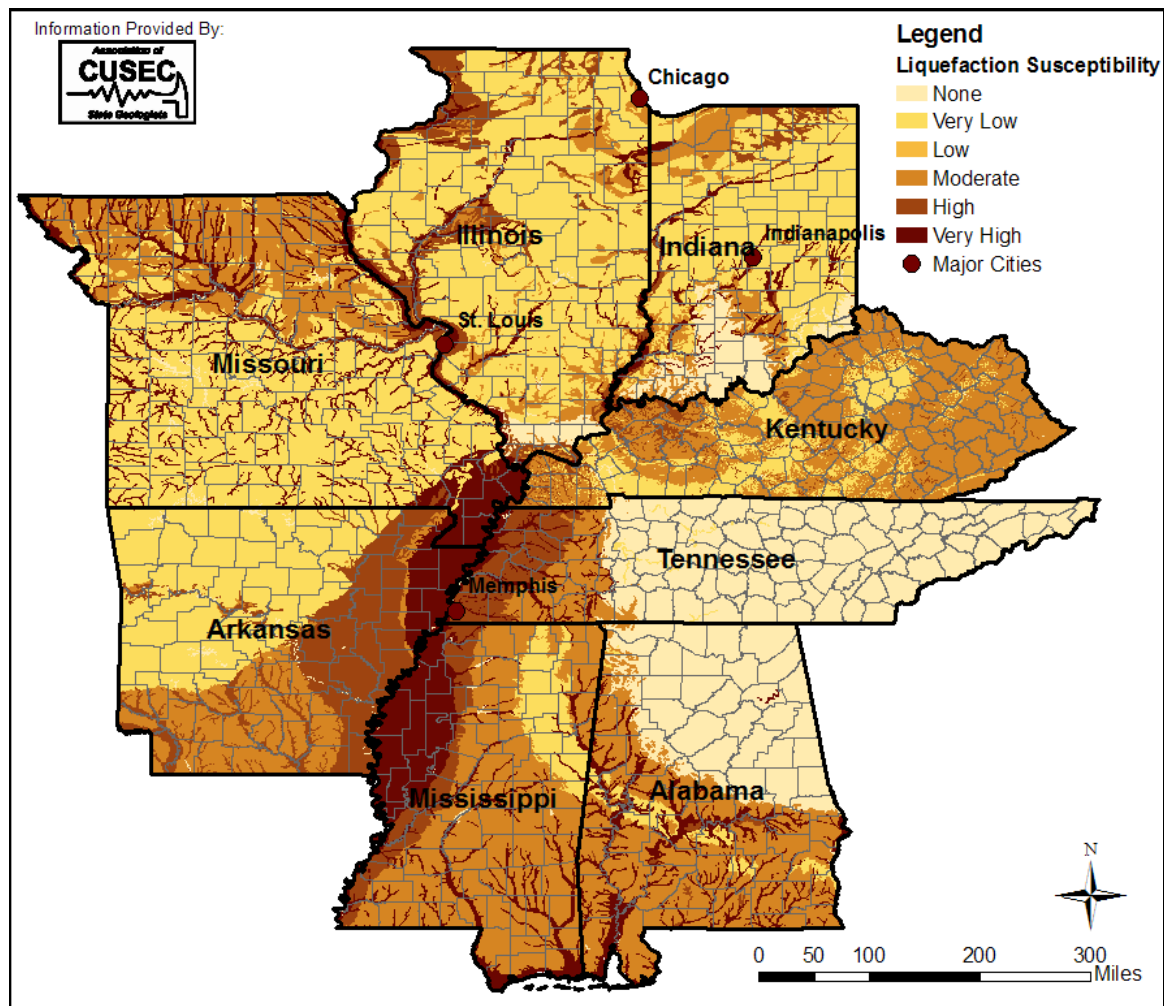


Figure 3: Liquefaction Susceptibility Map for NMSZ (CUSEC, 2008)

Soil Response Map

The CUSEC State Geologists originally produced a soil site classification map for the eight CUSEC states as outlined previously. The soil site class map is used, along with an earthquake magnitude and location, to calculate the surface ground motions throughout the study region. Due to various limitations in HAZUS all ground motion maps are developed externally and include soil amplification according to the soil site class information from the CUSEC State Geologists.

Dr. Chris Cramer, of the University of Memphis (previously of USGS), created the scenario ground motion maps using the methodology outlined in Cramer (2006). The Cramer (2006) methodology used earthquake events on all three segments of the New Madrid faults along with ground motions modified by soil site amplification based on a soil response map and reference shear wave velocity profiles for each soil type (Figure 4).

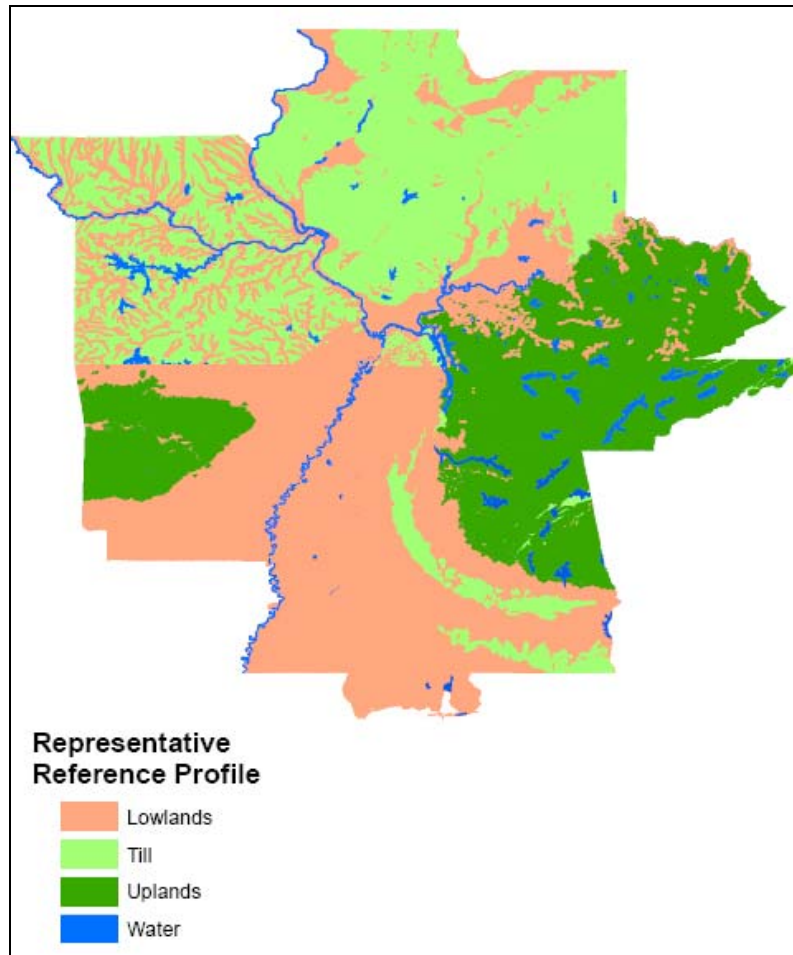


Figure 4: Soil Response Map (Cramer, 2006; Toro and Silva, 2001)

The scenario event it designed to represent a nationally-catastrophic earthquake event in the Central US. Historically, earthquakes on the New Madrid Fault occurred in groups of three where each of the three segments of the fault ruptured over a period of several months. Ideally, the scenario event includes three sequential earthquakes, though HAZUS limitations do not permit hazard modeling this complex. The best available approximation of three sequential fault ruptures is the simultaneous rupture of all three fault segments. The maps created for the NMSZ sequential rupture still utilize the procedure outlined in Cramer (2006), though it is applied to a total rupture length that includes the northeast, central (Reelfoot Thrust), and southwest segments of the New Madrid Fault. Each individual fault segment rupture was assigned a magnitude of 7.7 and this magnitude is retained for the simultaneous rupture. It is estimated that the impacts estimated in the simultaneous rupture scenario are less than the impacts that result from the sequential

rupture scenario since partially damaged structures from one event could be greatly affected by the second and third events. Currently, however, it is impossible to determine damage for successive earthquake events due to a lack of fragility relationships for damaged infrastructure.

As a result, all the ground motion maps were developed considering a sequential rupture of the three NMSZ segments, meaning that the ground motion maps represent the combined ground motion caused by the rupture of all three segments in a sequence. Figure 5 illustrates the three segments of the NMSZ. The ground motion was propagated horizontally through rock layer and then propagated vertically through soil layers above the bedrock. The ground motion maps for PGA, PGV, and both short- and long-period spectral acceleration were developed for the $M_w 7.7$ sequential rupture event and are illustrated in Figure 6 thru Figure 9.

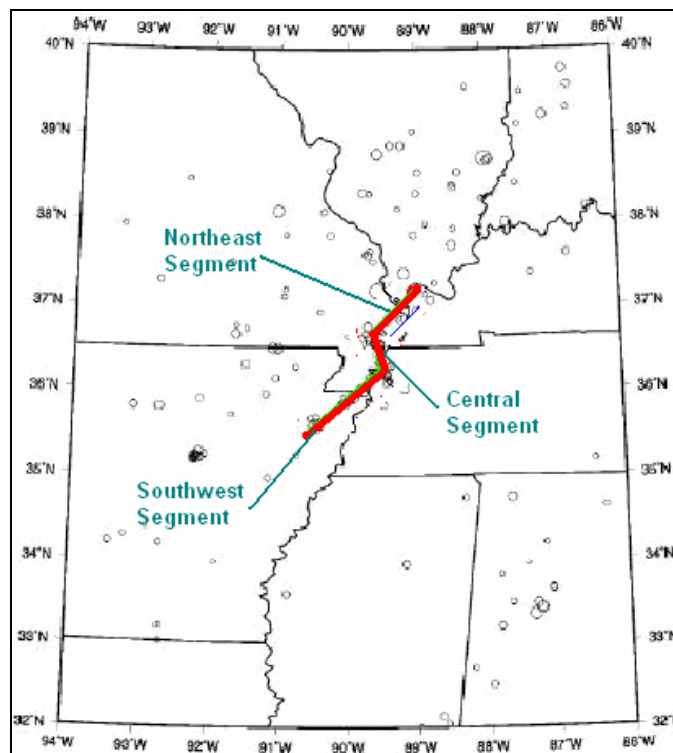


Figure 5: NMSZ Fault Segments

All new soil classification, liquefaction susceptibility, and ground motion maps are regionally-comprehensive and a substantial improvement upon previous maps that characterize hazard throughout a small portion of the eight-state study region. Additionally, all soil characterization maps utilize a consistent proceed as outlined in the NEHRP provisions or Youd and Perkins (1976), which was not available previously. These substantial improvements to the characterization of regional hazard greatly improve the overall quality and accuracy of Central US earthquake impact assessments as the most current and regionally-comprehensive hazard input data is utilized.

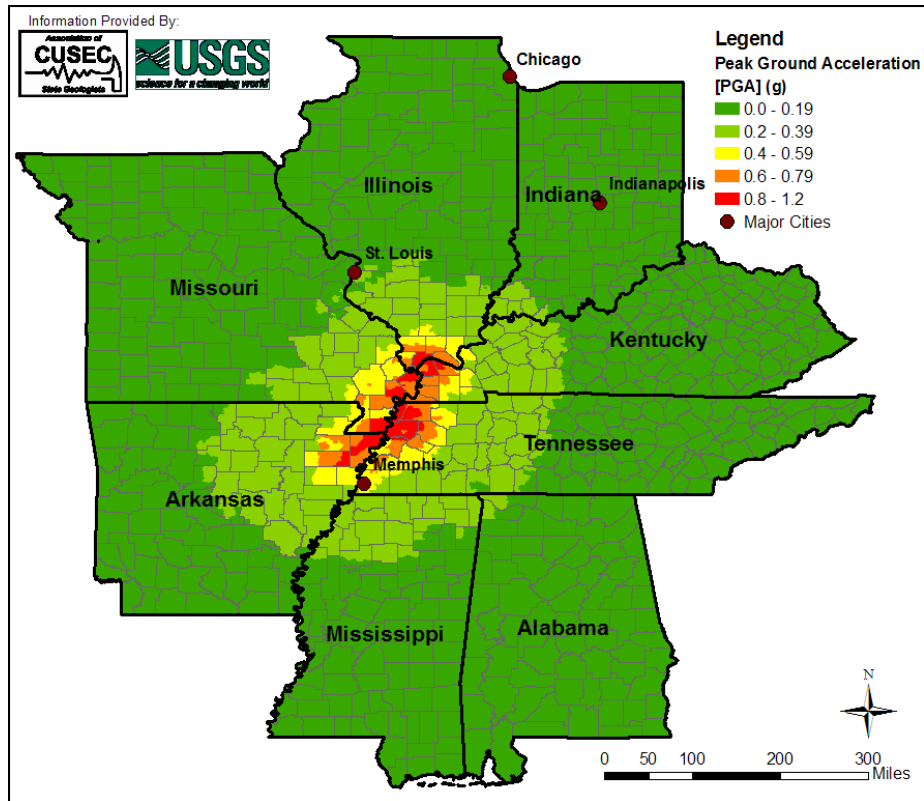


Figure 6: Peak Ground Acceleration (PGA) for NMSZ Scenario Event

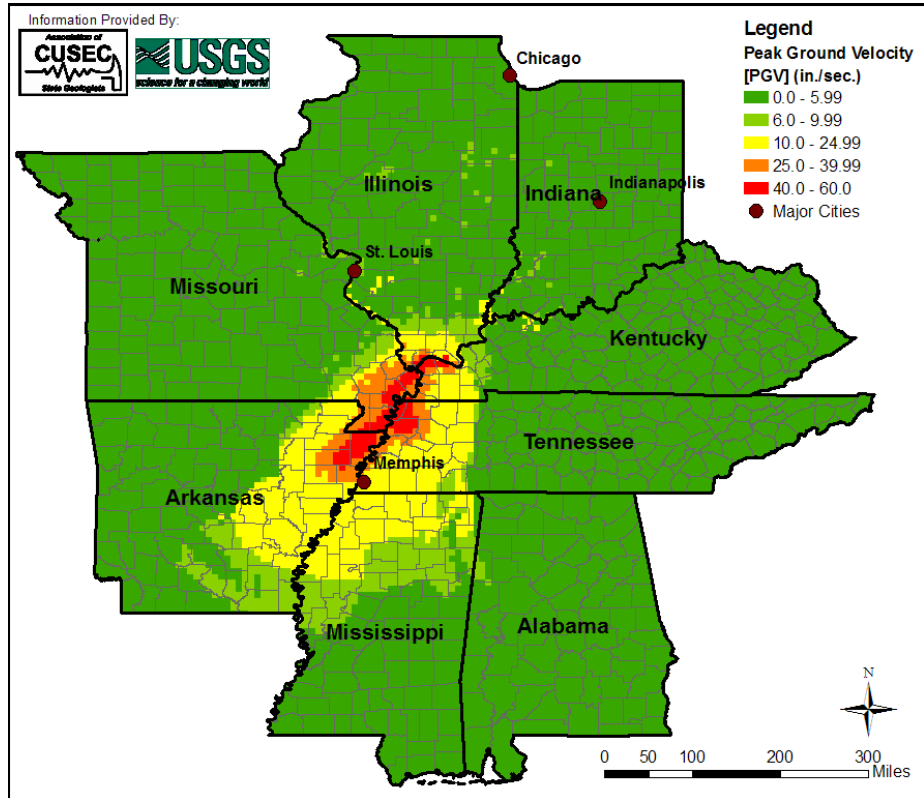


Figure 7: Peak Ground Velocity (PGV) for NMSZ Scenario Event

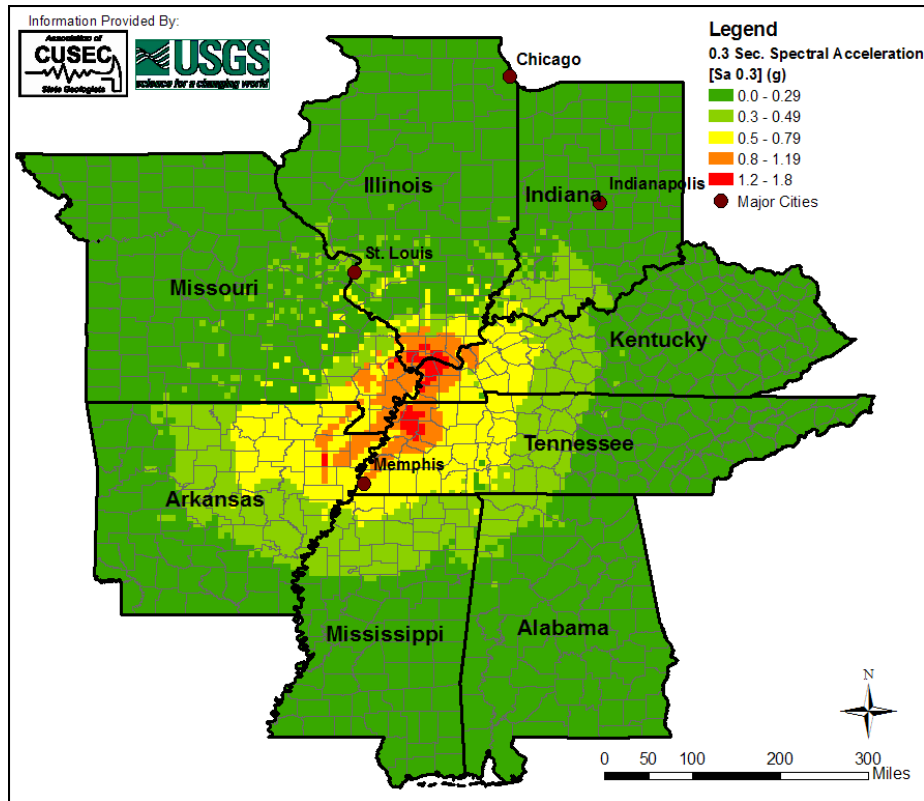


Figure 8: Short-Period (0.3 Second) Spectral Acceleration for NMSZ Scenario Event

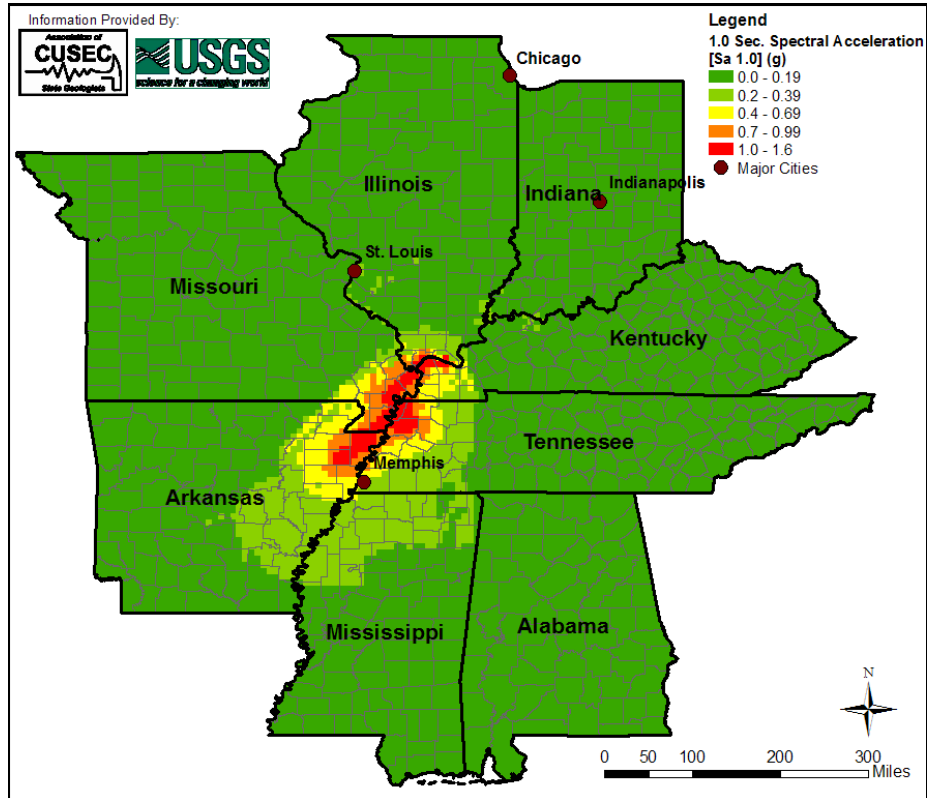


Figure 9: Long-Period (1.0 Second) Spectral Acceleration for NMSZ Scenario Event

References

Building Seismic Safety Council (2004). *NEHRP Recommended Provisions for Seismic Regulations for New Buildings and Other Structures* (2003 Edition, Part 1 Provisions. FEMA 450). FEMA, Washington, D.C., 355.

Cramer, C.H. (2006). Quantifying the Uncertainty in Site Amplification Modeling and Its Effects on Site-Specific Seismic-Hazard Estimation in the Upper Mississippi Embayment and Adjacent Areas. *Bulletin of the Seismological Society of America*, 96 (6), 2008-2020.

Central U.S. Earthquake Consortium (CUSEC) Association of the State Geologists (2008). *CUSEC State Geologists' Procedures for New Madrid Catastrophic Planning Initiative Phase II 8-State Soil Site Class, Liquefaction Susceptibility, and Soil Response Maps*. Memphis, TN. CUSEC.

Federal Emergency Management Agency [FEMA] (2008). *HAZUS-MH MR3 Technical Manual*. Washington, D.C. FEMA.

Fullerton, D. S., Bush, C. A., and Pennell, J. N. (2003). *Map of Surficial Deposits and Materials in the Eastern and Central United State (East of 102 degrees West Longitude)*. USGS Geologic Investigation Series I-2789. <http://pubs.usgs.gov/imap/i-2789/i-2789_p.pdf>.

International Code Council (2002). 2003 International Building Code, 668.

Toro, G.R. and W.J. Silva, (2001), *Scenario Earthquakes for St. Louis, MO, and Memphis, TN, and Seismic Hazard Maps for the Central United States Region Including the Effect of Site Conditions*. Final Technical Report, USGS External Grant 1434-HQ-GR-02981, 248 pp. < http://www.riskeng.com/PDF/Scen_CEUS_Rept.pdf >.

Youd, T. L., and Perkins, D. M. (1978). Mapping of Liquefaction Induced Ground Failure Potential. *Journal of the Geotechnical Engineering Division*. v 104, n 4, 433-446.

Appendix 2 – Inventory

HAZUS Impact Assessment Inventory

Inventory defines the assets in any region of interest and is required for any analytical earthquake impact assessment. HAZUS inventory comprises two main categories: population demographics and infrastructure. Population demographics are aggregated, typically to the census tract-level, meaning all demographic data in a tract is summed together. Demographics include total population, number of households, and divisions of population by age, ethnicity, income, as well as school- and working-populations, visitors, and other populations. The MR3 version of HAZUS (FEMA, 2008) is utilized in this study, and population data in this version represents Year 2000 US Census data, as shown in Table 1. No updates were made to these demographic numbers for this study.

Table 1: Population of Eight-State Study Region (Year 2000 Census)

State	Total Population	% Total Population
Alabama	4,447,100	10.2%
Arkansas	2,673,400	6.1%
Illinois	12,419,293	28.4%
Indiana	6,080,485	13.9%
Kentucky	4,041,769	9.2%
Mississippi	2,844,658	6.5%
Missouri	5,595,211	12.8%
Tennessee	5,689,283	13.0%
Total	43,791,199	100.0%

The description of infrastructure entails various types of facilities and structures, some of which are aggregated and others that are represented by specific coordinates. These types of facilities are referred to hereafter as point-wise infrastructure or inventory. The ‘general building stock’ in HAZUS is an aggregated representation of several building use groups (occupancy types) and structural systems (building types). All buildings and building square footages are summed at the census tract-level similar to population demographics. Building occupancy types include residential (single and multi-family homes), commercial, industrial, governmental, educational, religious, and agricultural buildings. These general occupancy types are further subdivided into 33 specific occupancy classes and are listed in the HAZUS Technical Manual (FEMA, 2008). Moreover, buildings are characterized by structure type including wood, reinforced masonry, unreinforced masonry, steel, cast-in-place concrete, precast concrete, and manufactured housing. General building types are also subdivided specific 36 building types which are listed in the HAZUS Technical Manual. Building counts, square footage and replacements costs in the MR3 version use data from 2005. No improvements were made to building data in this study, only baseline information from the HAZUS program was used. Furthermore, some local distribution pipelines are characterized with aggregated data. Potable and waste water, as well as natural gas, local distribution lines

are aggregated at the census tract-level and are left unchanged from baseline values for all impact assessments completed in this study.

Numerous infrastructure groups are represented by point-wise facilities or structures and these types are comprised of:

- Essential Facilities
 - Schools
 - Hospitals
 - Police Stations
 - Fire Stations
 - Emergency Operation Centers
- Transportation Lifelines
 - Highway Bridges (including major river crossings)
 - Railway Bridges
 - Ferry Facilities
 - Bus Stations
 - Airports
 - Light Rail Facilities and Bridges
- Utility Lifelines
 - Waste Water Facilities
 - Natural Gas Facilities
 - Major Natural Gas Transmission Pipelines
 - Oil Facilities
 - Major Oil Transmission Pipelines
 - Electric Power Facilities
 - Major Electric Transmission Lines
 - Communication Facilities
- High Potential-Loss Facilities
 - Dams
 - Nuclear Power Facilities
 - Military Installations
 - Hazardous Materials Facilities
 - Levees

These infrastructure types are the focus of all inventory updates to the baseline inventory in the HAZUS program. Sources of new inventory range from national datasets to independent, infrastructure type-specific investigations by the modeling team. The Homeland Security Infrastructure Program (HSIP) Gold Datasets from 2007 and 2008 (NGA, 2007 & 2008), the National Bridge Inventory (NBI) from 2008 (US Dept. of Transportation, 2008), and levee data from the US Army Corps. of Engineers are the national datasets utilized in this study. The HSIP data includes more than 200 datasets for various types of infrastructure while the NBI and US Army Corps. data refer to bridge and levee data only. State-specific data was incorporated for Illinois and Indiana. The Mid-America Earthquake (MAE) Center completed an investigation of essential facilities inventory on another earthquake impact assessment project and this information was

added to existing inventory for Illinois. Additionally, the POLIS Center at Purdue University, compiled extensive inventory databases for most types of point-wise infrastructure and these facilities were incorporated for the State of Indiana. Lastly, the MAE Center completed an independent search for major river crossings in the Central US. Major bridges on the Arkansas, Illinois, Mississippi, Missouri, and Ohio Rivers were geo-coded for use in HAZUS analysis. These major bridges are not part the baseline inventory and are added to inform end-users of potential damage to major river crossings in the region of interest.

The number of datasets used to improve inventory increases the likelihood of duplicating individual items in the characterization of infrastructure. All efforts were made to reduce the number of duplicate structures via geo-spatial and metadata filters. First, a geo-spatial buffer was applied to the existing inventory and all facilities falling inside the buffer zone were further examined. Facility/structure names and street addresses (where available) were cross-referenced against the existing inventory to further remove duplicate data. Even after this time-consuming and rigorous filtering process, it is still possible that duplicate facilities were added to the inventory. It is believed that there are minimal duplications and, thus the affect on impact assessment results is negligible. It is relevant to note that inventory is likely underrepresented despite all efforts to improve characterizations of infrastructure. With this in mind, the minimal duplication of facilities is not significant.

Each infrastructure type requires numerous metadata to complete an earthquake impact assessment. Such metadata include structure type, seismic design level, structure height/width, geo-spatial location/coordinates, address, replacement cost, backup power generation capability, and several others that are specific to certain infrastructure types. Sources of new inventory do not include all the required metadata and thus require the implementation of HAZUS ‘default’ values. This means certain metadata utilized in the HAZUS baseline inventory are applied to new inventory when no other metadata is available. Details of assumptions made regarding metadata for new inventory incorporated into HAZUS earthquake impact assessments are detailed in the following descriptions, denoted by infrastructure category: essential facilities, transportation lifelines, utility lifelines, and high potential-loss facilities.

NOTE: All POLIS Center data utilized was properly formatted for HAZUS and thus none of the metadata improvements discussed below were applied to that dataset. All metadata for these facilities was compiled by the POLIS Center.

Essential Facilities

Hospitals

Improvements to hospitals in HAZUS include those facilities that are hospitals as well as urgent care facilities. Hospitals are classified based on size, or bed capacity. When no

beds are specified, as is the case with urgent care facilities, facilities are specified as medical clinics, “EFMC.” When hospitals bed counts are available, facilities are specified as small, medium, or large, according to the bed counts in Table 3.11 of Chapter 3 in the HAZUS Technical Manual (FEMA, 2008). Structure type must also be specified and, since HSIP data does not include this metadata, the HAZUS default for each state is applied. For the State of Alabama, the default structure type is steel frame, “SL1”, and for the seven remaining states is precast concrete, “PC1”. Seismic design level is assumed to be pre-code, which corresponds to the HAZUS default assumption.

Replacement costs have been calculated by project collaborators on a per bed basis by state. When bed numbers are not available a bed count of 49 is assumed, making the facilities the size of a small hospital. These assumptions provide only approximate values. State per bed costs are as follows (Costs are in thousands of dollars):

- | | |
|-----------------------|-----------------------|
| • AL = \$201.1696/bed | • KY = \$217.7469/bed |
| • AR = \$193.1836/bed | • MS = \$186.7433/bed |
| • IL = \$262.3077/bed | • MO = \$235.43/bed |
| • IN = \$227.0436/bed | • TN = \$205.9109/bed |

Structure types and seismic design levels for facilities included from the MAE Center project in Illinois were assigned during that project and thus metadata assumptions were required.

Fire Stations

There is only one facility classification for fire stations, “EFFS,” and it is applied to all new fire stations. Additionally, the HAZUS default structure type seismic design level are assigned to all new items, unreinforced masonry low-rise, “URML”, and pre-code, “PC”, respectively. Replacement costs are applied, by state, based, on HAZUS default cost data (costs are in thousands of dollars):

- | | |
|----------------|----------------|
| • AL = \$1,250 | • KY = \$1,318 |
| • AR = \$1,200 | • MS = \$1,137 |
| • IL = \$1,613 | • MO = \$1,470 |
| • IN = \$1,425 | • TN = \$1,252 |

Structure types and seismic design levels for facilities included from the MAE Center project in Illinois were assigned during that project and thus now metadata assumptions were required.

Police Stations

Police stations taken from all HSIP data include local, state, and university police stations. All new facilities receive the same HAZUS facility classification, “EFPS,” as well as

default structure and seismic design classifications, “URML” and “PC,” respectively. Default replacement costs are also applied by state (costs are in thousands of dollars):

- AL = \$1,251
- AR = \$1,201
- IL = \$1,613
- IN = \$ 1,425
- KY = \$1,318
- MS = \$1,138
- MO = \$1,470
- TN = \$1,252

Structure types and seismic design levels for facilities included from the MAE Center project in Illinois were assigned during that project and thus now metadata assumptions were required.

Schools

Schools are classified as either elementary/primary education or colleges/universities. Corresponding layers from HSIP were isolated and new facilities identified then added to existing inventory. Colleges and universities include all medical schools, technical colleges, community colleges, and specialty institutions. Elementary/primary schools are classified as “EFS1”, and colleges/universities are classified as “ESF2”. Default structural and seismic design metadata were applied to all new facilities, “URML” and “PC”, respectively.

Replacement costs for HSIP 2007 data were determined by project collaborators based on the number of students per school. This information was not available to the MAE Center when 2008 HSIP data was incorporated. Replacement costs for all new HSIP 2008 schools were assigned the average replacement cost of all existing schools in the state inventory. State replacement costs for all new schools are as follows (costs are in thousands of dollars):

- AL = \$7,848
- AR = \$6,017
- IL = \$7,954
- IN = \$7,560
- KY = \$7,415
- MS = \$7,031
- MO = \$7,181
- TN = \$7,871

Structure types and seismic design levels for facilities included from the MAE Center project in Illinois were assigned during that project and thus now metadata assumptions were required.

Emergency Operation Centers

Emergency operation centers (EOCs) added to the regional inventory included emergency operation centers, state emergency operation centers and 9-1-1 call centers in the HSIP data. There is only one facility classification for these facility types, “EFEO”, and it was applied to all three facility types. As with other essential facility types,

HAZUS default structural and seismic design metadata were applied to EOCs, “URML” and “PC”, respectively. Default replacement costs are also applied by state (costs are in thousands of dollars):

- AL = \$900
- AR = \$870
- IL = \$1,110
- IN = \$1,030
- KY = \$980
- MS = \$850
- MO = \$1,030
- TN = \$880

Structure types and seismic design levels for facilities included from the MAE Center project in Illinois were assigned during that project and thus now metadata assumptions were required.

Transportation Lifelines

Major River Crossings

Major river crossings are uniquely configured bridges that are not suited for the bridge fragilities in the HAZUS program. A total of 127 major river crossings were identified and included in the regional analysis. Threshold values were used to determine damage for each major river crossing type and, as a result, independent bridge classes were required for analysis. Numerous bridge types are specific to California and these are not used in the Central US. Several of these bridge types were utilized for major river crossings, since no other Central US bridges exist for those classifications. HAZUS bridge classifications reserved specifically for California include highway bridge types:

- | | | |
|---------|----------|----------|
| 1. HWB6 | 4. HWB13 | 7. HWB21 |
| 2. HWB8 | 5. HWB18 | 8. HWB25 |
| 3. HWB9 | 6. HWB20 | 9. HWB27 |

Since only six major river crossing types were considered, the first six classifications were selected for use in this series of assessments. Fragility relationships for these bridge types were replaced with the threshold values identified for each type. Correlations between major river crossing type and HAZUS bridge class are listed in the following along with the number of bridges in each category:

- HWB6 → Cable-Stayed Bridges
- HWB8 → Multispan Continuous Steel Truss Bridges
- HWB9 → Multispan Simply Supported Steel Truss Bridges
- HWB13 → Multispan Continuous Steel Girder Bridge
- HWB18 → Multispan Simply Supported Steel Girder Bridges
- HWB20 → Multispan Simply Supported Concrete Girder Bridges

Geo-spatial data was also used to locate each bridge within the region of interest. Although other metadata was available for many bridges (i.e. length, width, number of spans, etc.), this was not added to the HAZUS analysis since it was not required. These metadata were a factor in the development of threshold values, however. Baseline replacement costs from HAZUS baseline inventory were not assigned to these bridges due to their unique construction.

Highway Bridges

Highway bridges in the HSIP data are taken from the NBI, so NBI bridge classifications must be converted to HAZUS bridge classifications. The tables below illustrate the correlation between NBI bridge type and HSIP bridge type:

NBI Classification	Material	HAZUS Classification	Comments
000 002 002 003 004 012 019	Other	HWB28	* These bridges are classified as 'Other' bridges since they do not fit any other HAZUS bridge types
100 101 102 103 104 105 106 107 109 110 111 112 114	Concrete	HWB5 or HWB7	* HWB5 constructed before 1990, HWB7 constructed in 1990 or later
118 119		HWB28	*Culverts and tunnels do not have a specific fragility in HAZUS and are classified as 'Other' bridges
121 122		HWB5 or HWB7	* HWB5 constructed before 1990, HWB7 constructed in 1990 or later

200 201 202 203 204 205 206 207 211 212 214	Continuous Concrete	HWB10 or HWB11	* HWB10 constructed before 1990, HWB11 constructed in 1990 or later
218 219		HWB28	*Culverts and tunnels do not have a specific fragility in HAZUS and are classified as 'Other' bridges
221 222		HWB10 or HWB11	* HWB10 constructed before 1990, HWB11 constructed in 1990 or later
300 301 302 303 304 305 306 307 308 309 310 311 312 313 314	Steel	HWB12 or HWB14 of HWB 24	* HWB12 constructed before 1990, HWB14 constructed in 1990 or later and HWB24 for all bridges meeting HWB12 classifications that are less than 20m (~66ft)
315		HWB28	*Movable-Lift bridges do not have a specific fragility in HAZUS and are classified as 'Other' bridges
316		HWB28	*Movable-Bascule bridges do not have a specific fragility in HAZUS and are classified as 'Other' bridges
317		HWB28	*Movable-Swing bridges do not have a specific fragility in HAZUS and are classified as 'Other' bridges
318		HWB28	*Tunnels do not have a specific fragility in HAZUS and are classified as 'Other' bridges
319		HWB28	*Culverts do not have a specific fragility in HAZUS and are classified as 'Other' bridges

400 401 402 403 404 405 406 407 409 410 411 412 413 414	Steel Continuous	HWB15 or HWB16 or HWB26	* HWB15 constructed before 1990, HWB16 constructed in 1990 or later and HWB26 for all bridges meeting HWB15 classifications that are less than 20m (~66ft)
416		HWB28	*Movable-Bascule bridges do not have a specific fragility in HAZUS and are classified as 'Other' bridges
419		HWB28	*Culverts do not have a specific fragility in HAZUS and are classified as 'Other' bridges
421		HWB15 or HWB16 or HWB26	* HWB15 constructed before 1990, HWB16 constructed in 1990 or later and HWB26 for all bridges meeting HWB15 classifications that are less than 20m (~66ft)
500 501 502 503 504 505 506 511	Prestressed Concrete	HWB17 or HWB19	* HWB17 constructed before 1990, HWB 19 constructed in 1990 or later
519		HWB28	*Culverts do not have a specific fragility in HAZUS and are classified as 'Other' bridges
522		HWB17 or HWB19	* HWB17 constructed before 1990, HWB 19 constructed in 1990 or later
601 602 603 604 605 606 613 614	Prestressed Concrete Continuous	HWB17 or HWB19	* HWB17 constructed before 1990, HWB 19 constructed in 1990 or later
619		HWB28	*Culverts do not have a specific fragility in HAZUS and are classified as 'Other' bridges
621 622		HWB17 or HWB19	* HWB17 constructed before 1990, HWB 19 constructed in 1990 or later
700 701 702 703 707 709 710 719	Timber	HWB28	* Timber bridges do not have specific fragilities in HAZUS and thus are classified as 'Other' bridges

800 801 802 804 811 819	Masonry	HWB28	* Masonry bridges do not have specific fragilities in HAZUS and thus are classified as 'Other' bridges
900 902 910 911 919	Aluminum, Wrought Iron, Cast Iron	HWB28	* Aluminum, Wrought Iron, and Cast Iron bridges do not have specific fragilities in HAZUS and thus are classified as 'Other' bridges

It is relevant to note that material and construction types are correlated HAZUS bridge types based on main span properties only. Approach properties are not considered since HAZUS does not analyze approaches. Various other metadata are added to HAZUS databases including length, width, number of spans, maximum span length, and skew angle. The default seismic design level is also applied to new bridges, low-code, “LC”.

Replacement costs for bridges are based on a per square foot cost by state. For this calculation, main span total length and bridge width are used. It is relevant to know that widths and lengths in the NBI, and thus, HSIP highway bridge datasets, are listed in tenths of meters, so all widths and lengths must be divided by ten to attain a width and length in meters. In some cases, bridge widths are not available so an average width of the remaining bridge widths in the state is applied. Average widths are only used to estimate replacement costs and are not added to the HAZUS model. Replacement costs and average widths used for replacement cost calculations are detailed in the following:

- AL = \$1.458/ m², ave. width = 11.9m
- AR = \$1.4094/ m², ave. width = 9.54m
- IL = \$1.7982/ m², ave. width = 28.95m
- IN = \$1.6686/ m², ave. width = 30.08m
- KY = \$1.5876/ m², ave. width = 11.2m
- MS = \$1.377/ m², ave. width = 9.7m
- MO = \$1.6686/ m², ave. width = N/A
- TN = \$1.4256/m², ave. width = 14.9m

Railway Bridges

New railway bridges added from HSIP data are correlated to HAZUS railway bridge types as follows:

HSIP Classifications		HAZUS Classification	
Span Material	Span Type	Bridge Type	Comments
0	0 3	RLB10	*'Other' materials in HSIP are classified as 'Other' bridges in HAZUS
1	0 1 2 3 4 6 7	RLB10 or RLB9	* Concrete is only specifically called out as RLB 9, though length is less than 66'. All other concrete bridges are classified as RLB10 which are 'Other' bridges
3	1 7	RLB1 or RLB3	*RLB1 constructed before 1990, RLB3 constructed in 1990 or later
4	4	RLB4 or RLB5	*RLB4 constructed before 1990, RLB5 constructed in 1990 or later
7	1	RLB10	*Timber is not specifically used in HAZUS, so these bridges are classified as 'Other'

As with highway bridges, various metadata are added to HAZUS databases including length, width, number of spans, maximum span length, and skew angle. The default seismic design level, “LC”, is applied.

Replacement costs for railway bridges are specified as costs per linear foot of bridge, by state. It is relevant to know that lengths in the HSIP railway bridge dataset are listed in tenths of meters, so all lengths must be divided by ten to attain a length in meters. Replacement costs for railway bridges in each state are listed in the following:

- AL = \$2.70/m
- AR = \$2.61/m
- IL = \$3.33/m
- IN = \$3.09/m
- KY = \$2.94/m
- MS = \$2.55/m
- MO = \$3.09/m
- TN = \$2.64/m

Bus Facilities

There is only one HAZUS classification for bus facilities, “BDFLT”, and it is applied to all new HSIP bus facilities. The HSIP layer ‘Bus Stations’ is used from this inventory update. The HAZUS default seismic design level, “LC”, is applied to all new facilities as well. Replacement costs for bus facilities are listed below by state (costs are in thousands of dollars):

- AL = \$981
- AR = \$948.30
- IL = \$1,209.90
- IN = \$1,122.70
- KY = \$1,068.20
- MS = \$926.50
- MO = \$1,122.70
- TN = \$959.20

Light Rail Facilities

There are two HSIP layers that are used to improve the light rail facilities inventory in HAZUS, 'Amtrak Stations' and 'Transit Stations'. Only the facilities in the 'Transit Stations' layer that are specified as 'Commuter Rail' are added to the light rail facilities inventory. The remaining facilities are added to the railway facilities inventory. Both layers employ the same HAZUS facility classification as there is only one class available, "LDFLT". The HAZUS default seismic design class is applied, "LC". Replacement costs for both HSIP layers are based on HAZUS default costs and are assigned to new facilities, by state, as follows (costs are in thousands of dollars):

- AL = \$1,962.00
- AR = \$1,896.60
- IL = \$2,419.80
- IN = \$2,245.40
- KY = \$2,136.40
- MS = \$1,853.00
- MO = \$2,245.40
- TN = \$1,918.40

Railway Tunnels

There is only one HAZUS classification for railway tunnels, "RDFLT", and it is applied to all new tunnels from the 'RR Tunnels' layer in the HSIP datasets. The HAZUS default seismic design level, "LC", is applied to all new tunnels. A replacement cost of \$11/m is used to determine replacement cost and is taken from HAZUS default replacement costs. The length of tunnels is included in the HSIP metadata and is also added to the HAZUS databases.

Railway Facilities

There are three HSIP layers that contribute to the railway facilities inventory, 'RR Yards,' 'Railroad Stations', and 'Transit Stations'. Only the facilities in the 'Transit Stations' layer that are specified as 'Line-Haul Railroads' are included in the railway facilities inventory. The remaining facilities are included in the light rail facilities inventory. Both 'RR Yards' and 'Railroad Stations' are classified as "RDF", and 'Transit Stations' are classified as "RMF". The HAZUS default seismic design level, "LC", is also applied to new facilities.

Replacement costs for new railway facilities are the same as those for light rail facilities and are as follows, by state (costs are in thousands of dollars):

- AL = \$1,962.00
- AR = \$1,896.60
- IL = \$2,419.80
- IN = \$2,245.40
- KY = \$2,136.40
- MS = \$1,853.00
- MO = \$2,245.40
- TN = \$1,918.40

Ports

The HSIP ‘Ports’ layer is the only layer used to improve the port facilities inventory. The single HAZUS port classification, “PDFLT”, is applied to all new facilities. The HAZUS default seismic design level, “LC”, is also assigned to all new facilities. Replacement costs are assigned to new facilities based on HAZUS default replacement costs by state (costs are in thousands of dollars):

- AL = \$1,962.00
- AR = \$1,896.60
- IL = \$2,245.40
- IN = \$2,158.20
- KY = \$1,940.20
- MS = \$2,245.40
- MO = \$2,158.20
- TN = \$1,940.20

Ferry Facilities

Only the HSIP layer ‘Ferries’ is used to improve the HAZUS representation of ferry facilities. The only HAZUS classification available for these facilities is, “FDFLT”, and it is applied to all new facilities. Additionally, the HAZUS default seismic design level, “LC”, is assigned to all new facilities. Replacement costs are assigned to new facilities, by state, based on HAZUS default replacement costs. These replacement costs are listed in the following (costs are in thousands of dollars):

- AL = \$1,122.70
- AR = \$948.30
- IL = \$1,209.90
- IN = \$1,122.70
- KY = \$1,068.20
- MS = \$926.50
- MO = \$1,122.70
- TN = \$959.20

Airports

Only one HSIP layer is used to improve the airport inventory, ‘Airports_Heliports’. There are several facility types included in this layer thus requiring several HAZUS facility classifications. Facility types in the HSIP layer are detailed in the “LAN_FA_TY” field. Facilities specified as ‘heliports’ in that field are assigned the HAZUS facility classification, “AFH”. All facilities specified as ‘airports’ are assigned the HAZUS classification, “ADFLT”. The remaining facilities classifications of ‘Gliderport’, ‘Seaplane Base’, ‘Stolport’, and ‘Ultralight’ are assigned HAZUS classification, “AFO”. The HAZUS default seismic design level, “LC”, is applied to all new facilities, regardless of HAZUS facility classification. Replacement costs for all new facilities are based on HAZUS default replacement costs by state and are applied as follows (costs are in thousands of dollars):

- AL = \$4,905.00
- AR = \$4,741.50
- IL = \$6,049.50
- IN = \$5,613.50
- KY = \$5,341.00
- MS = \$4,632.50
- MO = \$5,613.50
- TN = \$4,796.00

Utility Lifelines

Potable Water Facilities

There are no potable water facilities included in the HSIP datasets and thus none are added to the HAZUS inventory.

Waste Water Facilities

There is only one facility classification available in HAZUS for waste water facilities, “WDFLT,” and it was used for all new waste water facilities. Only on HSIP layer, ‘Waste Water Facs’, was used to improve the existing characterization of this facility type. The HAZUS default seismic design level, low-code, “LC”, was applied to all new facilities as well. Replacements costs are assigned to all new facilities, by state, based on HAZUS default replacement costs. Replacements costs are shown below (costs are in thousands of dollars):

- | | |
|-----------------|-----------------|
| • AL = \$59,940 | • KY = \$65,268 |
| • AR = \$57,942 | • MS = \$56,610 |
| • IL = \$73,926 | • MO = \$68,598 |
| • IN = \$68,598 | • TN = \$58,608 |

Oil Facilities

There are several sources of new inventory in the HSIP data that are classified as oil facilities in HAZUS. The HSIP layer ‘Oil Gas Facilities’ includes both oil and natural gas facilities. These facilities were separated based on the commodities each produces. Oil facilities are defined as though with an entry in the “COMMODITY” field of: ‘Crude,’ ‘Crude, Petrochemical,’ ‘Crude, Refined Products,’ ‘Crude, Refined Products, LPG/NGL,’ ‘Petrochemical,’ ‘Petrochemical, LPG/NGL,’ ‘Refined Products,’ ‘Refined Products, LPG/NGL,’ and ‘Refined Products, Miscellaneous.’ All new facilities from this layer were assigned the HAZUS facility classification, “ODFLT.”

Additionally, the HSIP layer ‘Oil Terminals’ is used to improve the existing oil facilities inventory. New facilities from this layer are also classified as, “ODFLT”. Oil refineries are also added to the existing inventory from the HSIP data layer, ‘Refineries.’ Specific HAZUS classifications are based on refinery capacities which are detailed in the “BSD_OPER” field. Refineries with a capacity of less than 100,000 lbs./day are classified as small refineries, “ORFS”, while refineries with capacities between 100,000 and 500,000 lbs./day are classified as medium-sized refineries, “ORFM”.

A fourth HSIP layer utilized in the oil facilities inventory improvement is ‘Liquid Petroleum Gas Stations’. All new facilities from that layer are classified as, “ODFLT”. Lastly, oil wells are added to the HAZUS existing inventory from the ‘Oil Gas Wells’ layer. As with oil and gas facilities, natural gas wells and oil wells are separated based on commodity stored. Only those wells deemed “ACTIVE” in the metadata are added to the inventory. Oil wells are those denoted by the following: ‘oil and gas wells,’ ‘oil wells,’ and ‘shut-in oil’. All new oil wells are classified as, “ODFLT”.

The HAZUS default seismic design level, “LC” is applied to all new oil facilities, regardless of the source layer in the HSIP data. The same replacement costs are applied to all new facilities and there costs are based on the HAZUS default replacement costs. The replacement costs applied to each facility, by state, are shown in the following (costs are in thousands of dollars):

- | | |
|--------------|--------------|
| • AL = \$90 | • KY = \$98 |
| • AR = \$87 | • MS = \$85 |
| • IL = \$111 | • MO = \$103 |
| • IN = \$103 | • TN = \$88 |

Natural Gas Facilities

There are also multiple HSIP data layers that were used to improve the existing natural gas facility inventory. All facilities related to natural gas from the ‘Oil Gas Facilities’ layer were added to the natural gas inventory. Facilities showing the following commodities were classified as natural gas facilities: ‘LPG/NGL,’ ‘Miscellaneous,’ ‘Natural Gas,’ ‘Natural Gas, Crude, Refined Products,’ ‘Natural Gas, Crude, Refined Products, LPG/NGL,’ ‘Natural Gas, LPG/NGL,’ ‘Natural Gas, Petrochemical,’ and ‘Natural Gas, Petrochemical, LPG/NGL.’ Those facilities specified as ‘Compressor or pump stations’ in the metadata were classified as, “NGC” in the HAZUS databases. All other facility types are classified as, “GDFLT”.

Natural gas wells from the HSIP data layer, ‘Oil Gas Wells’ are also added to the existing natural gas facilities dataset. As with oil wells, only those specified as “ACTIVE” are added to the inventory. Natural gas well were those specified as: gas injection well,’ ‘gas storage well,’ ‘gas storage,’ ‘gas well,’ and ‘shut-in gas.’ All natural gas wells are classified as, “GDFLT”. All new facilities, regardless of HSIP source layer, are assigned the HAZUS default seismic design level, “LC”. Additionally, new facilities are assigned the HAZUS default replacement cost for each state. Replacement costs for each state are shown in the following (costs are in thousands of dollars):

- | | |
|-------------------|-------------------|
| • AL = \$981.00 | • KY = \$1,068.20 |
| • AR = \$948.30 | • MS = \$926.50 |
| • IL = \$1,209.90 | • MO = \$1,122.70 |
| • IN = \$1,122.70 | • TN = \$959.20 |

Electric Power Facilities

Several layers in the HSIP data are used improve the characterization of electric power facilities. First, 'Electric Substations' are added and classified based on substations capacity. Low voltage substations are though with capacities less than 115KV and were classified as, "ESSL". Medium voltage substations were those with capacities between 115KV and 500KV. These substations are classified as, "ESSM". High voltage substations are those with capacities greater then 500KV and were classified as "ESSH".

Additionally, power plants were taken from HSIP data via the data layer, 'Electric Power Plants.' As with substations, power plants were classified based on generation capacity. Power plants with capacities less than 100MW were considered small plants and classified as, "EPPS." Power plants with capacities between 100MW and 500 MW were considered medium plants and classified as, "EPPM." Power plants with capacities greater than 500MW were considered large plants and classified as, "EPPL."

Further improvements utilized the 'Electric Generating Units' data layer in the HSIP data. Only those facilities specified as "ACTIVE" are included in the improved inventory data characterization utilized in HAZUS analysis. These facilities are classified similar to power plants, based on their power generation capacity. The same classifications are used for this HSIP data layer as for electric power plants.

Finally, the HSIP data layer 'Electric Control Centers' was added to the existing inventory. All new facilities from this data layer were classified as, "EDC". Regardless of HSIP source layer, new facilities were assigned the seismic design level, "LC". Furthermore, all new facilities are assigned the HAZS default replacement cost, by state. These replacements costs are as follows (costs are in thousands of dollars):

- | | |
|------------------|------------------|
| • AL = \$99,000 | • KY = \$107,800 |
| • AR = \$95,700 | • MS = \$93,500 |
| • IL = \$122,100 | • MO = \$113,300 |
| • IN = \$113,300 | • TN = \$96,800 |

Communication Facilities

A total of eleven HSIP layers are used to improve the characterization of communication facilities. The following details the HSIP layers used and the HAZUS classifications assigned to new facilities from each layer:

- Facilities from the HSIP data layer 'AM Antennas' were classified as, "CBR", for 'AM or FM transmitters and stations'
- Facilities from the HSIP data layer 'FM Antennas' were classified as, "CBR", for 'AM or FM transmitters and stations'
- Facilities from the HSIP data layer 'Land Mobile com' were classified as, "CBO", for 'Other transmitters and stations'

- Facilities from the HSIP data layer 'Land Mobile bcast' were classified as, "CBO", for 'Other transmitters and stations'
- Facilities from the HSIP data layer 'Microwave Towers' were classified as, "CBO", for 'Other transmitters and stations'
- Facilities from the HSIP data layer 'TV NTSC' were classified as, "CBT", for 'TV stations or transmitters'
- Facilities from the HSIP data layer 'TV DIGITAL' were classified as, "CBT", for 'TV stations or transmitters'
- Facilities from the HSIP data layer 'Central Office Locations' were classified as, "CCO", for 'Central offices'
- Facilities from the HSIP data layer 'Internet service providers' were classified as, "CCO", for 'Central offices'
- Facilities from the HSIP data layer 'Internet exchange points' were classified as, "CCO", for 'Central offices'

All new facilities were assigned the HAZUS default seismic design level, "LC". Additionally, all new facilities were assigned the HAZUS default replacement cost by state. Replacement costs for each state are as follows (costs are in thousands of dollars):

- | | |
|--------------|--------------|
| • AL = \$90 | • KY = \$98 |
| • AR = \$87 | • MS = \$85 |
| • IL = \$111 | • MO = \$103 |
| • IN = \$103 | • TN = \$88 |

High Potential-Loss Facilities

Dams

All new dam data is taken from HSIP 2007 and 2008 datasets. There are eleven dam types in the HAZUS classification scheme and many dam classifications in the HSIP data. The correlation between HSIP dam types and HAZUS dam types can be found in the following Table 2.

In cases where an HSIP dam type is not specified, the dam is classified as 'Other'. Various metadata describing dam configuration and capacity are also added to HAZUS metadata. Replacement costs are not included in the HAZUS modeling process for dams and thus not part of the metadata used in this project.

Table 2: Dam Classifications

Description	HAZUS Dam Type	HSIP Dam Type
Earth	HPDE	RECB, RECBPG, RECN, RECNPG, REER, REEROT, REERPG, REOT, REOTER, REST
Rockfill	HPDR	ERCN, ERCNPG, EROT, ERRE
Gravity	HPDG	PGCB, PGCN, PGCNRE, PGER, PGRE, PGRECN, PGRETC, PGVA, PGVAOT
Buttress	HPDB	CBCN, CBOT, CBRE
Arch	HPDA	VACB, VAPG, VAPGOT
Multi-Arch	HPDU	MV
Concrete	HPDC	CNMS, CNOT, CNPG, CNPGER, CNPGRE
Masonry	HPDM	MS
Stone	HPDS	ST
Timber Crib	HPDT	TC
Other	HPDZ	OT

Nuclear Power Facilities

Damage is not estimated for nuclear power facilities in the HAZUS framework though these facilities are included in HAZUS inventory databases. Three HSIP datasets are used to populate the HAZUS inventory, ‘Nuclear Fuel’, ‘Nuclear Plants’, and ‘Nuclear Research Facilities.’ All facilities are classified as ‘HPNP’ in the HAZUS facility classification scheme. No structural, seismic or replacement cost metadata are required since no damage or economic impact estimations are carried out in the HAZUS model.

Hazardous Materials Facilities

New hazardous materials facilities are identified in the HSIP dataset ‘RCRA hazardous waste.’ All facilities are classified as ‘HDFLT’ as it is the only facility class available for hazardous materials facilities. No replacement costs, structural or seismic metadata are required since HAZUS does not determine damage or economic loss internally. Only facility locations are required.

Levees

Levees were not analyzed in HAZUS, but rather analyzed externally meaning levee inventory did not have to comply with all HAZUS metadata requirements. A structure type classification was required to match the ground shaking with likely levels of damage. All levees are earthen structure and thus only one structure type is used which corresponds to one set of threshold values. Additionally, geo-spatial information was used to properly locate each levee within the study region. Though other metadata were available, none were required for the damage analysis. For flood risk analysis, levee crest elevations are required, though this information was not included in the metadata.

NOTE: Though not stated specifically under each inventory item category, geo-spatial location metadata, facility names, and street addresses are added to the HAZUS inventory to help identify each facility.

The following tables detail the critical infrastructure available at the beginning of Central US earthquake impact assessments by the project team. The inventory from ‘Project Year 1’ comprises HAZUS default data only. The critical infrastructure inventory shown by state in Table 3 through Table 10 represents three years of data collection from numerous sources. Sources of inventory have been previously discussed in this section. The inventory in the ‘Regional Modeling Inventory’ column was used in the earthquake impact assessments detailed in this report.

Table 3: Inventory Statistics for State of Alabama

Infrastructure Category	Baseline Inventory (Project Yr. 1)	Regional Modeling Inventory (Project Yr. 3)	Additional Infrastructure from Baseline
Essential Facilities			
Hospitals	122	210	88
Schools	1,857	1,903	46
Fire Stations	729	1,388	659
Police Stations	470	496	26
Emergency Operation Centers	27	124	97
Transportation Facilities			
Highway Bridges	11,857	17,491	5,634
Highway Tunnels	0	0	0
Railway Bridges	88	118	30
Railway Facilities	104	115	11
Railway Tunnel	0	9	9
Bus Facilities	16	24	8
Port Facilities	274	327	53
Ferry Facilities	0	6	6
Airports	180	469	289
Light Rail Facilities	0	11	11
Light Rail Bridges	0	0	0
Utility Facilities			
Communication Facilities	418	15,895	15,477
Electric Power Facilities	78	1,629	1,551
Natural Gas Facilities	81	458	377
Oil Facilities	17	425	408
Potable Water Facilities	30	30	0
Waste Water Facilities	299	9,315	9,016
High Potential Loss Facilities			
Dams	2,101	2,233	132
Hazardous Materials Facilities	2,199	3,656	1,457
Levees	0	5	5
Nuclear Power Facilities	3	3	0

Table 4: Inventory Statistics for State of Arkansas

Infrastructure Category	Baseline Inventory (Project Yr. 1)	Regional Modeling Inventory (Project Yr. 3)	Additional Infrastructure from Baseline
Essential Facilities			
Hospitals	93	125	32
Schools	1,059	1,328	269
Fire Stations	435	1,330	895
Police Stations	378	515	137
Emergency Operation Centers	11	113	102
Transportation Facilities			
Highway Bridges	5,634	14,060	8,426
Highway Tunnels	2	2	0
Railway Bridges	48	68	20
Railway Facilities	68	69	1
Railway Tunnel	0	5	5
Bus Facilities	16	18	2
Port Facilities	99	3	-96
Ferry Facilities	1	3	2
Airports	216	335	119
Light Rail Facilities	0	7	7
Light Rail Bridges	0	0	0
Utility Facilities			
Communication Facilities	310	4,626	4,316
Electric Power Facilities	31	800	769
Natural Gas Facilities	97	422	325
Oil Facilities	10	96	86
Potable Water Facilities	69	69	0
Waste Water Facilities	411	2,107	1,696
High Potential Loss Facilities			
Dams	1,173	1,228	55
Hazardous Materials Facilities	1,475	1,834	359
Levees	0	124	124
Nuclear Power Facilities	1	1	0

Table 5: Inventory Statistics for State of Illinois

Infrastructure Category	Baseline Inventory (Project Yr. 1)	Regional Modeling Inventory (Project Yr. 3)	Additional Infrastructure from Baseline
Essential Facilities			
Hospitals	227	413	186
Schools	5,283	5,795	512
Fire Stations	1,007	1,822	815
Police Stations	866	1,082	216
Emergency Operation Centers	149	221	72
Transportation Facilities			
Highway Bridges	22,854	29,967	7,113
Highway Tunnels	0	0	0
Railway Bridges	963	1,030	67
Railway Facilities	285	304	19
Railway Tunnel	0	4	4
Bus Facilities	101	120	19
Port Facilities	438	517	79
Ferry Facilities	2	11	9
Airports	624	935	311
Light Rail Facilities	0	409	409
Light Rail Bridges	38	38	0
Utility Facilities			
Communication Facilities	518	36,436	35,918
Electric Power Facilities	153	2,231	2,078
Natural Gas Facilities	62	3,778	3,716
Oil Facilities	39	41,105	41,066
Potable Water Facilities	242	242	0
Waste Water Facilities	876	9,807	8,931
High Potential Loss Facilities			
Dams	1,255	1,562	307
Hazardous Materials Facilities	4,870	17,310	12,440
Levees	0	576	576
Nuclear Power Facilities	7	9	2

Table 6: Inventory Statistics for State of Indiana

Infrastructure Category	Baseline Inventory (Project Yr. 1)	Regional Modeling Inventory (Project Yr. 3)	Additional Infrastructure from Baseline
Essential Facilities			
Hospitals	128	1,285	1,157
Schools	2,630	2,874	244
Fire Stations	605	1,247	642
Police Stations	502	537	35
Emergency Operation Centers	51	113	62
Transportation Facilities			
Highway Bridges	16,505	20,387	3,882
Highway Tunnels	0	0	0
Railway Bridges	80	92	12
Railway Facilities	91	149	58
Railway Tunnel	0	8	8
Bus Facilities	32	46	14
Port Facilities	84	100	16
Ferry Facilities	0	0	0
Airports	496	675	179
Light Rail Facilities	0	26	26
Light Rail Bridges	0	0	0
Utility Facilities			
Communication Facilities	386	22,806	22,420
Electric Power Facilities	54	975	921
Natural Gas Facilities	29	3,556	3,527
Oil Facilities	11	5,771	5,760
Potable Water Facilities	96	203	107
Waste Water Facilities	446	4,531	4,085
High Potential Loss Facilities			
Dams	1,026	1,187	161
Hazardous Materials Facilities	3,793	5,112	1,319
Levees	0	101	101
Nuclear Power Facilities	0	1	1

Table 7: Inventory Statistics for State of Kentucky

Infrastructure Category	Baseline Inventory (Project Yr. 1)	Regional Modeling Inventory (Project Yr. 3)	Additional Infrastructure from Baseline
Essential Facilities			
Hospitals	121	189	68
Schools	1,666	1,871	205
Fire Stations	625	1,066	441
Police Stations	381	407	26
Emergency Operation Centers	9	146	137
Transportation Facilities			
Highway Bridges	6,443	15,418	8,975
Highway Tunnels	4	4	0
Railway Bridges	143	166	23
Railway Facilities	117	125	8
Railway Tunnel	1	18	17
Bus Facilities	21	26	5
Port Facilities	277	301	24
Ferry Facilities	1	16	15
Airports	142	222	80
Light Rail Facilities	0	6	6
Light Rail Bridges	0	0	0
Utility Facilities			
Communication Facilities	374	17,099	16,725
Electric Power Facilities	68	1,976	1,908
Natural Gas Facilities	75	22,146	22,071
Oil Facilities	20	34,492	34,472
Potable Water Facilities	179	179	0
Waste Water Facilities	335	9,447	9,112
High Potential Loss Facilities			
Dams	1,134	1,196	62
Hazardous Materials Facilities	2,060	2,865	805
Levees	0	90	90
Nuclear Power Facilities	0	2	2

Table 8: Inventory Statistics for State of Mississippi

Infrastructure Category	Baseline Inventory (Project Yr. 1)	Regional Modeling Inventory (Project Yr. 3)	Additional Infrastructure from Baseline
Essential Facilities			
Hospitals	105	163	58
Schools	1,124	1,297	173
Fire Stations	430	984	554
Police Stations	368	365	-3
Emergency Operation Centers	37	121	84
Transportation Facilities			
Highway Bridges	13,692	18,293	4,601
Highway Tunnels	0	0	0
Railway Bridges	56	63	7
Railway Facilities	71	76	5
Railway Tunnel	1	1	0
Bus Facilities	27	41	14
Port Facilities	205	222	17
Ferry Facilities	0	2	2
Airports	192	257	65
Light Rail Facilities	0	20	20
Light Rail Bridges	0	0	0
Utility Facilities			
Communication Facilities	299	9,915	9,616
Electric Power Facilities	32	853	821
Natural Gas Facilities	55	3,442	3,387
Oil Facilities	10	7,405	7,395
Potable Water Facilities	17	17	0
Waste Water Facilities	335	3,406	3,071
High Potential Loss Facilities			
Dams	3,307	3,544	237
Hazardous Materials Facilities	1,154	2,042	888
Levees	0	50	50
Nuclear Power Facilities	1	1	0

Table 9: Inventory Statistics for State of Missouri

Infrastructure Category	Baseline Inventory (Project Yr. 1)	Regional Modeling Inventory (Project Yr. 3)	Additional Infrastructure from Baseline
Essential Facilities			
Hospitals	143	208	65
Schools	2,863	2,871	8
Fire Stations	636	1,399	763
Police Stations	592	654	62
Emergency Operation Centers	33	173	140
Transportation Facilities			
Highway Bridges	21,765	27,258	5,493
Highway Tunnels	0	0	0
Railway Bridges	163	200	37
Railway Facilities	125	139	14
Railway Tunnel	0	12	12
Bus Facilities	62	72	10
Port Facilities	193	232	39
Ferry Facilities	1	8	7
Airports	401	562	161
Light Rail Facilities	0	32	32
Light Rail Bridges	0	0	0
Utility Facilities			
Communication Facilities	397	21,789	21,392
Electric Power Facilities	79	1,855	1,776
Natural Gas Facilities	9	354	345
Oil Facilities	10	167	157
Potable Water Facilities	187	357	170
Waste Water Facilities	1,312	7,816	6,504
High Potential Loss Facilities			
Dams	4,108	5,408	1,300
Hazardous Materials Facilities	2,113	3,040	927
Levees	0	369	369
Nuclear Power Facilities	1	3	2

Table 10: Inventory Statistics for State of Tennessee

Infrastructure Category	Baseline Inventory (Project Yr. 1)	Regional Modeling Inventory (Project Yr. 3)	Additional Infrastructure from Baseline
Essential Facilities			
Hospitals	135	232	97
Schools	1,973	2,352	379
Fire Stations	565	1,110	545
Police Stations	425	424	-1
Emergency Operation Centers	36	171	135
Transportation Facilities			
Highway Bridges	5,298	22,897	17,599
Highway Tunnels	5	5	0
Railway Bridges	122	151	29
Railway Facilities	129	141	12
Railway Tunnel	0	15	15
Bus Facilities	35	58	23
Port Facilities	168	202	34
Ferry Facilities	1	6	5
Airports	184	318	134
Light Rail Facilities	0	26	26
Light Rail Bridges	0	0	0
Utility Facilities			
Communication Facilities	458	17,156	16,698
Electric Power Facilities	59	574	515
Natural Gas Facilities	56	183	127
Oil Facilities	21	160	139
Potable Water Facilities	98	98	0
Waste Water Facilities	504	2,001	1,497
High Potential Loss Facilities			
Dams	994	1,215	221
Hazardous Materials Facilities	2,489	4,080	1,591
Levees	0	11	11
Nuclear Power Facilities	2	5	3

Table 11: Inventory Statistics for Eight-State Region

Infrastructure Category	Baseline Inventory (Project Yr. 1)	Regional Modeling Inventory (Project Yr. 3)	Additional Infrastructure from Baseline
Essential Facilities			
Hospitals	1,074	2,825	1,751
Schools	18,455	20,291	1,836
Fire Stations	5,032	10,346	5,314
Police Stations	3,982	4,480	498
Emergency Operation Centers	353	1,182	829
Essential Facilities Total	28,896	39,124	10,228
Transportation Facilities			
Highway Bridges	104,048	165,771	61,723
Highway Tunnels	11	11	0
Railway Bridges	1,663	1,888	225
Railway Facilities	990	1,118	128
Railway Tunnel	2	72	70
Bus Facilities	310	405	95
Port Facilities	1,738	1,904	166
Ferry Facilities	6	52	46
Airports	2,435	3,773	1,338
Light Rail Facilities	0	537	537
Light Rail Bridges	38	38	0
Transportation Facilities Total	111,241	175,569	64,328
Utility Facilities			
Communication Facilities	3,160	145,722	142,562
Electric Power Facilities	554	10,893	10,339
Natural Gas Facilities	464	34,339	33,875
Oil Facilities	138	89,621	89,483
Potable Water Facilities	918	1,195	277
Waste Water Facilities	4,518	48,430	43,912
Utility Facilities Total	9,752	330,200	320,448
High Potential-Loss Facilities			
Dams	15,098	17,573	2,475
Hazardous Materials Facilities	20,153	39,939	19,786
Levees	0	1,326	1,326
Nuclear Power Facilities	15	25	10
High Potential-Loss Facilities Total	35,266	58,863	23,597
Total Number of Facilities	185,155	603,756	418,601

Transportation Network Model Inventory

The road network data for the two metropolitan areas, including locations of node and link, road characteristics, and travel demand are collected from the local metropolitan planning organizations (MPO) (i.e., the East-West Gateway Council of Governments at St. Louis, MO, and the Memphis Urban Area MPO at Memphis, TN). The road network databases contain over 100 fields with descriptive characteristics for each link that is used to estimate capacity and speed setting for traffic modeling.

The East-West Gateway Council of Governments (EWGCOG) consists of the City of St. Louis, Franklin, Jefferson, St. Charles, and St. Louis Counties in Missouri, and Madison, Monroe, and St. Clair Counties in Illinois. The Memphis Urban Area MPO consists of Shelby, Fayette, and Tipton Counties in Tennessee, and Desoto and Marshall Counties in Mississippi. The road network database and the associated travel demand are extracted from the 2004 highway network model from the Memphis MPO. The St. Louis MPO road network and travel demand are extracted from the 2002 loaded highway network product from the EWGCOG's TransEval transportation model.

The Memphis network consists of 12,399 nodes and 29,308 links, and travel demand of the network are represented by 1,605,289 origin-destination (OD) pairs. The St. Louis network is even larger, containing 17,352 nodes, 40,432 links, and 7,263,025 OD pairs.

Bridge information is extracted from the 2002 National Bridge Inventory (NBI) database from the Federal Highway Administration (FHWA). The 2002 version of the NBI database is compatible with the road network information provided by the local MPOs. From the NBI database, a total number of 3,095 and 615 bridges within the MPO boundaries are filtered in GIS on the St. Louis and Memphis MPO network, respectively.

Utility Network Model Inventory

Utility network models also require additional inventory investigations. As with transportation network modeling, advanced utility network modeling is completed for St. Louis and Memphis only since these are the two primary metropolitan areas significantly impacted by a NMSZ event. Water network data was obtained from The City of St. Louis Water Division. The MAE Center was not permitted to retain any of the inventory data so researchers completed all analyses at the St. Louis Water Division headquarters. The aforementioned HSIP 2008 data provided the basis for electric power network data in the St. Louis area.

St. Louis Natural Gas data was provided by Laclede Gas Company. Due to the confidential nature of this proprietary data, the MAE Center is not in a position to display the pipeline inventory, though results are included in subsequent sections and are represented in an aggregated form. All data for Memphis, Tennessee, utility network analyses was obtained from Memphis Light, Gas, and Water (MLGW). Network datasets included natural gas, potable water and sewage pipelines as well as electric network data.

References

Federal Emergency Management Agency [FEMA] (2008). HAZUS-MH MR3 Technical Manual. Washington, D.C. FEMA.

NGA Office of Americas/North America and Homeland Security Division (PMH) (2007). Homeland Security Infrastructure Program (HSIP) Gold Dataset 2007. Bethesda, MD 20816-5003. May.

NGA Office of Americas/North America and Homeland Security Division (PMH) (2008). Homeland Security Infrastructure Program (HSIP) Gold Dataset 2008. Bethesda, MD 20816-5003. October.

US Department of Transportation – Federal Highway Administration (2008). National Bridge Inventory. 1200 New Jersey Avenue SE, Washington, D.C., 20590. (2008).

Appendix 3 – Fragility Relationships

General Overview

Structural fragility, or vulnerability, functions relate the severity of shaking to the probability of reaching or exceeding pre-determined damage limit states. The shaking intensity is defined by peak ground parameters or spectral values of acceleration, velocity, or displacement. The maximum structural performance is estimated through capacity curves, specific to building or other infrastructure types. Furthermore, the intensity measure selected in fragility derivations is dependent upon the type of structure that the fragility relationships are developed for. It is generally recognized that structures with long natural periods, such as long span bridges or pipelines, are more sensitive to displacement; thus, peak ground displacement is a suitable choice as an intensity measure for the derivation of fragility relationships. Conversely, structures with short periods of vibration such as low rise masonry buildings are more sensitive to acceleration; hence peak ground acceleration is a better choice as an intensity measure in this case.

Limit states are essential in fragility curve derivation. HAZUS limit states include slight, moderate, extensive, and complete damage. The probability of reaching a defined limit state is given by equation (1):

$$P[LS] = \sum P[LS|D = d] P[D = d] \quad (1)$$

where D is a variable that describes the demand imposed on the system, $P[LS|D = d]$ is the conditional probability for the exceedance of the limit state (LS), given that $D = d$, and the summation is taken over all possible values of D , and the probability $P[D = d]$ defines the hazard. The variable, d , is the control, or interface, variable. The conditional probability, $P[LS|D = d]$, is the vulnerability function (Wen et al., 2003).

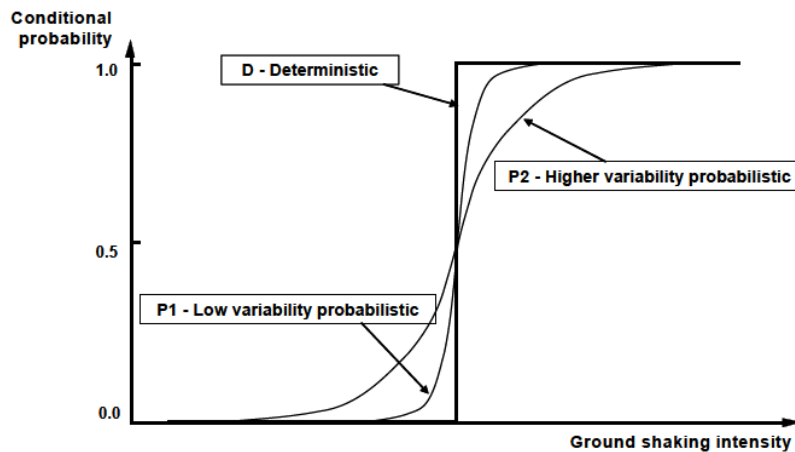


Figure 1: Conventional Fragility Curves (MAEC, 2007)

Figure 1 shows a typical fragility curve. The vertical line represents a system with deterministic limit state, while the other two curves represent probabilistic limit states

with different variability. The curve closer to the vertical line (deterministic) has lower uncertainty than the curve that is farther from the vertical line

Building Fragilities

HAZUS Building Fragility Relationships

HAZUS defines four damage limit states (slight, moderate, extensive, and complete), and thus four fragility curves, per building type. Fragilities are represented with lognormal cumulative distribution functions that estimate the probability of reaching or exceeding a certain damage state, for a certain level of ground shaking or ground deformation. Equation (2) expresses the mathematical relationship that describes the fragility curves:

$$P[\text{Exceedance}_i | S_d] = \Phi \left[\frac{1}{\beta_{\text{TOT}i}} \ln \left(\frac{S_d}{LS_i} \right) \right] \quad (2)$$

where Φ is the standard normal cumulative distribution function, $\beta_{\text{TOT}i}$ is the total uncertainty associated with damage state, i , S_d is spectral displacement, and LS_i is the median value of S_d at which the building reaches the damage limit state, i . Figure 2 depicts a typical set of fragility curves used in HAZUS, illustrating the four damage limit states (from left to right): slight, moderate, extensive, and complete.

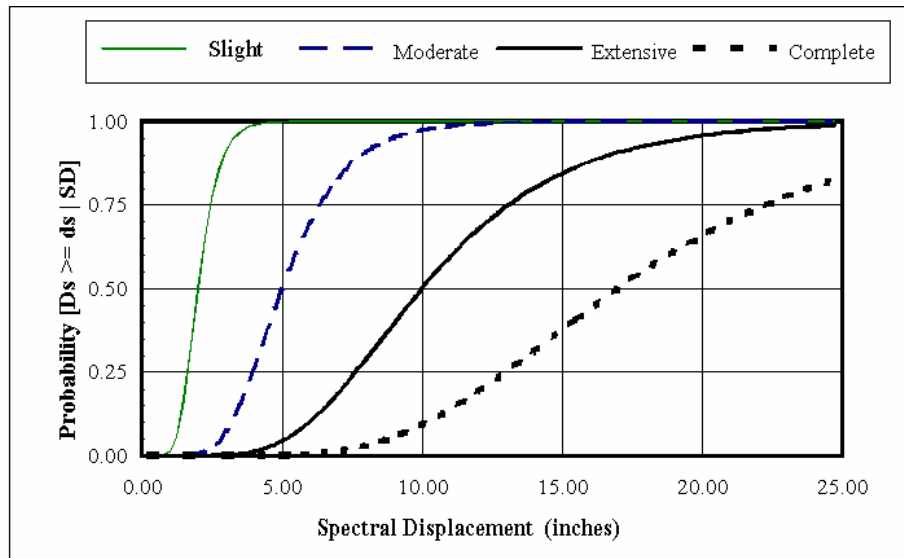


Figure 2: Characteristic Fragility Relationships for Slight, Moderate, Extensive, and Complete Damage States (FEMA, 2008)

As previously mentioned, there are four fragility curves in each set that are specific to each HAZUS building type. Damage functions require various metadata to properly apply building fragilities including, construction material, building height (low, medium,

or high rise), and response spectrum of the structure. There are 36 model building types defined in HAZUS. Table 1 illustrates model building types included in HAZUS.

Table 1: HAZUS Model Building Types (FEMA, 2008)

No.	Label	Description	Height			
			Range		Typical	
			Name	Stories	Stories	Feet
1	W1	Wood, Light Frame ($\leq 5,000$ sq. ft.)		1 - 2	1	14
2	W2	Wood, Commercial and Industrial ($> 5,000$ sq. ft.)		All	2	24
3	S1L	Steel Moment Frame	Low-Rise	1 - 3	2	24
4	S1M		Mid-Rise	4 - 7	5	60
5	S1H		High-Rise	8+	13	156
6	S2L	Steel Braced Frame	Low-Rise	1 - 3	2	24
7	S2M		Mid-Rise	4 - 7	5	60
8	S2H		High-Rise	8+	13	156
9	S3	Steel Light Frame		All	1	15
10	S4L	Steel Frame with Cast-in-Place Concrete Shear Walls	Low-Rise	1 - 3	2	24
11	S4M		Mid-Rise	4 - 7	5	60
12	S4H		High-Rise	8+	13	156
13	S5L	Steel Frame with Unreinforced Masonry Infill Walls	Low-Rise	1 - 3	2	24
14	S5M		Mid-Rise	4 - 7	5	60
15	S5H		High-Rise	8+	13	156
16	C1L	Concrete Moment Frame	Low-Rise	1 - 3	2	20
17	C1M		Mid-Rise	4 - 7	5	50
18	C1H		High-Rise	8+	12	120
19	C2L	Concrete Shear Walls	Low-Rise	1 - 3	2	20
20	C2M		Mid-Rise	4 - 7	5	50
21	C2H		High-Rise	8+	12	120
22	C3L	Concrete Frame with Unreinforced Masonry Infill Walls	Low-Rise	1 - 3	2	20
23	C3M		Mid-Rise	4 - 7	5	50
24	C3H		High-Rise	8+	12	120
25	PC1	Precast Concrete Tilt-Up Walls		All	1	15
26	PC2L	Precast Concrete Frames with Concrete Shear Walls	Low-Rise	1 - 3	2	20
27	PC2M		Mid-Rise	4 - 7	5	50
28	PC2H		High-Rise	8+	12	120
29	RM1L	Reinforced Masonry Bearing Walls with Wood or Metal Deck Diaphragms	Low-Rise	1-3	2	20
30	RM1M		Mid-Rise	4+	5	50
31	RM2L	Reinforced Masonry Bearing Walls with Precast Concrete Diaphragms	Low-Rise	1 - 3	2	20
32	RM2M		Mid-Rise	4 - 7	5	50
33	RM2H		High-Rise	8+	12	120
34	URML	Unreinforced Masonry Bearing Walls	Low-Rise	1 - 2	1	15
35	URMM		Mid-Rise	3+	3	35
36	MH	Mobile Homes		All	1	10

The fragility curves implemented in HAZUS are functions of structural response. The structural response required to utilize the vulnerability functions is determined by applying the capacity spectrum approach, thus requiring the derivation of the capacity, defined by pushover curves. Fragility curves are further delineated by the level of seismic

design inherent in building construction. Four seismic design levels are available in HAZUS, pre-, low-, moderate-, and high-code, and are applicable to each building type. There are a total of 144 combinations of building types and seismic design levels in HAZUS representing 144 individual capacity curves. The capacity spectrum method (CSM) and building capacity curves provide reasonable structural damage estimates adequate for structural loss assessment.

A capacity curve relates the lateral displacement to the lateral force. Typically, lateral displacement is top (roof) displacement, while base shear is utilized for a static-equivalent lateral force representation. In order to obtain HAZUS-compatible relationships, total base shear is converted to spectral acceleration (S_a) and roof displacement is converted to spectral displacement (S_d), by applying the following equations:

$$S_a = \frac{V/W}{\alpha_1} \quad (3)$$

$$\alpha_1 = \frac{\left[\sum_{i=1}^N w_i \phi_{i1} / g \right]^2}{\left[\sum_{i=1}^N w_i / g \right] \left[\sum_{i=1}^N (w_i \phi_{i1}^2) / g \right]} \quad (4)$$

$$S_d = \frac{\Delta_{\text{roof}}}{PF_1 \phi_{\text{roof},1}} \quad (5)$$

$$PF_1 = \frac{\left[\sum_{i=1}^N w_i \phi_{i1} / g \right]}{\left[\sum_{i=1}^N (w_i \phi_{i1}^2) / g \right]} \quad (6)$$

where V is the base shear, W is total building weight, g is the acceleration of gravity, w_i is the weight of i -th story, and ϕ_i is the magnitude of the fundamental mode shape at story, i . The parameters α_1 and PF_1 are defined by equations (4) and (6), respectively. The methodology is adapted from Applied Technology Council Report, ATC-40 (1996).

The building capacity curves are constructed based on estimates of engineering properties that affect the design, i.e. the yield and the ultimate capacities of each model building type. The parameters required to define the limit states are as follows:

- C_s : Design strength coefficient (fraction of building's weight)
- T_e : True "elastic" fundamental-mode period of building in seconds
- α_1 : Fraction of building weight effective in push-over mode

- α_2 : Fraction of building height at location of push-over mode displacement
- γ : Overstrength factor relating “true” yield strength to design strength
- λ : Overstrength factor relating ultimate strength to yield strength
- μ : Ductility factor relating ultimate displacement to λ times the yield displacement (i.e., assumed point of significant yielding of the structure)

The design strength, C_s , is approximately based on the lateral-force design requirements of current seismic codes (e.g., 1994 NEHRP Provisions). These requirements are functions of the building seismic zone location and other factors such as the type of lateral force resisting systems, the local soil conditions, and the building fundamental period. In the HAZUS Technical Manual (FEMA, 2008), Tables 5.4, 5.5, and 5.6 provide values for the parameters C_s , T_e , the response factors α_1 and α_2 , the overstrength factors λ and γ , and the ductility factor μ . Figure 3 illustrates the derivation procedure for HAZUS fragility curves and relates the definition of the yield and ultimate points to the previously discussed parameters.

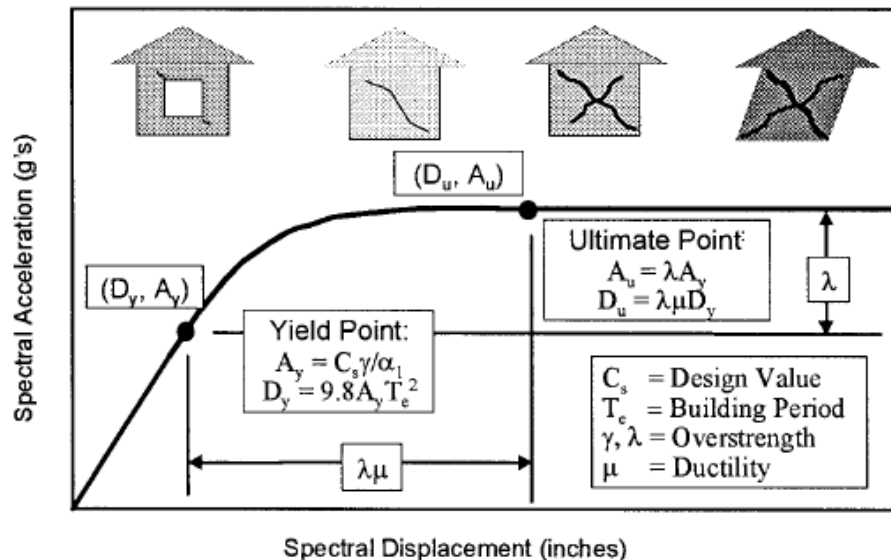


Figure 3: Derivation of HAZUS Fragilities (MAEC, 2007)

The four damage states (slight, moderate, extensive, and complete) are defined through drift threshold median values of buildings. Comprehensive drift values for different building types, seismic design levels, and heights are included in the HAZUS Technical Manual, Tables 5.9a-d. Though drift threshold values vary depending upon construction materials, building height, and seismic design level, general assumptions are applied for specific categories as follows:

- Drift ratio values of complete damage of moderate-code buildings are assumed to be 75% of drift ratio values that define complete damage of high-code buildings
- Drift ratio values of complete damage of low-code buildings are assumed to be 63% of drift ratio values that define complete damage of high-code buildings

- Slight damage ratios are assumed to have approximately same drift ratio values for all code design levels

The previous statements are based on the assumption that low- and moderate-code structures have lower ductility capacity than high-code buildings, thus having lower post-yield capacity. Most structures still exhibit elastic behavior even when slightly damaged that leads to the assumption of equal drift ratio for all code levels. For pre-code buildings, low-code parameters are reduced to 80% of the original values, in order to account for inferior seismic design. For all damage states, drift ratios are reduced as building height increases. Drift ratio values of mid-rise buildings are reduced to 67% of the low-rise building values, while high-rise building values are assumed to be 50% of the low-rise building drift ratios.

The uncertainty associated with damage levels in fragility relationships is obtained by the combination of three lognormal standard deviation values. The total variability for each limit state is evaluated using the following equation:

$$\beta_{Sds} = \sqrt{\left(\text{CONV}[\beta_C, \beta_D, \bar{S}_{d,Sds}]\right)^2 + \left(\beta_{M(Sds)}\right)^2} \quad (7)$$

where β_{Sds} is the lognormal standard deviation that describes the total variability in structural damage state, ds, β_C is the lognormal standard deviation parameter that describes the variability in the capacity curve, β_D is the lognormal standard deviation parameter that describes the variability in the demand spectrum, $\bar{S}_{d,Sds}$ is the median value of spectral displacement, in inches, of structural components for damage state, ds, $\beta_{M(Sds)}$ is the lognormal standard deviation parameter that describes the uncertainty in the estimate of the median value of the threshold of structural damage state, ds. “CONV” refers to a convolution function which is necessary to account for the interdependency between the lognormal standard deviations of capacity and demand values. $\beta_{M(Sds)}$ is assumed as 0.4 for all buildings, while the lognormal standard deviation parameter, β_C , takes the values of 0.3 for pre-code structures and 0.25 for all post-code seismic design levels. The β_D term is taken as 0.45 for short periods and 0.5 for long periods.

HAZUS default fragilities are applied to the entire U.S. though the observational data used to develop the fragilities is heavily based on California earthquake damage data. The resulting fragilities are applied to the entire U.S. even though they are not specific to the Central US; therefore, the uncertainty associated with the default fragilities is high. In order to reduce the uncertainty and provide more accurate and structure-specific fragilities, new fragilities derived by the Mid-America Earthquake (MAE) Center are implemented in the earthquake impact assessment conducted in this study.

Building Fragility Improvements

A new method to derive fragilities is used to improve upon the HAZUS default fragility functions. The methodology employed to develop the new building fragilities allows for a more accurate damage assessment and is used to derive sets of fragility curves for all HAZUS building types. The HAZUS-compatible fragility derivation methodology developed by Gencturk (2007) consists of several main components: capacity, demand, structural analysis, and fragility curve generation.

The capacity of structures is represented by either analytical (for wood frame structures) or expert opinion (for other building types) pushover curves. Demand refers to the earthquake event a structure is subjected to and represented using artificially generated earthquake ground motions. HAZUS provides default capacity for all infrastructure types, though the demand curves are adjusted to represent Central US events during the development of new building fragilities. With regard to demand, synthetic records are often used in the Central US for large magnitude earthquakes due to a lack of adequate existing earthquake records. Synthetic, site-specific ground motions were used in order to capture site-specific factors such as frequency distribution, duration, and site conditions (Gencturk et al., 2008). Finally, structural assessment is completed by applying an advanced Capacity Spectrum Method (CSM) (Gencturk and Elnashai, 2008), and fragilities are derived and presented in two different forms: conventional and HAZUS-compatible. Only the HAZUS compatible fragility relationships are used in this study.

Capacity and demand are critical to the process of fragility relationship derivation. A better representation of the real behavior both in terms of building capacity and earthquake demand generate more dependable results. The proposed fragility derivation method produces fragility relationships that are easily implemented in loss assessment methodology. In order to develop a comprehensive set of fragility relationships that apply to a wide variety of building types numerous structural parameters must be considered, including construction type, height, and seismic design level, among others. Furthermore, a simple representation of lateral force resisting capacity is implemented which accurately reflects real behavior (pushover curves are utilized for this purpose). A similar methodology as described in HAZUS Technical Manual was implemented to estimate building capacity.

The spectral displacement ground motion parameter is employed in HAZUS building fragility curves and thus is the basis for all new HAZUS-compatible fragility relationships incorporated in this study. Building capacity curves for all building types included in the HAZUS program were not modified for these HAZUS-compatible fragilities. In other words, fragility curves are derived using the default capacity curves as provided by HAZUS, the site specific ground motions for Central US, and the developed method for structural assessment, i.e. advanced CSM.

Ground motion processes are highly unpredictable and variable, thus they are responsible for a large portion of the uncertainty in the derivation of fragility relationships. This emphasizes the importance of earthquake record selection, since the accuracy of the representation of the demand is directly related to the reliability of fragility derivation. Due to the lack of natural records in the Central US, synthetic artificial records are used.

The regional differences in ground motion characteristics are small in seismically active areas; therefore, natural time histories selected from one high-seismicity zone can be carried to other high-seismicity regions, given that magnitude, depth, fault mechanism, and site conditions are represented accurately. However, strong motion characteristics in inter-plate and intra-plate regions exhibit significant differences. In fact, ground motion attenuates faster in more fragmented inter-plate regions than unfractured intra-plate regions such as the Central and Eastern US (CEUS). It is necessary that these features are considered in order to obtain reliable fragility relationships.

One example of a cohesive intra-plate region is the Upper Mississippi Embayment. The Upper Mississippi Embayment has unique ground motion attenuation due to the soft soil sediments located on top of the bedrock. Thickness varies from only a few feet up to 4,000 feet throughout the Embayment. With this in mind, attenuation relationships were derived for two soil profiles, uplands and lowlands. The upland profile represents extremely stiff soils or rock, while the lowland profile represents soft soil conditions. Figure 4 illustrates the soil profile of the Upper Mississippi Embayment and the cities for which synthetic ground motions were developed (Fernandez, 2007).

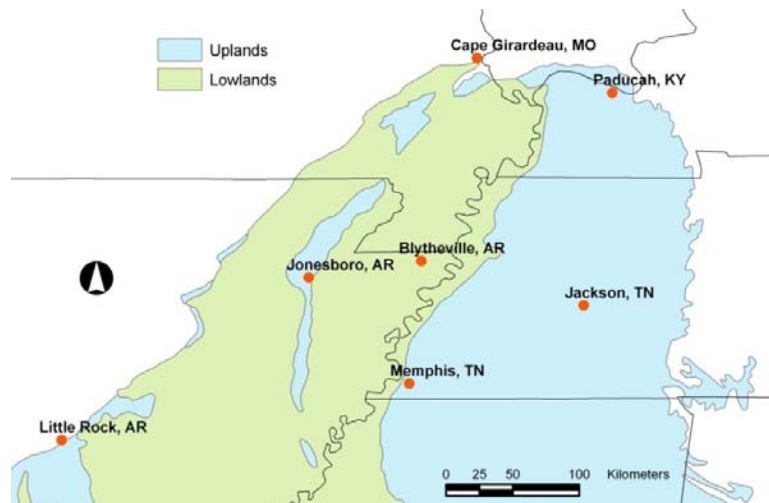


Figure 4: Soil Profiles for the Upper Mississippi Embayment (Fernandez, 2007)

A set of ground motions consistent with hazard levels of 10%, 5% and 2% probabilities of exceedance in 50 years (with corresponding return periods of 475, 975 and 2,475 years) were considered. The ground motions representing the 975-year return period event were selected for this study. Each set includes ten acceleration time histories for both upland and lowland profiles. Table 2 illustrates the ground motion parameters for both soil profiles.

Table 2: Single Value Representations of Earthquake Record Sets

Record #	Lowlands			Uplands		
	PGA (g)	PGV (in/sec)	PGD (in)	PGA (g)	PGV (in/sec)	PGD (in)
1	0.204	13.580	6.938	0.201	9.007	3.851
2	0.212	10.733	5.884	0.224	12.048	7.554
3	0.185	8.785	6.902	0.230	17.364	11.546
4	0.207	10.870	7.034	0.226	11.240	6.176
5	0.198	9.821	11.615	0.198	9.808	12.338
6	0.237	17.385	18.182	0.239	13.772	23.945
7	0.192	7.812	6.120	0.275	9.737	8.396
8	0.208	9.511	10.684	0.223	13.614	14.424
9	0.178	17.592	7.321	0.213	13.490	5.489
10	0.213	16.352	6.444	0.250	15.601	13.397
Mean	0.203	12.244	8.712	0.228	12.568	10.712
Standard Deviation	0.017	3.694	3.845	0.023	2.707	5.866

It is relevant to note the necessity of having two different soil profiles, since local soil conditions greatly affect the ground shaking at the surface. It is commonly known that stiff soils behave elastically, while soft soils exhibit highly inelastic behavior and typically cause high period elongation. The behavioral differences of the two soil types are illustrated in Figure 5, where 5% damped elastic spectra is presented for lowland and upland profiles.

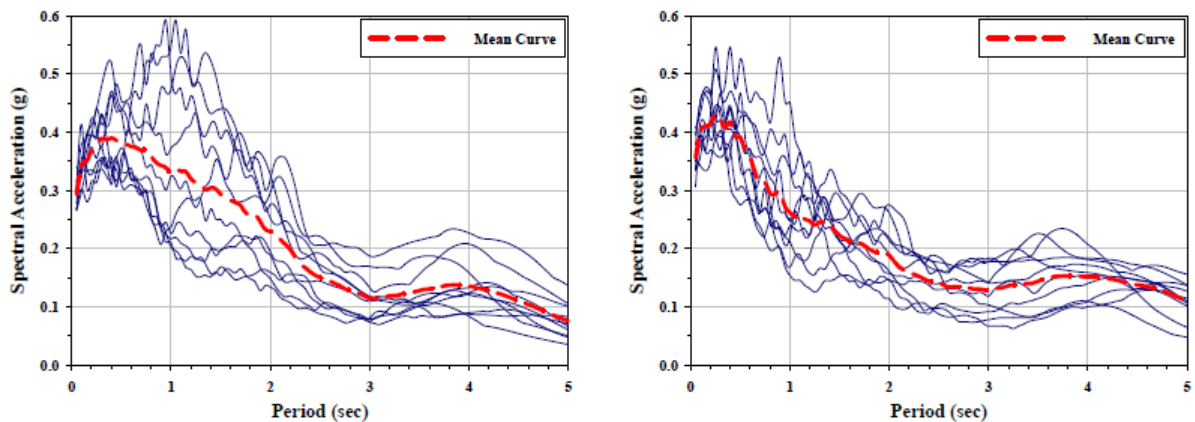


Figure 5: Spectral Acceleration Elastic Spectra (5% damping) for Lowlands (left) and Uplands (right) (Gencturk, 2007)

It is important that the ground motions used represent the characteristics of the New Madrid Seismic Zone (NMSZ), therefore, the demand is represented by synthetically generated ground motion records compatible with the seismo-tectonic and geotechnical characteristics (e.g. magnitude, distance, and site conditions) of the NMSZ.

Another very important factor in the derivation of fragility relationships is the methodology employed for structural assessment. The implemented methodology must predict accurately the displacement response under the applied ground motion. An advanced Capacity Spectrum Method is developed that provides more accurate results than existing CSM methods.

The advanced CSM is designed to overcome the difficulties encountered in nonlinear static analysis and provide better estimates of structural response. The fundamental idea is to use inelastic dynamic analysis of single degree of freedom (SDOF) systems represented by bilinear force-deformation relationships. The advanced method eliminates approximations and hence errors introduced into the solution through the use of: equivalent linear systems, design spectra (when actual spectra area are not available), and force reduction factors.

A step-by-step procedure to determine the displacement demand with the advanced method is given below:

1. A set of trial performance points are chosen on the capacity diagram
2. A bilinear representation is developed for each trial performance point
3. Peak responses of SDOF systems, whose force-deformation relationship is defined as a bilinear representation, are obtained using nonlinear time history analyses. Kinematic hardening behavior is assumed for hysteretic response (the implemented hysteretic model is shown in Figure 6).
4. The intersection of the curve constructed by joining the points found in Step 3 with the capacity diagram gives the displacement demand imposed on the structure

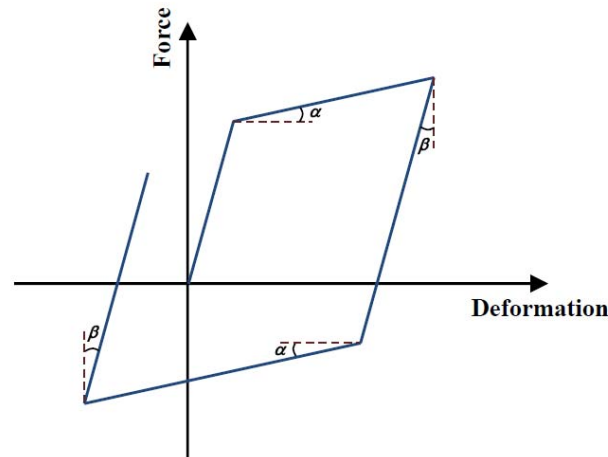


Figure 6: Force-Deformation Relationship for Kinematic Hardening Behavior (Gencturk, 2007)

This advanced method is utilized to analyze structures, whose pushover curves are available, under any desired ground motion without convergence problems even under very severe ground motions. Additionally, the methodology provides a reliable alternative to computationally expensive inelastic dynamic analysis of multiple degree of freedom (MDOF) structures.

One major limitation of the methodology is that MDOF structures are represented as SDOF structures, as it is the case with all CSMs. The reduction of degrees of freedom is a concern for structures where torsional effects are significant due to irregularities in plan and/or elevation of buildings. In these cases, the higher modes can contribute

significantly to the structural response, thus, analysis based solely on the first mode can yield inaccurate results.

Another limitation of the CSM is that it relies on the pushover curve. Pushover curves do not account for any local behavior and may not include all features of the buildings, such as soft stories and higher mode phenomena. Additionally, structures behave differently in two opposite directions, namely, pull and push. Therefore, the irregularities in the plan and elevation of a structure can significantly affect the accuracy of pushover curve. Given that the above limitations do not impair the required accuracy, the proposed CSM provides reliable and accurate results for estimating displacement demands imposed on structures behaving beyond their elastic limits.

Finally, fragility relationships are generated by conducting statistical analysis of the results obtained from the structural response assessment of the variations of capacity of buildings under the variations of ground motions using the methodology for structural response assessment described in the preceding section. This final component of the proposed framework for fragility analysis yields the desired relationships and completes the entire procedure.

Conventional fragilities differ from HAZUS fragilities in terms of intensity measures. The majority of conventional fragilities utilize peak ground parameters (acceleration [PGA], velocity [PGV], or displacement [PGD]) or spectral values to represent the ground shaking intensity. HAZUS fragilities are presented differently. In HAZUS, the fragility relationships are expressed by damage state exceedance probabilities related to structural response and the only parameter required to derive the HAZUS-compatible fragility curves is the combined uncertainty of capacity and demand, which is obtained through the “convolution” process (Gencturk, 2007).

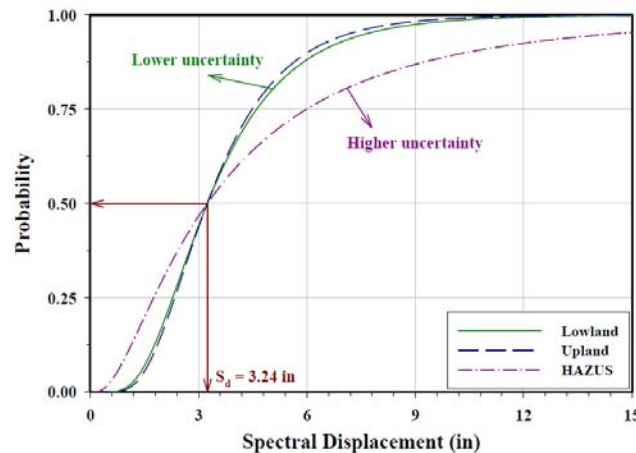


Figure 7: Comparison of Improved Fragility Relationships to HAZUS Default Fragility Curves

Figure 7 illustrates the improved fragility curves for upland and lowland soil profiles as well as the HAZUS default damage function for building type S3, high-code, for the extensive damage state. Both upland and lowland profiles are illustrated in Figure 7 and show a lesser level of uncertainty than the HAZUS default fragility. By reducing the level

of uncertainty in the building fragility relationships, better estimates of the building damage for the Central US are obtained.

Bridge Fragilities

As with all other infrastructure included in the HAZUS inventory databases, default fragility relationships are provided for each bridge type identified within the program. Sets of fragility curves are provided for each of 28 bridge types though only 19 of them are applicable to the Central US. Several bridge types are reserved for bridges in California due the stringent seismic provisions and unique configurations used in that portion of the country. Fragility relationships for the bridge types relevant to the Central US are updated in this study with more regionally-appropriate curves. The methodology used to develop the default bridge fragilities is discussed and compared to the methodology employed in the new fragilities used in this study to determine bridge damage. A discussion on new bridge fragility implementation is provided as well.

HAZUS Default Bridge Fragility Relationships

Default bridge fragilities were developed with the Capacity Spectrum Method (CSM) where demand is based on an effective damping formulation. The formulation requires the lesser of the following values:

$$C_d = \frac{2.5 * A}{B_s} \quad \text{or} \quad C_d = \frac{S * A}{T_{eff} * B_L} \quad (8)$$

where A is peak ground acceleration normalized by gravitational acceleration (g), S is soil type, T_{eff} is effective/secant period, B_s is the short period range spectral reduction factor, and B_L is the long period range spectral reduction factor. Both reduction factors are specified as a function of the effective damping ratio of the bridge which is obtained previously as a function of ductility (Basoz and Mander, 1999).

Calculating structural capacity requires normalized base shear of the entire bridge structure, which is obtained from analysis of bridge piers and abutments for cases of lateral loading. Under the transverse loading produced by earthquakes the arching action of the bridge deck between abutments must be considered. The total bridge capacity is then formulated as follows:

$$C_c = C_{cp} + C_d \quad (9)$$

where C_c is base shear capacity, C_{cp} is the base shear capacity of the critical pier, and here C_d is the additional capacity provided by arch action. Note that the magnitude of deck arching is dependent upon number of spans in the bridge. Both concrete arching action and resistance from steel truss action are combined to determine pier capacity which

requires several geometric factors. A strength reduction factor that accounts for cyclic loading is considered, among others.

The capacity of single span bridges is only dependent upon bridge bearings according to Basoz and Mander (1999). Upon considering both transverse and rotational modes of a single span bridge, it was determined that the translational mode governs. Additional formulations are also provided which consider three-dimensional effects such as bridges with strong bearings and weak piers or conversely, weak bearings and strong piers. Using this framework the capacity of a single span bridge equates to twice its pier capacity. Drift limits are greater for bridges with weak bearings and strong piers than for the opposite configuration, primarily based on experimental reinforced concrete tests. Damage functions were developed further to include displacements, allowing for factors such as skew angle.

All validation of the Basoz and Mander (1999) bridge fragility relationships is based on earthquake records from California events, specifically the 1989 Loma Prieta event and the 1994 Northridge event. Ground motions from these events were used and replicate, as closely as possible, the actual damage reported in the California earthquakes. Figure 8 illustrates the comparison between Basoz and Mander (1999) fragility relationships with actual earthquake damage for simply supported, multispan bridges with multiple column bents and non-monolithic abutment type. Though only one example bridge type is included here, other bridge types show similar results. These fragility relationships were reformatted and presented in terms of spectral acceleration.

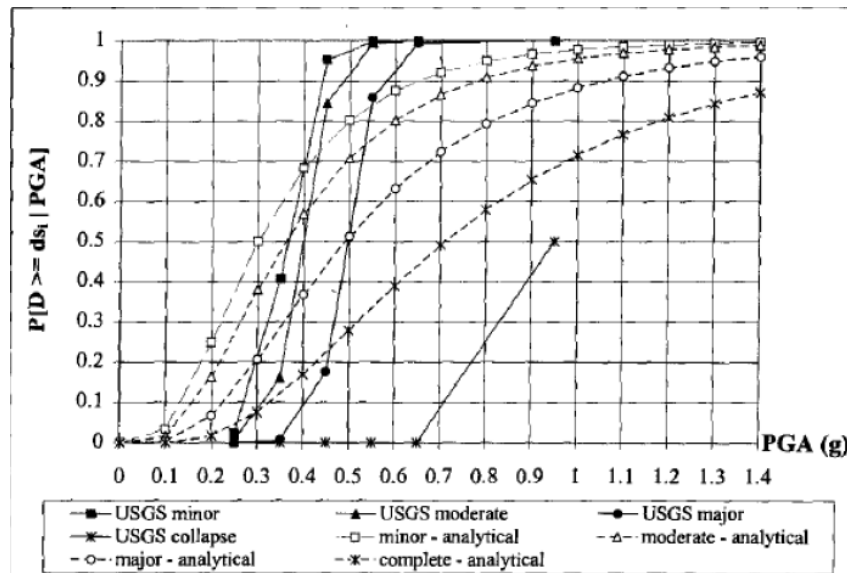


Figure 8: Comparison of Actual Earthquake Damage with Basoz and Mander Fragility Relationships (Basoz and Mander, 1999)

Bridge Fragility Improvements

The bridge fragility relationships used in this study were specifically created for bridges common to the CEUS. Three-dimensional analytical models and non-linear time history analyses were utilized to create a more accurate set of curves for each bridge type investigated. Additionally, the new methodology considers the performance of multiple bridge components unlike the default fragilities. A total of nine bridge types common to the CEUS were developed, only five of which are utilized in this study due to the constraints of the classification scheme inherent in HAZUS.

A total of 96 synthetic ground motions were used to define the demand placed on each bridge. Half of the ground motions were obtained from uniform hazard motions developed for three CEUS cities by Wen and Wu (2001). The other half was developed by Rix and Fernandez-Leon (2004). Regional soil profiles were incorporated in both sets of ground motions. Since synthetic records represent the geometric mean of two orthogonal components each record was used to develop the two orthogonal components required for three-dimensional analysis based on the procedure in Baker and Cornell (2006). Note that vertical components of ground motion were not considered in this case.

Capacity is defined for several bridge components based on both experimental results and expert opinion (Padgett and DesRoches, 2006). Bridge components considered in the fragility development process include columns, fixed bearings, expansion bearings, and both longitudinal and transverse abutments. As with the default fragilities, four damage states are considered: slight, moderate, extensive, and complete. These component limit states were intended to have a physical meaning and are shown in Table 3. Those values denoted with 'N/A' indicate survey responses asserting that considerable damage to those components may not cause long-term bridge closures (Padgett and DesRoches, 2006).

Table 3: Bridge Component Limit States (Nielson and DesRoches, 2007)

Component	Slight		Moderate		Extensive		Complete	
	median	dispersion	median	dispersion	median	dispersion	median	dispersion
Column (m)	1.29	0.59	2.10	0.51	3.52	0.64	5.24	0.65
Steel Fixed Bearing - Long. (mm)	6.00	0.25	20.00	0.25	40.00	0.47	187.00	0.65
Steel Fixed Bearing - Trans. (mm)	6.00	0.25	20.00	0.25	40.00	0.47	186.60	0.65
Steel Rocker Bearing - Long. (mm)	37.40	0.60	104.20	0.55	136.10	0.59	186.60	0.65
Steel Rocker Bearing - Trans. (mm)	6.00	0.25	20.00	0.25	40.00	0.47	187.00	0.65
Elasto Fixed Bearing - Long. (mm)	28.90	0.60	104.20	0.55	136.10	0.59	186.00	0.65
Elasto Fixed Bearing - Trans. (mm)	28.80	0.79	90.90	0.68	142.20	0.73	195.00	0.66
Elasto Expansion Bearing - Long. (mm)	28.90	0.60	104.20	0.55	136.10	0.59	186.60	0.65
Elasto Expansion Bearing - Trans. (mm)	28.80	0.79	90.90	0.68	142.20	0.73	195.00	0.66
Abutment - Passive (mm)	37.00	0.46	146.00	0.46	N/A	N/A	N/A	N/A
Abutment - Active (mm)	9.80	0.70	37.90	0.90	77.20	0.85	N/A	N/A
Abutment - Trans. (mm)	9.80	0.70	37.90	0.90	77.20	0.85	N/A	N/A

Three-dimensional models of each CEUS bridge type are created based on common bridge configurations. Elastic beam-column elements are used to model the bridge superstructure in a lumped centerline method that considered the composite action of both deck and girders. All columns and bent beams are modeled as non-linear beam-column elements with fiber cross-sections. The advantage of this distributed plasticity model is that non-linear hysteretic behavior of the elements is captured. Moreover, non-linear springs are used to model bearings and both longitudinal and transverse abutments.

Finally, pile foundations are modeled with lumped translational and rotational springs at the bases of each column. Figure 9 illustrates the general model scheme for a Multispan Continuous Steel (MSC) Girder Bridge, though models for other bridge types, including concrete and other steel bridges, are presented in the original works by Nielson and DesRoches (2004, 2006a, 2006b, 2007). Once all models were built full non-linear time history analyses were performed for each combination of synthetic ground motion record and bridge type where all components were modeled and maximum demand was recorded.

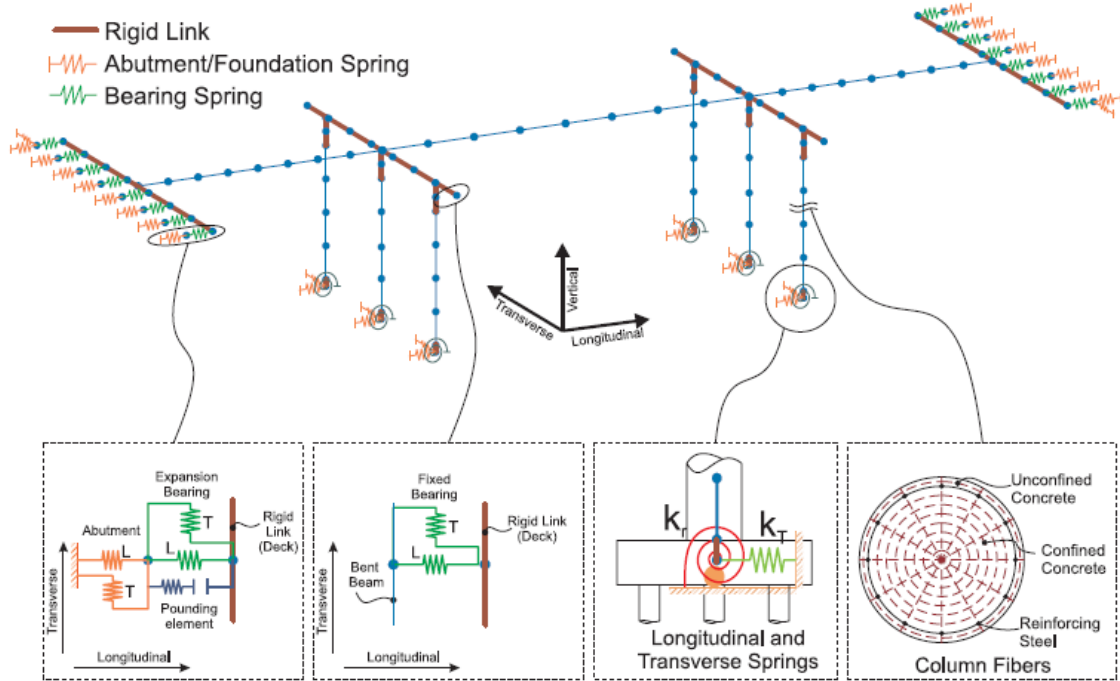


Figure 9: General Model Scheme for 3-D MSC Steel Girder Bridge (Nielson and DesRoches, 2007)

Bridge fragilities are constructed by first examining individual components. Component-level fragility relationships were developed based on component demand and limit states that were discussed previously. Finally, system-level fragilities were created by integrating over all possible failures and joint probabilistic demand models (Nielson and DesRoches, 2006b, 2007). New bridge fragility curves for the various types of CEUS bridges were presented in terms of a median peak ground acceleration (PGA) value and a dispersion value. Actual curves were drawn based on the equation:

$$P[\text{Damage State}_i \text{ or greater} | \text{PGA}] = \Phi \left[\frac{\ln(\text{PGA}) - \ln(\text{med}_i)}{\zeta_i} \right] \quad (10)$$

where med_i and ζ_i represent the i^{th} damage state. Figure 10 illustrates the fragility curves for the three types of Multispan Continuous (MSC) bridges at each of the four damage states included in the HAZUS methodology. Fragility curves were also developed for multispan simply supported and simple span bridges, though the fragility curves are not shown here.

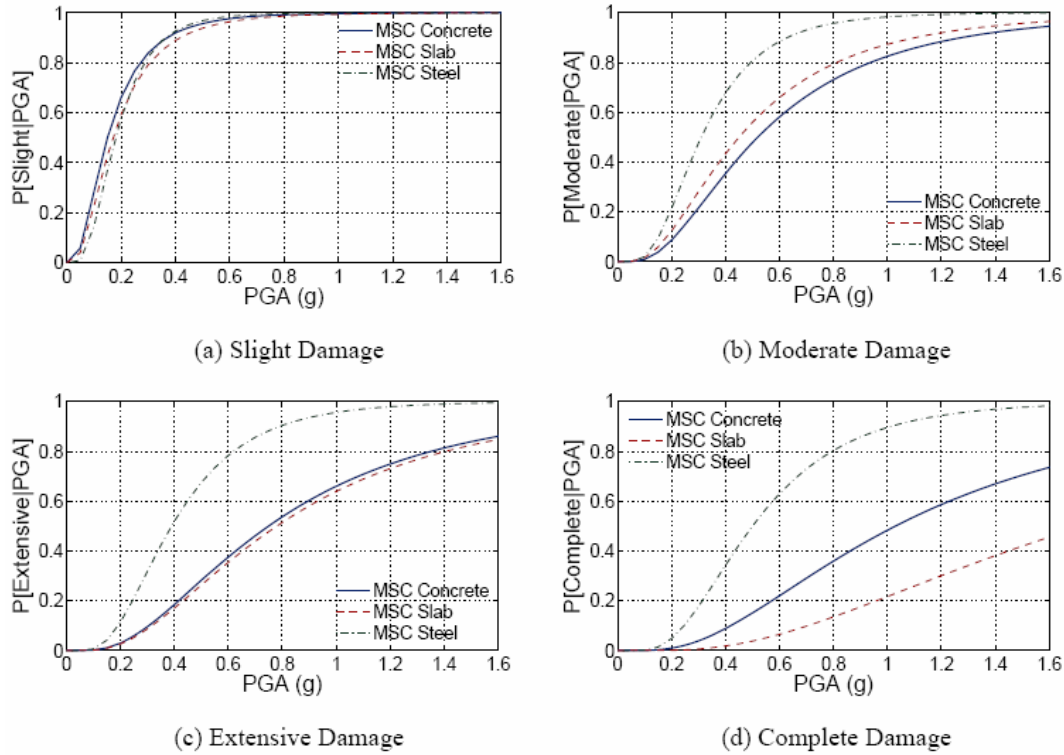


Figure 10: Fragility Curves for MSC Bridge Type (Nielson and DesRoches, 2007)

Only five of the bridge types considered in Nielson and DesRoches (2004, 2006a, 2006b, 2007) are applicable to the bridges included in this study. All bridge types included in the new bridge fragility study are shown in Table 4. Several bridge types considered by Neilson and DesRoches are not compatible with HAZUS bridge types and are not incorporated as a result. Bridge types incompatible with HAZUS include multispans simply supported concrete box girder, multispans simply supported slab, multispans continuous concrete box girder, multispans continuous slab, and single span concrete box girder.

Table 4: CEUS Bridge Types

Reference No.	Bridge Description
Concrete Bridges	
9	Multispan Simply Supported Concrete Box Girder (A,B)
2	Multispan Simply Supported Concrete Girder (A,B)
8	Multispan Simply Supported Slab (A,B)
1	Single Span Concrete Girder (A,B)
7	Multispan Continuous Concrete Box Girder (A,B)
3	Multispan Continuous Concrete Girder (A,B)
6	Multispan Continuous Slab (A,B)
Steel Bridges	
4	Multispan Simply Supported Steel Girder (A,B)
10	Single Span Steel Girder (A,B)
5	Multispan Continuous Steel Girder (A,B)
Miscellaneous Bridges (HAZUS fragilities recommended)	
11	Tunnel/Culvert
12	Truss
13	Other

A = Conventional Design; B = Seismic Design

New CEUS fragilities, similar to HAZUS default fragilities, consider both conventionally and seismically designed bridges. Table 5 illustrates the correlation between HAZUS bridge types and new CEUS bridge types from the aforementioned fragility study. Conventional and seismic bridge types are shown along with the bridge classification number. Several bridge types are applicable to California only and thus are not correlated to any CEUS bridge types. Additionally, three bridge types, HWB1, HWB2, and HWB28, retain the HAZUS default fragility values. These types are not specifically addressed in the CEUS bridge fragility research so the default values are left unchanged. The highway bridge types that appear in Table 5 are replicated in Table 6 along with the fragility median and dispersion values that are implemented in NMSZ earthquake impact assessments discussed in this report. Generally, new fragilities indicate that multispan steel girder bridges are the most vulnerable bridge type and single span bridges are far less vulnerable to seismic activity. Again, the bridge types in gray are those that retain the HAZUS default fragility values since they are not included in the work of Nielson and DesRoches (2004, 2006a, 2006b, 2007) for the CEUS.

Table 5: Correlation Between HAZUS Default Fragilities and New CEUS Fragilities

HAZUS-MH Bridge Classification	HAZUS Bridge Description	Design Level	New Fragility Reference No.	New Fragility Bridge Description
HWB1	Major Bridge w/ length > ~500ft.	Conventional	NONE	N/A
HWB2	Major Bridge w/ length > ~500ft.	Seismic	NONE	N/A
HWB3	Single Span	Conventional	1A	Single Span Concrete Girder
HWB4	Single Span	Seismic	1B	Single Span Concrete Girder
HWB5	Multi-Column Bent, Simple Support, Concrete	Conventional	2A	Multi-Span, Simple Support, Concrete Girder
HWB6	N/A --> CA Bridge ONLY		NONE	N/A
HWB7	Multi-Column Bent, Simple Support, Concrete	Seismic	2B	Multi-Span, Simple Support, Concrete Girder
HWB8	N/A --> CA Bridge ONLY		NONE	N/A
HWB9	N/A --> CA Bridge ONLY		NONE	N/A
HWB10	Continuous Concrete	Conventional	3A	Multi-Span Continuous Concrete Girder
HWB11	Continuous Concrete	Seismic	3B	Multi-Span Continuous Concrete Girder
HWB12	Multi-Column Bent, Simple Support, Steel	Conventional	4A	Multi-Span, Simple Support, Steel Girder
HWB13	N/A --> CA Bridge ONLY		NONE	N/A
HWB14	Multi-Column Bent, Simple Support, Steel	Seismic	4B	Multi-Span, Simple Support, Steel Girder
HWB15	Continuous Steel	Conventional	5A	Multi-Span Continuous Steel Girder
HWB16	Continuous Steel	Seismic	5B	Multi-Span Continuous Steel Girder
HWB17	Multi-Column Bent, Simple Support, Prestressed Concrete	Conventional	2A	Multi-Span, Simple Support, Concrete Girder
HWB18	N/A --> CA Bridge ONLY		NONE	N/A
HWB19	Multi-Column Bent, Simple Support, Prestressed Concrete	Seismic	2B	Multi-Span, Simple Support, Concrete Girder
HWB20	N/A --> CA Bridge ONLY		NONE	N/A
HWB21	N/A --> CA Bridge ONLY		NONE	N/A
HWB22	Continuous Concrete	Conventional	3A	Multi-Span Continuous Concrete Girder
HWB23	Continuous Concrete	Seismic	3B	Multi-Span Continuous Concrete Girder
HWB24	Multi-Column Bent, Simple Support, Steel	Conventional	4A	Multi-Span, Simple Support, Steel Girder
HWB25	N/A --> CA Bridge ONLY		NONE	N/A
HWB26	Continuous Steel	Conventional	5A	Multi-Span Continuous Steel Girder
HWB27	N/A --> CA Bridge ONLY		NONE	N/A
HWB28	All Other Bridges	N/A	NONE	N/A

NOTE: Rows appearing in gray indicate bridge types not applicable in the Central US, thus no bridge types corresponding to new bridge fragilities are assigned. This applies to Table 5 and Table 6.

Table 6: New CEUS Bridge Fragility Values

HAZUS Bridge Class	Slight Median	Slight Beta	Moderate Median	Moderate Beta	Extensive Median	Extensive Beta	Complete Median	Complete Beta
HWB1	0.4	0.6	0.5	0.6	0.7	0.6	0.9	0.6
HWB2	0.6	0.6	0.9	0.6	1.1	0.6	1.7	0.6
HWB3	0.35	0.9	1.33	0.9	1.83	0.9	2.5	0.9
HWB4	0.35	0.9	1.33	0.9	1.83	0.9	2.5	0.9
HWB5	0.2	0.7	0.63	0.7	0.91	0.7	1.28	0.7
HWB6	0.3	0.6	0.5	0.6	0.6	0.6	0.9	0.6
HWB7	0.4	0.7	1.45	0.7	2.16	0.7	3.07	0.7
HWB8	0.35	0.6	0.45	0.6	0.55	0.6	0.8	0.6
HWB9	0.6	0.6	0.9	0.6	1.3	0.6	1.6	0.6
HWB10	0.16	0.7	0.53	0.7	0.75	0.7	1.01	0.7
HWB11	0.24	0.7	0.53	0.7	0.75	0.7	1.01	0.7
HWB12	0.24	0.5	0.45	0.5	0.58	0.5	0.85	0.5
HWB13	0.3	0.6	0.5	0.6	0.6	0.6	0.9	0.6
HWB14	0.48	0.5	1.04	0.5	1.39	0.5	2.04	0.5
HWB15	0.19	0.5	0.32	0.5	0.41	0.5	0.51	0.5
HWB16	0.23	0.5	0.38	0.5	0.62	0.5	0.71	0.5
HWB17	0.2	0.7	0.63	0.7	0.91	0.7	1.28	0.7
HWB18	0.3	0.6	0.5	0.6	0.6	0.6	0.9	0.6
HWB19	0.4	0.7	1.45	0.7	2.16	0.7	3.07	0.7
HWB20	0.35	0.6	0.45	0.6	0.55	0.6	0.8	0.6
HWB21	0.6	0.6	0.9	0.6	1.3	0.6	1.6	0.6
HWB22	0.16	0.7	0.53	0.7	0.75	0.7	1.01	0.7
HWB23	0.24	0.7	0.53	0.7	0.75	0.7	1.01	0.7
HWB24	0.24	0.5	0.45	0.5	0.58	0.5	0.85	0.5
HWB25	0.6	0.6	0.8	0.6	10	0.6	10	0.6
HWB26	0.19	0.5	0.32	0.5	0.41	0.5	0.51	0.5
HWB27	0.75	0.6	0.75	0.6	0.75	0.6	1.1	0.6
HWB28	0.8	0.6	1.0	0.6	1.2	0.6	1.7	0.6

References

- Applied Technology Council [ATC] (1996). Seismic Evaluation and Retrofit of Concrete Buildings. Report No. ATC-40. Applied Technology Council. Redwood City, CA.
- Baker, J.W. and C.A. Cornell (2006). Correlation of Response Spectral Values for Multicomponent Ground Motions. *Bulletin of the Seismological Society of America*. v 96, 215-227.
- Basoz, Nesrin, and John Mander (1999). *Enhancement of the Highway Transportation Lifeline Module in HAZUS*. Report No. Draft 7. National Institute of Building Sciences. Washington, D.C.
- Federal Emergency Management Agency [FEMA] (2008). HAZUS-MH MR3 Technical Manual. Washington, D.C. FEMA.
- Fernandez, A (2007). “Numerical Simulation of Earthquake Ground Motions in Upper Mississippi Embayment.” School of Civil and Environmental Engineering, Georgia Institute of Technology, Atlanta, Georgia.
- Gencturk, B. (2007). Improved Fragility Relationships for Populations of Buildings Based on Inelastic Response. MS Thesis, Department of Civil and Environmental Engineering, University of Illinois at Urbana-Champaign, Urbana, IL.
- Gencturk, B., Elnashai, A. S., and Song, J. (2008). Improved Fragility Relationships for Populations of Buildings Based on Inelastic Response. *The 14th World Conference on Earthquake Engineering*. Beijing, China. October 12-17.
- Gencturk, B., Elnashai, A. S. (2008). Development and Application of an Advanced Capacity Spectrum Method. *Engineering Structures*. v 30, 3345-3354.
- Mid-America Earthquake Center [MAEC] (2007). “Comprehensive Seismic Loss Modeling for the State of Illinois” Report: Appendix III, Fragility Functions. June.
- Nielson, B. G. and R. DesRoches (2004). Improved Methodology for Generation of Analytical Fragility Curves for Highway Bridges, *9th ASCE Specialty Conference on Probabilistic Mechanics and Structural Reliability*, ASCE, July. Albuquerque, NM.
- Nielson, B. and R. DesRoches (2006a). Effect of using PGA versus Sa on the uncertainty in probabilistic seismic demand models of highway bridges. *8th National Conference on Earthquake Engineering*. Earthquake Engineering Research Institute, April 18-22. San Francisco.

Nielson, B. G. and R. DesRoches (2006b). Influence of modeling assumptions on the seismic response of multi-span simply supported steel girder bridges in moderate seismic zones. *Engineering Structures*. v28, n 8, 1083-1092.

Nielson, B.G. and R. DesRoches (2007). Analytical Seismic Fragility Curves for Typical Bridges in the Central and Southeastern United States. *Earthquake Spectra*. v 23, n 3. 615-623.

Padgett, J.E. and R DesRcohes (2006). Bridge Damage-Functionality Using Expert Opinion Survey. *8th National Conference on Earthquake Engineering*. Earthquake Engineering Research Institute. April 18-21. San Francisco, CA.

Rix, G.J. and J.A. Fernandez-Leon (2004). Synthetic Ground Motions for Memphis, TN. Retrieved July 2 2004. <http://www.ce.gatech.edu/research/mae_ground_motion>

Wen, Y.K, B.E. Ellingwood and J. Bracci (2003). "Vulnerability Function Derivation for Consequence-Based Engineering." Mid-America Earthquake Center Report.

Wen, Y.K. and C.L. Wu (2001). Uniform Hazard Ground Motions for Mid-America Cities. *Earthquake Spectra*. v 17, 359-384.

Appendix 4 – Threshold Values

Introduction

A series of powerful earthquakes in North America occurred on the New Madrid Fault at the beginning of the 19th century. The seismic events occurred over a three month period, between Dec. 16, 1811, and February 7, 1812. The estimated magnitudes of the major earthquakes were nearly 8. Thousands of additional earthquakes of lesser magnitudes occurred over that three month period (MNDR, 2008).

Moreover, more than 4,000 earthquakes have been reported in the New Madrid Seismic Zone (NMSZ) since 1974. Figure 1 shows the distribution of epicenters throughout the region (USGS). More recently an earthquake of magnitude 5.4 occurred on April 18, 2008, in southern Illinois (blue dot in Figure 2 shows its epicenter). Though this event is associated with the Wabash Valley Seismic Zone, it provides further evidence of continuous, moderate seismic activity in the Central US.

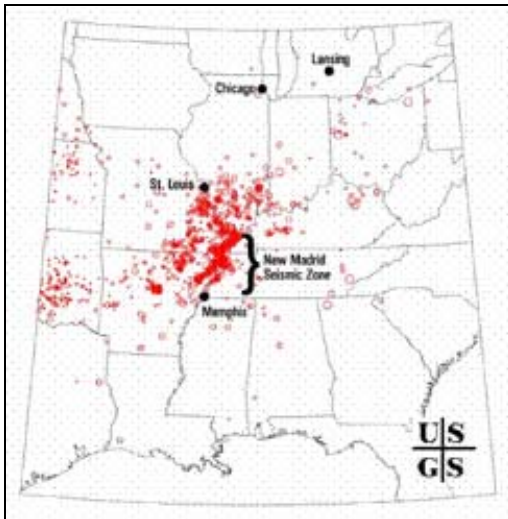


Figure 1: Earthquakes in the NMSZ since 1974

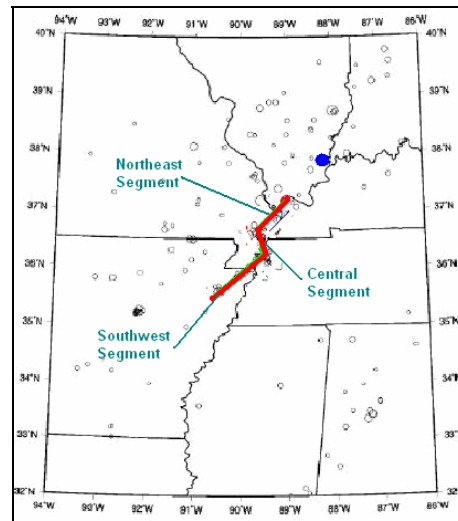


Figure 2: NMSZ Fault Segments



Figure 3: Rivers in the Central US



In the Central US, the Mississippi River divides the region into two parts, namely the eastern and western parts. Additionally the Ohio, Missouri, Illinois, and Arkansas Rivers divide the geography. There are more than one hundred long-span bridges crossing these rivers. Highway, as well as railway, connections between states are provided by these structures. Incidentally, some of these bridges, located on the Mississippi and Ohio rivers, cross near the Central and Northeast segments of the New Madrid Fault. Major bridges are identified in seven of the eight states included in this study: Arkansas, Illinois, Indiana, Kentucky, Mississippi, Missouri, and Tennessee. No major river crossings are identified in Alabama.

It is likely that an earthquake similar to the NMSZ events of 1811 and 1812 would cause damage to both highway and railway transportation infrastructure as well as dams, levees, and hazardous materials facilities. Such an event would likely interrupt transportation services and cause substantial economic loss (Hildenbrand et al., 1996; Elnashai et al., 2008). Reasonable approximate threshold values, which are primarily the median peak ground acceleration (PGA) values of fragility relationships, are established for the damage states described in HAZUS (slight, moderate, extensive, and complete) and are designed to be utilized in the rapid assessment of the damage to selected infrastructure systems in the Central US.

Problem Definition

This report presents an approximate procedure for the rapid evaluation of seismic vulnerability of selected major infrastructure components including major river crossings, dams, levees, and storage tanks for hazardous materials located within the eight-state study region in the Central US. It is evident that comprehensive damage assessment analyses of these unique and complex structural systems are rather complicated, tedious and time-consuming. On the other hand, seismic vulnerability of these infrastructure components are needed to evaluate damage.

The methodology adopted for deriving approximate damage measures is based on engineering judgement. Previous research which focused on the development of bridge fragility curves and damage evaluation of the infrastructure systems subjected to several earthquakes have been reviewed thoroughly. The purpose of such an extensive literature review was not only to reduce the uncertainties in the final damage measures but also to provide a more realistic vulnerability assessment. Due to time constraints and the large inventories of unique infrastructure, analytically- or experimentally-based fragility relationships are unrealistic, and instead ‘threshold values’ are employed to determine damage. A ‘threshold value’ is a limiting ground shaking value, above which damage is considered ‘likely’, and below which is considered ‘unlikely’. Threshold values are approximate measures and are designed for rapid assessment, though further investigation and development of full fragility relationships is recommended. A comparison of a threshold value and a conventional fragility relationship is illustrated in Figure 5.

The methodology utilized to generate the approximate damage measures is summarized as follows:

- PGA is the ground shaking parameter used for the generation of the approximate threshold values since it is readily available from earthquake records

- Reasonable approximate threshold values have been selected from the developed fragility curves using engineering judgment for damage states as described in HAZUS, namely slight, moderate, extensive, and complete
- The median PGA values of the fragility curves have been selected as approximate threshold values (see Figure 4)
- Fragility curves for infrastructure exemplifying the identified infrastructure element groups have been taken into consideration as much as possible to minimize the uncertainties and provide a more realistic vulnerability assessment
- When fragility curves were unavailable, previous research containing damage data collected via field-survey after earthquakes has been taken into consideration
- Reasonable lower bounds were kept as the threshold values for each infrastructure category
- Finally, four ranges of approximate threshold values have been established for each infrastructure type and damage state to be utilized in rapid assessment of the damage to the selected infrastructure components

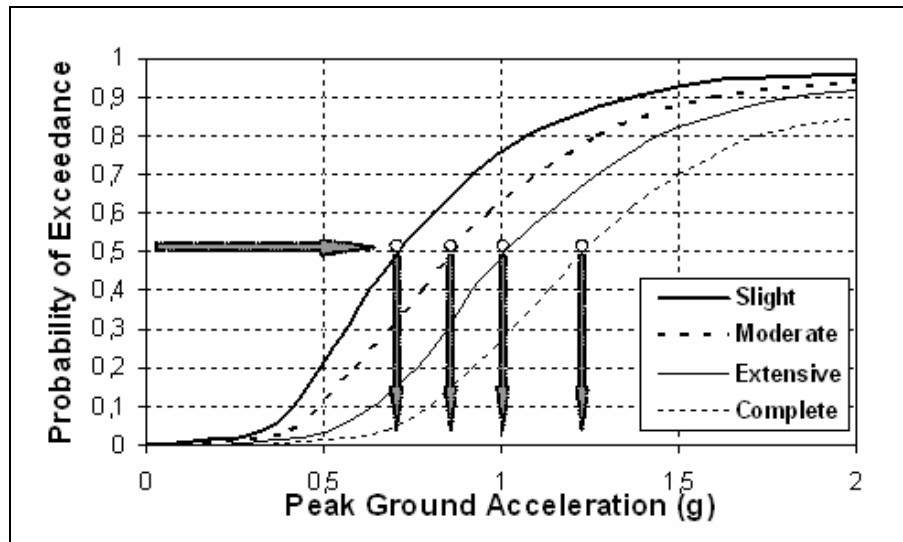


Figure 4: Generation of Approximate Threshold Values from Fragility Curves

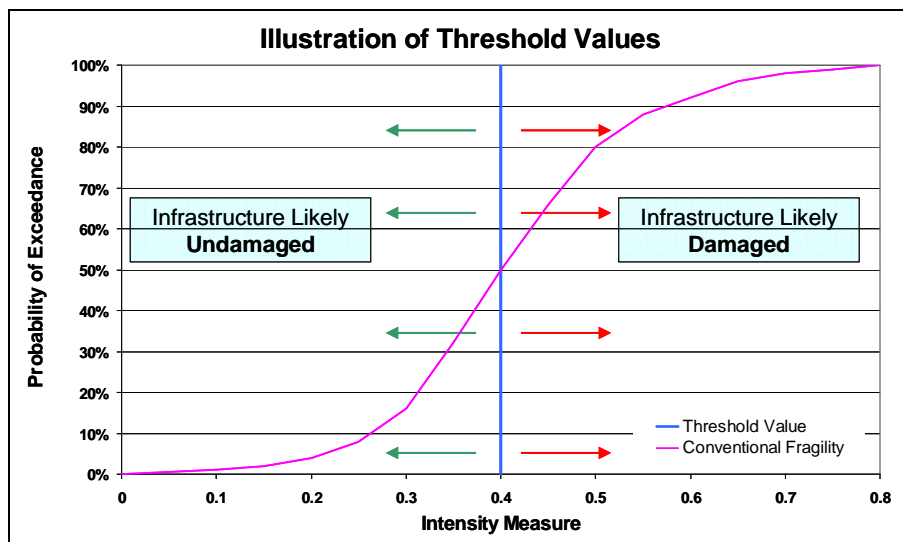


Figure 5: Comparison of Threshold Value and Typical Fragility Relationship

Threshold Values for Bridges

Survey of Major River Crossings

The Mississippi, Ohio, Missouri, Illinois, and Arkansas Rivers are the only major rivers considered in the eight-state study region. There are many different long-span bridges crossing these rivers. The bridge approaches for the major river crossing are not considered in this study. The bridges located on these five rivers included in this investigation are presented in Table 1. Some of the bridges on the canals, waterways, and rivers are vertical lift or side- or center-mounted swing bridges. Vertical lift bridges lift without tilting to provide sufficient clearance over the navigation channel for marine traffic.

More detailed information about each of these complex river crossings is provided in the “Additional Bridge Data” section at the conclusion of this appendix.

Table 1: Bridge Inventory

Bridge	Location
1 Caruthersville Bridge	Caruthersville, Missouri and Dyersburg, Tennessee
2 Harahan Bridge	West Memphis, Arkansas and Memphis, Tennessee
3 Lyons-Fulton Bridge	Clinton, Iowa and Fulton, Illinois
4 Quincy Bayview Bridge	West Quincy, Missouri Quincy, Illinois
5 Cairo Mississippi River Bridge	Bird's Point, Missouri and Cairo, Illinois
6 Cairo I-57 Bridge	Charleston, Missouri and Cairo, Illinois
7 Thebes Bridge	Illmo, Missouri and Thebes, Illinois
8 Bill Emerson Memorial Bridge	Cape Girardeau, Missouri and East Cape Girardeau, Illinois
9 Chester Bridge	Perryville, Missouri and Chester, Illinois
10 Crescent City Connection	New Orleans, Louisiana
11 Hernando de Soto Bridge	West Memphis, Arkansas and Memphis, Tennessee
12 Frisco Bridge	West Memphis, Arkansas and Memphis, Tennessee
13 Memphis & Arkansas Bridge	West Memphis, Arkansas and Memphis, Tennessee
14 Savanna-Sabula Bridge	Savanna, Illinois and Sabula, Iowa, River Mile 537.8
15 Sabula Rail Bridge	Sabula, Iowa and Savanna, Illinois
16 Huey P. Long Bridge	Jefferson Parish, Louisiana
17 New Chain Of Rocks Bridge	River Mile 190.8
18 Chain of Rocks Bridge	St. Louis, Missouri
19 Clark Bridge	West Alton, Missouri and Alton, Illinois
20 Martin Luther King Bridge	St. Louis, Missouri and East St. Louis, Illinois
21 Eads Bridge	St. Louis, Missouri and East St. Louis, Illinois
22 McKinley Bridge	St. Louis, Missouri and Venice, Illinois
23 Poplar Street Bridge	St. Louis, Missouri and East St. Louis, Illinois
24 MacArthur Bridge	St. Louis, Missouri and East St. Louis, Illinois
25 Gateway Bridge	Clinton, Iowa and Fulton, Illinois
26 Merchants Bridge	St. Louis, MO
27 Jefferson Barracks Bridge	St. Louis, Missouri and Columbia, Illinois
28 Fred Schwengel Memorial Bridge	Le Claire, Iowa and Rapids City, Illinois
29 I-74 Bridge	Bettendorf, Iowa and Moline, Illinois
30 Rock Island Government Bridge	Davenport, Iowa and Rock Island, Illinois
31 Rock Island Centennial Bridge	Davenport, Iowa and Rock Island, Illinois

	Bridge	Location
32	Helena Bridge	Helena-West Helena, Arkansas and Lula, Mississippi
33	I-280 Bridge	Davenport, Iowa and Rock Island, Illinois
34	Dubuque-Wisconsin Bridge	Dubuque, Iowa, with Grant County, Wisconsin
35	Julien Dubuque Bridge	Dubuque, Iowa, and East Dubuque, Illinois
36	Old Vicksburg Bridge	Delta, Louisiana and Vicksburg, Mississippi
37	Vicksburg Bridge	Delta, Louisiana and Vicksburg, Mississippi
38	Sunshine Bridge	Sorrento, Louisiana and Donaldsonville, Louisiana
39	Norbert F. Beckey Bridge	Muscatine, Iowa and Illinois
40	Louisiana Rail Bridge	Louisiana, Missouri and Illinois
41	Champ Clark Bridge	Louisiana, Missouri and Illinois
42	Burlington Rail Bridge	Burlington, Iowa and Gulf Port, Illinois
43	Great River Bridge	Burlington, Iowa and Gulf Port, Illinois
44	Greenville Bridge	Lake Village, Arkansas and Greenville, Mississippi
45	Benjamin G. Humphreys Bridge	Lake Village, Arkansas and Greenville, Mississippi
46	Horace Wilkinson Bridge	Baton Rouge, Louisiana
47	Black Hawk Bridge	Lansing, Iowa and Crawford County, Wisconsin, River Mile 663.4
48	Fort Madison Toll Bridge	Fort Madison, Iowa and Niota, Illinois
49	John James Audubon Bridge	Pointe Coupee Parish, Louisiana, West Feliciana Parish, Louisiana
50	Mark Twain Memorial Bridge	Hannibal, Missouri
51	Wabash Bridge (w/ vertical lift)	Hannibal, Missouri and Illinois
52	Keokuk Rail Bridge	Keokuk, Iowa and Hamilton, Illinois
53	Keokuk-Hamilton Bridge	Keokuk, Iowa and Hamilton, Illinois
54	Natchez-Vidalia Bridge	Vidalia, Louisiana and Natchez, Mississippi
55	Quincy Memorial Bridge	West Quincy, Missouri and Quincy, Illinois
56	Bayview Bridge	West Quincy, Missouri Quincy, Illinois
57	Quincy Rail Bridge	West Quincy, Missouri and Quincy, Illinois
58	Moline-Arsenal Bridge	River Mile 485.7
59	Crescent Railroad Bridge	River Mile 481.4
60	Double Chain Bridge	St. Louis, MO
61	Single Chain Bridge	St. Louis, MO
62	Grand Tower Pipeline Bridge	Grand Tower, Illinois
63	A. W. Willis, Jr. Bridge	River Mile 737.1
64	Mud Island Monorail/ Memphis Suspension Railway	Memphis, Tennessee
65	Cairo Ohio River Bridge	Wickliffe, Kentucky and Cairo, Illinois
66	Cairo Rail Bridge	Wickliffe, Kentucky and Cairo, Illinois
67	Metropolis Bridge	Metropolis, Illinois
68	Interstate 24 Bridge	Metropolis, Illinois
69	Irvin S. Cobb Bridge	Paducah, KY and Brookport, IL
70	Shawneetown Bridge	Old Shawneetown, Illinois
71	Henderson Bridge	Henderson, Kentucky
72	Bi-State Vietnam Gold Star Bridges/ Twin Bridges	Henderson, Kentucky and Evansville, Indiana
73	Glover H. Cary Bridge	Owensboro, Kentucky and Spencer County, Indiana
74	William H. Natcher Bridge	Owensboro, Kentucky to Rockport, Indiana
75	Bob Cummings - Lincoln Trail Bridge	Indiana-Kentucky State Line
76	Matthew E. Welsh Bridge	Brandenburg, Kentucky and Mauckport, Indiana
77	Lewis Bridge	St. Louis County and St. Charles County, Missouri
78	Bellefontaine Bridge	St. Louis County and St. Charles County, Missouri

	Bridge	Location
79	Discovery Bridge	St. Louis County and St. Charles County, Missouri
80	Wabash Bridge	Bridgeton and Saint Charles, MO
81	Blanchette Memorial Bridge	St. Louis County and St. Charles County, Missouri
82	Veterans Memorial Bridge	St. Louis County and St. Charles County, Missouri
83	Daniel Boone Bridge	St. Louis County and St. Charles County, Missouri
84	Washington Bridge	Washington, Missouri
85	Christopher S. Bond Bridge	Hermann, MO
86	Jefferson City Bridge	Jefferson City, Missouri
87	Rocheport Interstate 70 Bridge	Cooper County and Boone County , MO
88	Boonslick Bridge	Boonville, Missouri
89	Glasgow Bridge	Glasgow, Missouri
90	Glasgow Railroad Bridge	Glasgow, Missouri
91	Hardin Bridge	Hardin, IL
92	Florence Bridge	Florence, IL
93	Valley City Eagle Bridges	Valley City, IL
94	Meredosia Bridge	Meredosia, IL
95	Beardstown Bridge	Beardstown, IL
96	Scott W. Lucas Bridge	Havana, IL
97	Pekin Bridge	Pekin, IL
98	Shade-Lohmann Bridge	Bartonville, IL and Creve Coeur, IL
99	Cedar Street Bridge	Peoria, Illinois and East Peoria, Illinois
100	Bob Michel Bridge	Peoria, Illinois and East Peoria, Illinois
101	Murray Baker Bridge	Peoria, Illinois and East Peoria, Illinois
102	McClugage Bridge	Peoria, IL
103	Lacon Bridge	Sparland and Lacon, IL
104	Henry Bridge	Henry, IL
105	Gudmund "Sonny" Jessen Bridge	Hennepin, IL
106	Spring Valley Bridge	Spring Valley, IL
107	Peru Bridge	Peru, IL
108	Abraham Lincoln Memorial Bridge	La Salle, Illinois and Oglesby, Illinois
109	Utica Bridge	Utica, IL
110	Ottawa Bridge	Ottawa, IL
111	Seneca Bridge	Seneca, IL
112	Morris Bridge	Morris, IL
113	Pendleton Bridge	Arkansas Post, Arkansas
114	Lawrence Blackwell Bridge	Pine Bluff, Arkansas
115	Rob Roy Bridge	Pine Bluff, Arkansas
116	79-B Bridge	Pine Bluff, Arkansas
117	Pipeline bridge	Redfield, Arkansas
118	I-440 Bridge	Little Rock, Arkansas
119	Rock Island Bridge	Little Rock, Arkansas
120	I-30 Bridge	Little Rock, Arkansas
121	Junction Bridge	Little Rock, Arkansas
122	Main Street Bridge	Little Rock, Arkansas
123	Broadway Bridge	Little Rock, Arkansas
124	Union Pacific Rail Bridge	Little Rock, Arkansas
125	Big Dam Bridge	Little Rock, Arkansas
126	I-430 Bridge	Little Rock, Arkansas
127	Highway 9 Bridge	Morrilton, Arkansas

Classification of Major River Crossings

Bridges are classified based on material, age, length, soil conditions, among others. In this study, however, classification of the Major River Crossings (MRCs) is based on construction type and construction material only. Six types of MRCs have been identified and grouped by common features leading to the following classifications:

- 1) Cable Stayed/Suspension Bridges (CSS)
- 2) Multispan Continuous Steel Truss Bridges (MCST)
- 3) Multispan Simply Supported Steel Truss Bridges (MSSST)
- 4) Multispan Continuous Steel Girder Bridges (MCSG)
- 5) Multispan Simply Supported Steel Girder Bridges (MSSSG)
- 6) Multispan Simply Supported Concrete Girder Bridges (MSSCG)

Based on these categories, the majority of the bridges fall into the ‘Multispan Simply Supported Steel Truss’ or ‘Multispan Continuous Steel Truss’ groups. These two bridge categories comprise nearly 75% of the total MRC inventory considered in this study. It is relevant to note that this study does not contain seismic response assessments or evaluations of damage to bridge approaches. The “Additional Bridge Data” section at the conclusion of this appendix contains information on each bridges accompanied by images of each.

Cable Stayed & Suspension Bridges

Cable stayed bridges and suspension bridges constitute 9% of the total bridge inventory investigated in this study. Figure 6 shows two examples of this type of MRC.



Figure 6: Quincy Bayview Bridge, 1987 (left) and I-74 Bridge, 1935 & 1959 (right)

Cable stayed bridges and suspension bridges included in the inventory are listed in Table 2.

Table 2: Cable Stayed & Suspension Bridges

Bridge	
4	Quincy Bayview Bridge
8	Bill Emerson Memorial Bridge
19	Clark Bridge
25	Gateway Bridge
29	I-74 Bridge
43	Great River Bridge
44	Greenville Bridge
49	John James Audubon Bridge
56	Bayview Bridge
62	Grand Tower Pipeline Bridge
74	William H. Natcher Bridge
117	Pipeline bridge

Multispan Continuous Steel Truss Bridges

The majority of the MRCs investigated are steel truss bridges. ‘Multispan Continuous Steel Truss Bridges’ comprise 42% of the total bridge inventory. Figure 7 shows two examples of this type of MRC. Multispan continuous steel truss bridges examined in this study are listed in Table 3.



Figure 7: Savanna-Sabula Bridge, 1932 (left) and Crescent City Connection Bridge, 1988 (right)

Table 3: Multispan Continuous Steel Truss Bridges

Bridge	
1	Caruthersville Bridge
2	Harahan Bridge
3	Lyons-Fulton Bridge
5	Cairo Mississippi River Bridge
6	Cairo I-57 Bridge
7	Thebes Bridge
9	Chester Bridge
10	Crescent City Connection
11	Hernando de Soto Bridge
12	Frisco Bridge
13	Memphis & Arkansas Bridge
14	Savanna-Sabula Bridge
15	Sabula Rail Bridge
16	Huey P. Long Bridge
17	New Chain of Rocks Bridge
18	Chain of Rocks Bridge
20	Martin Luther King Bridge
32	Helena Bridge

35	Julien Dubuque Bridge
36	Old Vicksburg Bridge
37	Vicksburg Bridge
38	Sunshine Bridge
45	Benjamin G. Humphreys Bridge
46	Horace Wilkinson Bridge
47	Black Hawk Bridge
50	Mark Twain Memorial Bridge
54	Natchez-Vidalia Bridge
55	Quincy [Soldier's] Memorial Bridge
60	Double Chain Bridge
61	Single Chain Bridge
64	Mud Island Monorail/ Memphis Suspension Railway
65	Cairo Ohio River Bridge
70	Shawneetown Bridge
72	Bi-State Vietnam Gold Star Bridges/ Twin Bridges
73	Glover H. Cary Bridge
75	Bob Cummings - Lincoln Trail Bridge
80	Wabash Bridge
81	Blanchette Memorial Bridge
82	Veterans Memorial Bridge
83	Daniel Boone Bridge
84	Washington Bridge
85	Christopher S. Bond Bridge
86	Jefferson City Bridge
87	Rocheport Interstate 70 Bridge
94	Meredosia Bridge
96	Scott W. Lucas Bridge
98	Shade-Lohmann Bridge
99	Cedar Street Bridge
101	Murray Baker Bridge
102	McClugage Bridge
103	Lacon Bridge
107	Peru Bridge
109	Utica Bridge

Multispan Simply Supported Steel Truss Bridges

‘Multispan Simply Supported Steel Truss Bridges’ constitute 31% of the total bridge inventory investigated in this study. Two examples of this type of MRC are shown in Figure 8. Multispan simply supported steel truss bridges are listed in Table 4.



Figure 8: Metropolis Bridge, 1917 (left) and Merchants Bridge, 1889 (right)

Table 4: Multispan Simply Supported Steel Truss Bridges

Bridge	
21	Eads Bridge
22	McKinley Bridge
24	MacArthur Bridge
26	Merchants Bridge
30	Rock Island Government Bridge
31	Rock Island Centennial Bridge
33	I-280 Bridge
34	Dubuque-Wisconsin Bridge
39	Norbert F. Beckey Bridge
40	Louisiana Rail Bridge
41	Champ Clark Bridge
42	Burlington Rail Bridge
48	Fort Madison Toll Bridge
51	Wabash Bridge
52	Keokuk Rail Bridge
57	Quincy Rail Bridge
59	Crescent Railroad Bridge
66	Cairo Rail Bridge
67	Metropolis Bridge
69	Irvin S. Cobb Bridge
71	Henderson Bridge
76	Matthew E. Welsh Bridge
78	Bellefontaine Bridge
79	Discovery Bridge
89	Glasgow Bridge
90	Glasgow Railroad Bridge
91	Hardin Bridge
92	Florence Bridge
95	Beardstown Bridge
104	Henry Bridge
106	Spring Valley Bridge
108	Abraham Lincoln Memorial Bridge
110	Ottawa Bridge
111	Seneca Bridge
115	Rob Roy Bridge
119	Rock Island Bridge
121	Junction Bridge
124	Union Pacific Rail Bridge
127	Highway 9 Bridge

Multispan Continuous Steel Girder Bridges

‘Multispan Continuous Steel Girder Bridges’ constitute only 6% of the total bridge inventory. Figure 9 shows two examples of this type of MRC. Multispan continuous steel girder bridges are listed in Table 5.



Figure 9: Lewis Bridge, 1979 (left) and Moline-Arsenal Bridge, 1982 (right)

Table 5: Multispan Continuous Steel Girder Bridges

Bridge	
53	Keokuk-Hamilton Bridge
58	Moline-Arsenal Bridge
68	Interstate 24 Bridge
77	Lewis Bridge
97	Pekin Bridge
100	Bob Michel Bridge
113	Pendleton Bridge
120	I-30 Bridge
126	I-430 Bridge

Multispan Simply Supported Steel Girder Bridges

‘Multispan Simply Supported Steel Girder Bridges’ constitute only 9% of the total bridge inventory. Figure 10 shows two examples of this type of MRC. Multispan simply supported steel girder bridges are listed in Table 6.



Figure 10: Poplar Street Bridge, 1967 (left) and Morris Bridge, 2002 (right)

Table 6: Multispan Simply Supported Steel Girder Bridges

Bridge	
23	Poplar Street Bridge
27	Jefferson Barracks Bridge
28	Fred Schwengel Memorial Bridge
63	A. W. Willis, Jr. Bridge
88	Boonslick Bridge
105	Gudmund "Sonny" Jessen Bridge
112	Morris Bridge
118	I-440 Bridge
123	Broadway Bridge
125	Big Dam Bridge

Multispan Simply Supported Concrete Girder Bridges

‘Multispan Simply Supported Concrete Girder Bridges’ constitute only 3%, or 4 bridges, of the 127 long-span bridges investigated in this study. Figure 11 shows an example of this type of MRC. Multispan Simply Supported Concrete Girder Bridges are listed in Table 7.



Figure 11: Valley City Eagle Bridges, 1988

Table 7: Multispan Simply Supported Concrete Girder Bridges

Bridge	
93	Valley City Eagle Bridges
114	Lawrence Blackwell Bridge
116	79-B Bridge
122	Main Street Bridge

Survey of Published Works

Previous studies performed by several authors on topics related to aspects of this study have been summarized. The majority of previous research focused on the development of bridge fragility curves. The bridge types considered in the previous studies are as follows: Multispan Continuous Concrete Girder Bridges (MCCG), Multispan Continuous Steel Girder Bridges (MCSG), Multispan Continuous Slab Bridges (MCS), Multispan Simply Supported Concrete Girder Bridges (MSSCG), Multispan Simply Supported Concrete Box Bridges (MSSCB), Multispan Simply Supported Slab Bridges (MSSS), Multispan Simply Supported Steel Girder Bridges (MSSSG), Single Span Concrete Girder Bridges (SSCG), and Multispan Prestressed-deck Bridges (MPD).

In one particular study, Nielsen and DesRoshes (2007) have developed seismic fragility curves for nine classes of bridges located in the Central and Southeastern US. Three dimensional models and nonlinear time-history analyses were used. The authors emphasized that multispan steel girder bridges were most vulnerable of all the bridge classes considered. Additionally, single-span bridges tended to be the least vulnerable. A comparison of the proposed fragility curves with those currently found in HAZUS (FEMA, 2008) revealed that there is strong agreement in the multispan simply supported steel girder bridge class. However, for other simply supported bridge classes (concrete girder, slab), the proposed fragility curves suggest a lower vulnerability level than those presented in HAZUS.

The span lengths of eight representative bridge configurations of the ‘Multispan Continuous Steel Girder’ bridges range between 43.95 feet (13.4m) and 133.82 feet (40.8m). Based on the fragility relationships, the median values suggested by the authors for several bridge classes are presented in Table 8.

Table 8: Threshold Values Suggested for Several Bridge Types

Bridge Type	Slight	Moderate	Extensive	Complete
MCCG	0.15	0.52	0.75	1.03
MCSG	0.18	0.31	0.39	0.50
MCS	0.17	0.45	0.78	1.73
MSSCG	0.20	0.57	0.83	1.17
MSSCB	0.21	0.65	1.19	2.92
MSSS	0.18	0.52	0.94	1.92
MSSSG	0.24	0.44	0.56	0.82
SSCG 1	0.41	1.84	2.62	3.64
SSCG 2	0.63	1.14	1.52	2.49

In a study by Elnashai et al. (2004), vulnerability functions for reinforced concrete bridges were derived analytically. Deformation-based limit states were employed. The analytically-derived vulnerability functions were then compared to a data set comprised of observational damage data from the Northridge (California, 1994) and Hyogo-ken Nanbu (Kobe, 1995) earthquakes. By varying the dimensions of the prototype bridge used in the study and the span lengths supported by piers, three more bridges were obtained with different overstrength ratios (ratio of design-to-available base shear). The prototype bridge analyzed was straight, 60 meters long, and 16 meters wide. The superstructure was a hollow prestressed concrete deck supported by the abutments and two rows of piers. To quantify the deformational capacity of the piers, static inelastic pushover analysis was employed. Inelastic time-history analyses were undertaken to evaluate the displacement on the bridge piers using seven accelerograms, which had been selected to represent earthquakes with various magnitudes. These magnitudes were typical of areas with moderate seismic hazard, which constitutes the majority of seismically active areas around the world. The threshold values suggested by the authors for the ‘Multispan Prestressed-Deck Bridge’ class are as follows:

Table 9: Threshold Values Suggested for Multispan Prestressed-Deck Bridges

Damage State Level	Slight	Moderate	Extensive	Complete
PGA (g)	0.43	0.56	0.67	N/A
Standard Deviation (g)	0.165	0.178	0.180	N/A

Choi et al. (2004) developed a set of fragility curves for bridges commonly found in the Central and Southeastern United States. Using the results of an inventory analysis, four typical bridge types were identified. Using non-linear analytical models, analytical fragility curves were developed for the four bridge types. The authors stated that, comparison of the fragility curves showed the most vulnerable bridge types were multi-span simply supported and multi-span continuous steel-girder bridges. In addition, it was emphasized that the least vulnerable bridges were the multi-span, continuous, pre-stressed, concrete-girder bridges. Consequently, the median values suggested by the authors for several bridge classes are presented in Table 10.

Table 10: Threshold Values Suggested for Several Bridge Types

Bridge Type	Slight	Moderate	Extensive	Complete
MSSSG	0.20	0.33	0.47	0.61
MSSCG	0.20	0.56	0.77	1.14
MCSG	0.20	0.34	0.48	0.69
MCCG	0.24	1.31	2.01	3.47

In the research conducted by Karim and Yamazaki (2000) an analytical method was utilized to construct fragility curves for highway bridge piers considering both structural parameters and variation of input ground motion. A typical bridge structure was considered, and its piers were designed using the seismic design codes of Japan. Earthquake records were selected from the 1995 Hyokogen-Nanbu earthquake based on peak ground acceleration and peak ground velocity. Nonlinear dynamic response analyses of a typical bridge with reinforced concrete piers, girder, and deck were performed using the earthquake records from Japan and the United States as input ground motion. Damage indices for the bridge piers were obtained. Using the damage indices and ground motion indices, fragility curves for the bridge piers were then constructed. Median values from the relationships developed by the authors for ‘Multispan Simply Supported Concrete Girder Bridges’ are as follows:

Table 11: Threshold Values Suggested for MSSCG Bridges

Bridge Type	Slight	Moderate	Extensive	Complete
MSSCG	N/A	N/A	0.82	1.01

Shinozuka et al. (2000a) presented a statistical analysis of structural fragility curves. The authors stated that both empirical and analytical fragility curves were considered. Empirical fragility curves were developed by utilizing bridge damage data obtained from the 1995 Hyogo-ken-Nanbu (Kobe) earthquake. The analytical fragility curves were constructed by performing nonlinear dynamic analysis. Empirical fragility curves for the Hanshin Expressway Public Cooperation’s (HEPC’s) bridge (columns) were developed based on damage resulting from the 1995 Kobe earthquake. To demonstrate the development of analytical fragility curves, two representative bridges with a precast, prestressed continuous deck in the Memphis area were used. The median values generated for ‘Multispan Continuous Prestressed-Deck Bridges (MCPD)’ are as follows:

Table 12: Threshold Values Suggested for MCPD Bridges

Damage State Level	Slight	Moderate	Extensive	Complete
PGA (g)	0.47	0.68	0.80	N/A

In a study by Shinozuka et al. (2000b) the fragility relationships of a bridge created via two different analytical approaches are described. One method utilized time-history analysis while the other method used the capacity spectrum method. A sample of 10 nominally identical but statistically different bridges and 80 ground-motion time histories were considered to account for the uncertainties related to the structural capacity and ground motion, respectively. The comparison of fragility curves developed with the nonlinear static procedure to those developed with time-history analysis indicated that the agreement was excellent for the at least minor damage state, but not as good for the severe damage state. However, the agreement was adequate even in the severe damage state considering the large number of typical assumptions under which the analyses of fragility

characteristics are performed. Median values generated from analyses for ‘Multispan Continuous Prestressed-Deck Bridges (MCPD)’ are as follows:

Table 13: Threshold Values Suggested by Shinozuka et al. (2000b) for MCPD Bridges

Damage State Level	Slight	Moderate	Extensive	Complete
PGA (g)	0.20	N/A	0.27	N/A

Hwang et al. (2000) presented a procedure for the evaluation of the expected seismic damage to bridges and highway systems in the City of Memphis and Shelby County, Tennessee. Data pertinent to 452 bridges and major arterial routes was collected and implemented in a geographic information system (GIS) database. The following bridge damage states were considered: none/minor damage, repairable damage, significant damage. Fragility curves corresponding to these damage states were established for various bridge types. The median values generated from the developed fragility curves for ‘Multispan Simply Supported Prestressed Girder Bridges (MSSPG)’ are shown in Table 14.

Table 14: Threshold values suggested by Hwang et al. (2000) for MSSPG bridges

Damage State Level	Slight	Moderate	Extensive	Complete
PGA (g)	N/A	0.12	0.17	N/A

Filiatrault et al. (1993) stated that the Shipshaw Cable-Stayed Bridge, which crosses the Saguenay River near Jonquiere, Quebec, suffered significant structural damage during the 1988 Saguenay Earthquake. This earthquake was the largest seismic event recorded in eastern Canada. The peak horizontal acceleration recorded in the epicentral region was 0.15g. One of four anchorage plates connecting the steel box girders to the abutments failed due to ground shaking. This paper dealt with the dynamic analyses and testing of the Shipshaw Cable-Stayed Bridge that was performed to confirm the cause of failure. Threshold values generated for ‘Cable-Stayed Bridges (CSB)’ using bridge damage data collected via field-survey after the earthquake are as follows:

Table 15: Threshold Values Suggested by Filiatrault et al. (1993) for Cable Stayed Bridges

Damage State Level	Slight	Moderate	Extensive	Complete
PGA (g)	N/A	0.15	N/A	N/A

An analytical approach was adopted to construct fragility curves for highway bridge piers of specific bridges in Karim and Yamazaki (2001). Nonlinear dynamic response analyses were performed, and the damage indices for the bridge piers were obtained using strong ground motion records from Japan and the United States. Fragility curves for the bridge piers were constructed assuming a lognormal distribution using damage and ground motion indices. Based on the actual damage data of highway bridges from the 1995 Hyokogen-Nanbu (Kobe) earthquake, a set of empirical fragility curves was constructed. The analytical fragility curves were then compared with the empirical fragility curves. The median values generated for ‘Multispan Simply Supported Prestressed Girder Bridges (MSSPG)’ are as follows:

Table 16: Threshold Values Suggested by Karim and Yamazaki (2001) for MSSPG Bridges

Damage State Level	Slight	Moderate	Extensive	Complete
PGA (g)	0.28	0.61	0.73	1.00

Ranf et al. (2007) evaluated the influence of ground motion and bridge properties on the likelihood of a bridge suffering damage during an earthquake in the Pacific Northwest. The

2001 Nisqually earthquake damaged 78 bridges, of which 67 had slight or mild damage. The authors emphasized that the percentage of bridges damaged correlated best with the estimated spectral acceleration at a period of 0.3 sec., the year of construction, and whether the bridge was movable or an older steel truss. The mechanical components of movable bridges make them particularly vulnerable. Older truss bridges suffered a disproportionate amount of damage to their movable joints and bracing members. In addition, it was emphasized that the data suggested that simply supported bridges were not more vulnerable than continuous bridges to low-level damage. Furthermore, the authors stated that damage to movable bridges and truss type bridges were greatly underestimated by the HAZUS procedure, which categorizes movable bridges and older trusses as “other” bridges.

In Bessason et al. (2004) the authors evaluated the damage of a base-isolated, cable-stayed bridge subjected to two strong ground motions. The Thjorsa River Bridge, built in 1950 and retrofitted with base isolation in 1991, was instrumented by strong-motion accelerometers. The bridge has one 83 meter long main span and two 12 meter long approach spans. Only the main span, a steel arch truss with concrete deck, was base isolated. The bridge was subjected to moderate earthquakes of magnitudes 6.6 and 6.5 which occurred in south Iceland on June 17th and June 21st, 2000, respectively. The epicenters were too close to the bridge. The PGA recorded during the first and second earthquakes were 0.53g and 0.84g, respectively. The authors emphasized that the bridge survived the earthquakes without any significant damage and was open to traffic immediately after the earthquakes. The recorded data showed that the earthquake excitation on each side of the river was significantly different in the short period range. For the longer periods, which are most important for the response of the long base-isolated bridge, the difference is less. The recorded earthquake action showed considerably higher reaction force than the bearings were expected to resist prior to retrofitting. The loads were also higher than the superstructure was expected to resist. It was highly emphasized that the bridge would probably have been severely damaged in the June 2000, south Iceland earthquakes if it had not been base-isolated.

Definitions of Bridge Damage States

Four structural damage limit states are considered: slight, moderate, extensive, and complete. Primarily, damage state definitions are based on recommendations from previous studies and the qualitative descriptions of the damage states as provided by HAZUS. However, since the damage limit states depend upon the bridge type, condition and year of construction, as well as soil liquefaction beneath the bridge, engineering judgment is used in determination of the damage state levels (Choi et al., 2004). Descriptions of the bridge damage states considered in this study are summarized below:

Slight Damage

- Minor cracking and spalling to the abutment, cracks in shear keys at abutments, minor spalling and cracks at hinges, minor spalling at the column (damage requires no more than cosmetic repair) or minor cracking to the deck
- For cable-stayed bridges: small deck movement and nonstructural damage

Moderate Damage

- Any column experiencing moderate (shear cracks) cracking and spalling (column still structurally sound), moderate movement of the abutment (<2"), extensive

cracking and spalling of shear keys, any connection having cracked shear keys or bent bolts, keeper bar failure without unseating, rocker bearing failure or moderate settlement of the approach

- For cable-stayed bridges: anchorage plate failure, small number of hangers breaking off from the deck

Extensive Damage

- Any column degrading without collapse – shear failure - (column structurally unsafe), significant residual movement at connections, or major settlement approach, vertical offset of the abutment, differential settlement at connections, shear key failure at abutments

Complete Damage

- Any column collapsing and connection losing all bearing support, which may lead to imminent deck collapse, tilting of substructure due to foundation failure

Performance Threshold Values

The threshold values identified in previous research activities are shown in the following tables for each of the four damage states. Reasonable approximate threshold values, which are the median PGA values of the fragility relationships, are selected for damage states described in HAZUS (slight, moderate, extensive, and complete) and are based on engineering judgment.

Some of the previous work emphasized truss bridges because they are thought to be the most vulnerable bridge types. Additionally, the mechanical components of movable bridges, such as the swing bridges and vertical lift bridges that provide clearance for marine traffic, are also especially vulnerable. Moreover, it was emphasized that simply supported bridges are less vulnerable than continuous bridges (Ranf et al., 2007). There has been significant research conducted on the fragility of steel and concrete girder bridges as well. Since there have been a limited number of studies conducted on development of the fragility relationships for cable stayed and suspension bridges, the threshold values generated for these bridge types are primarily based on the damage data gathered via field-surveys after earthquakes.

Table 17. Threshold Values Suggested for Several Bridge Types

BridgeType	Reference	Slight	Moderate	Extensive	Complete
CSS	Filiatrault et al. (1993)	N/A	0.15	N/A	N/A
MCST	Nielsen and DesRoshes (2007)	0.18	0.31	0.39	0.50
	Choi et al. (2004)	0.20	0.34	0.48	0.69
MSSST	Nielsen and DesRoshes (2007)	0.24	0.44	0.56	0.82
	Choi et al. (2004)	0.20	0.33	0.47	0.61
MCSG	Nielsen and DesRoshes (2007)	0.18	0.31	0.39	0.50
	Choi et al. (2004)	0.20	0.34	0.48	0.69
MSSSG	Nielsen and DesRoshes (2007)	0.24	0.44	0.56	0.82
	Choi et al. (2004)	0.20	0.33	0.47	0.61
MSSCG	Nielsen and DesRoshes (2007)	0.24	0.44	0.56	0.82
	Choi et al. (2004)	0.20	0.33	0.47	0.61
	Karim and Yamazaki (2000)	N/A	N/A	0.82	1.01
	Hwang et al. (2000)	N/A	0.12	0.17	N/A
	Karim and Yamazaki (2001)	0.28	0.61	0.73	1.00
	Elnashai et al. (2004)	0.43	0.56	0.67	N/A

Suggested Threshold Values

After a thorough review of all results presented in the previous work and damage data provided by post-earthquake field observations, threshold values for each bridge class have been proposed for four damage states. The proposed approximate threshold values are as follows:

Table 18. Threshold Values Proposed for Long-Span Bridges

Bridge Type	Slight	Moderate	Extensive	Complete
CSS	N/A	0.15	N/A	N/A
MCST	0.18	0.31	0.39	0.50
MSSST	0.20	0.33	0.47	0.61
MCSG	0.18	0.31	0.39	0.50
MSSSG	0.20	0.33	0.47	0.61
MSSCG	0.28	0.61	0.73	1.00

Threshold Values for Dams and Levees

Dams and levees are man-made infrastructure components which restrain naturally flowing water and serve several purposes including water storage for farm irrigation, prevention of flooding, hydro-electric power, water supply to towns or industry, maintenance of safe water levels and many others.

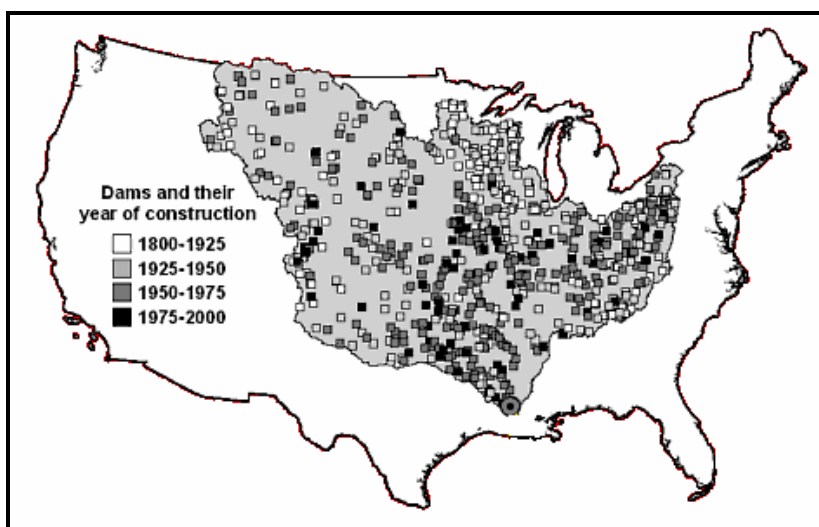


Figure 12: Large Dams Located in Central US

Dams and levees are critical infrastructure components in modern societies which are also vulnerable to natural hazards, especially earthquake hazards. If damaged or destroyed, dam and levee failures may disrupt the security, economic health, safety, and welfare of the general public. In September 2005, in the aftermath of Hurricane Katrina, the City of New Orleans, Louisiana, was largely submerged in floodwaters, mainly caused by levee failure (Luther, 2008). It is important to note that floods continue to pose an important threat to property and safety of population centers in the US. Inhabitants face a serious threat of flooding because of earthquake damage to dams and levees. The annual economic loss due to floods is estimated in the billions of dollars (FEMA 549, 2006). As a result, dam and

levee performance is a critical concern for engineers when considering economic impacts as well as public safety. Engineering decisions are based on lessons learned from previous hazard events, and subsequent preventative measures are taken to reduce failure risks. Figure 12 shows a map of large dams constructed in Central US and their respective years of construction.

Classification of Dams

Dams are classified based on the building material used, such as earth or concrete. Earth dams are built with earth and/or rockfill and are resistant to water pressure because of their weight. These types of dams are commonly referred to as gravity dams. If the material is not inherently watertight, dams are lined with an impervious material or have a watertight core. Earth dams are the oldest and most common type of dams. Concrete dams have several types: gravity, arch, buttress, multiple arch, barrages, and several others. Concrete gravity dams have a roughly triangular cross section and are also resistant to water pressure because of their weight. This type of dam is the most common type of concrete dam (ICOLD - International Commission of Large Dams). Concrete arch dams transmit most of the water load into the surrounding earth or large concrete thrust blocks.

There are many different dams within the eight-state study region that are investigated in this study. The majority of the dams located in these states are either earth dams, concrete gravity dams, or concrete arch dams. Seismic vulnerability of these dams must be addressed when assessing risk from earthquake hazards because these infrastructure types create substantial secondary hazards when damaged. This report presents approximate threshold values for use in rapid damage assessment of earth dams, concrete gravity dams, and concrete arch dams.



Figure 13. Damage at the Lower Van Norman Dam by the February 9, 1971, San Fernando, California, Earthquake (FEMA, 2005)

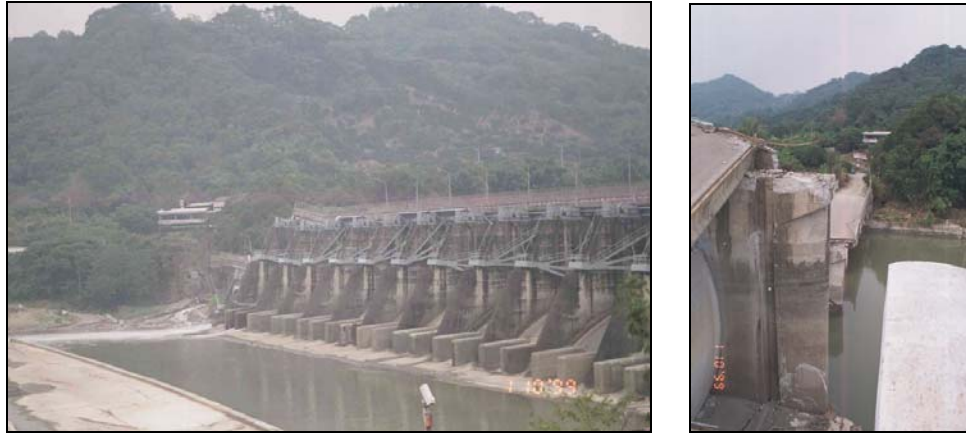


Figure 14. Dam Suffered Damage During the 7.6 magnitude 1999 Chi-Chi earthquake, Taiwan
(Images by Prof.Y. Hashash, University of Illinois)

Survey of Published Works

There is a relatively large number of dams and levees which have suffered damage during past earthquakes. Observational post-earthquake damage data is a very reliable form of data to use in the generation of threshold values. A summary of previous investigations predominantly based on the records from post-earthquake surveys of dams and levees subjected to strong ground motions are presented below.

The main purpose of the study performed by Tepel (1985), was to report the effects, or lack of effects, of a moderate earthquake (Morgan Hill Earthquake of April 24, 1984) on the well-designed facilities of a major water utility. These facilities were located from six to twenty-seven miles (10km to 43 km) from the epicenter. The Santa Clara Valley Water District, a public agency with flood control and water supply management authority in Santa Clara County, California, operates ten dams and reservoirs. Immediately after the April 24, 1984, Morgan Hill Earthquake, the District's Emergency Operations Center was activated. Major dams were inspected immediately following the event by operations staff in accordance with standard procedures. It was stated that no damage occurred at eight out of the District's ten dams. Functionally insignificant (or minor) damage was found at the Leroy Anderson and Coyote earth dams.

The earthquake caused two linear sets of longitudinal cracks on the crest of Leroy Anderson Dam, which were roughly twenty feet apart and extended 1,100 feet and 920 feet longitudinally along the surface of the dam. The Coyote Dam is one of the few dams in the U.S. knowingly built across an active fault. Minor surficial cracks were found in three areas of the dam: the upstream face, the crest, and in the vicinity of the spillway. The author concluded that the damaging effects of the earthquake were less severe than what was previously thought likely following a cursory review of peak acceleration response data. The author also emphasized that the damaging effects were less severe than anticipated by many (including the author) who personally experienced the earthquake shaking. As a result of dam damage data collected via field observations after the earthquake, the threshold values suggested by the author are as follows:

Table 19: Threshold Values Suggested for Several Dams

Dam	Slight	Moderate	Extensive	Complete
Leroy Anderson dam - downstream	0.41	N/A	N/A	N/A
Leroy Anderson dam - crest	0.63	N/A	N/A	N/A
Coyote dam	1.29	N/A	N/A	N/A

Boulanger and Duncan (n.d) stated that the upstream slope of the Lower San Fernando Dam in California failed due to liquefaction during the 1971 San Fernando earthquake. The peak ground acceleration of the earthquake was 1.25g at the Pacoima Dam. The dam was constructed by hydraulic filling, which involves mixing the fill soil with a large amount of water, transporting it to the dam site by pipeline, depositing the soil and water on the embankment in stages, and allowing the excess water to drain away. The fill that remains is loose and liquefied during the extended period of earthquake shaking. Figure 15 shows the aerial view and slide in the upstream shell of the dam after the earthquake.

**Figure 15: Aerial View of the Crest (left) and the Slide in the Upstream Shell of the Lower San Fernando Dam, in California, After the 1971 San Fernando Earthquake****Table 20: Threshold Values Suggested for Lower San Fernando Dam**

Damage State Level	Slight	Moderate	Extensive	Complete
PGA (g)	N/A	N/A	1.25	N/A

Performance evaluations of two reservoirs were conducted after the 1994 Northridge Earthquake by Davis and Bardet (1996). The authors concluded that this earthquake affected each of the dams in different ways. The Los Angeles Dam (LAD) and North Dike of the Los Angeles Reservoir (LAR) both moved slightly and settled, sustaining small, superficial cracks. The left abutment of the North Dike experienced a noticeable increase in seepage without significantly impeding the reservoir operations. The earthquake uplifted and shifted the foundation of the LAR by 30cm, causing tectonic effects on embankments. The tectonic tilt created a differential settlement across the embankments. Moreover, the authors stated that the Power Plant Tailrace, which is a small reservoir serving as the afterbay for the San Francisco Power Plant and channels aqueduct water to a filtration plant, slowly failed by piping due to transverse cracks and differential lateral spreading induced by liquefaction. The threshold values suggested by the authors as a result of the field survey performed after the earthquake are shown in Table 21.

Table 21: Threshold Values Suggested for Los Angeles Dam and Los Angeles Reservoir

Damage State Level	Slight	Moderate	Extensive	Complete
PGA (g)	N/A	0.56	N/A	N/A

Rathje et al. (2006) evaluated the behavior of earth dams and levees which survived the 2004 Niigata Ken Chuetsu, Japan, earthquake, stating that significant induced geotechnical and geologic failures occurred throughout the affected region. The most prevalent geotechnical observations from this earthquake were related to ground failure, including landslides in natural ground, failures of highway embankments and residential earth fills, and limited liquefaction in alluvial deposits. The absence of considerable levee deformations and surface faulting was also noted. The authors reported that one earth dam experienced significant deformation but did not release its reservoir. The levee system adjacent to the Shinano and Uono Rivers performed well, with only minor deformation observed in a few areas. Strong ground motions with PGA values of 0.82g-1.73g were observed at stations located immediately above the source region (Honda et al., 2005). The threshold values suggested in this study are presented in the following table:

Table 22: Threshold Values Suggested for Earth Dams and Levees

Dams/Levee	Slight	Moderate	Extensive	Complete
Earth dams	N/A	0.82	N/A	N/A
Levees	0.82	N/A	N/A	N/A

Nusier and Alawneh (2006) dealt with the seismic hazard assessment of earth dams subjected to earthquake events. The authors investigated the seismic hazard of the Kafrein Earth Dam located in Jordan. They stated that the site of the dam had been affected by multiple earthquakes of magnitudes greater than 6.0 over the last seven decades. They reported that the Jordan Valley Fault is a very significant strike-slip fault, similar to the Wabash Valley Fault in southeastern Illinois and southwestern Indiana which extends about 60 miles north-northeastward from just north of Shawneetown, Illinois and the Rough Creek Fault Zone. They concluded that, according to ICOLD (International Commission on Large Dams, 1989), the operating basis earthquake should have a 50% probability of non-exceedance throughout the 100-year lifetime of dam structures. For the Kafrein Dam, this non-exceedance probability represents a return period of 145 years and a design acceleration of 0.11g. The equivalent 90% confidence level results in a design acceleration of 0.25g.

A Safety Evaluation Earthquake is defined as the earthquake that produces the most severe level of ground motion under which the safety of the dam should be insured. The authors also concluded that the return period quoted for the Safety Evaluation Earthquake for the Kafrein Dam (Risk Class II Dam) is 3,000 years, representing an annual probability of exceedance of 0.03%. The resulting Maximum Design Earthquake, which produces the maximum ground motion values for design, should be 0.486g at bedrock. The suggested threshold value for Kafrein Dam is given in Table 23.

Table 23: Threshold Values suggested for Kafrein Dam

Damage State Level	Slight	Moderate	Extensive	Complete
PGA (g)	0.49	N/A	N/A	N/A

The main design characteristics of Karamah Dam located in the Jordan Valley were presented in a paper by Al-Homoud (1995). The author pointed out that the primary seismic source contributing to the hazard at the dam site is the active Jordan Valley Fault, which extends from the Dead Sea to the Sea of Galilee with an expected maximum earthquake magnitude of 7.8. A probabilistic method was used to evaluate the seismic hazard at the dam site. PGA was selected as the measure of ground motion severity.

Analyses were completed for 50%, 90%, and 95% exceedance probabilities throughout the structure lifetimes of 50, 100, and 200 years. According to the guidelines of ICOLD, PGA for a Maximum Design Earthquake (MDE) is 0.50g, and for Operating Basis Earthquake (OBE), which has a 50% probability of non-exceedence in 100 years lifetime of the dam, it is 0.17g. It is anticipated that OBE results in slight damage but the structure is still expected to be functional. It is reported that a PGA of 0.50g associated with the MDE triggers liquefaction of the sand layers in the dam foundation. Similarly, liquefaction may occur beneath the dam's foundation layers for a magnitude 7.8 earthquake, resulting in an expected crest settlement of 14.43 feet (4.4m). The expected horizontal rupture displacement for an earthquake of this magnitude is approximately 39.36 feet (12m). Slope stability analysis indicated deep failure planes in the foundation zone. The threshold value generated in this study is shown in Table 24.

Table 24. Threshold Values Suggested for Karamah Dam

Damage State Level	Slight	Moderate	Extensive	Complete
PGA (g)	0.17	N/A	N/A	N/A

Miller and Roycroft (2004) examine the seismic performance and deformation of levees via four case studies. The authors stated that, during the 7.1 magnitude Loma Prieta earthquake of October 17, 1989, severe ground shaking caused permanent ground displacement of levees at many locations along the Pajaro River near Watsonville, California. The area is in the seismically active region adjoining the San Andreas Fault Zone. The authors estimated the bedrock acceleration to have been 0.25g at the sites. The bedrock acceleration was amplified to an estimated 0.33g at the ground surface of soft soil sites. The yield accelerations for the critical failure surface are 0.50g and 0.49g, depending upon the depth of the assumed crack. They also concluded that one levee was severely damaged and three levees sustained minor damage. At the Artichoke Farm site, the levee experienced 24 inches (60 cm) of lateral spreading. There were major longitudinal cracks 2 feet wide and 8 feet deep in this section of levee. The South Side Levee experienced 2 inches (5 cm) lateral spreading. The threshold value suggested by the authors is shown in the following table:

Table 25: Threshold Values Suggested by Miller and Roycroft (2004) for Levees

Damage State Level	Slight	Moderate	Extensive	Complete
PGA (g)	0.33	N/A	N/A	N/A

The study by Trinufac and Hudson (1971) related to the 6.6 magnitude San Fernando, California, earthquake of February 9, 1971, where over 200 accelerographs were recorded. The horizontal peak ground acceleration of this earthquake was 1.25g. Although this earthquake did not have a large magnitude, it was associated with very severe ground motions and must be considered a major event from the standpoint of damage. However, it was stated that strong earthquake ground motion with large ground acceleration amplitudes do not necessarily indicate severe damage to structures. The threshold value based on the post-earthquake field survey is shown in Table 26.

Table 26: Threshold Values Suggested for Pacoima Concrete Gravity Dam

Damage State Level	Slight	Moderate	Extensive	Complete
PGA (g)	N/A	1.25	N/A	N/A

It was reported by Chopra (1992) that the Pacoima Dam, a concrete arch structure located in San Fernando, California, sustained damage to one abutment during the 1971 San

Fernando earthquake. Its reservoir was only partially full at the time of the strong ground motion. The median PGA value resulting from this research is given in the following table:

Table 27: Threshold Values Suggested by Chopra (1992) for Pacoima Dam

Damage State Level	Slight	Moderate	Extensive	Complete
PGA (g)	N/A	1.25	N/A	N/A

Behr et al. (1998) is related to structural deformation monitoring at the Pacoima Dam. The authors stated that the structure experienced severe shaking (>1 g) during the 1971 San Fernando and 1994 Northridge earthquakes (Swanson and Sharma, 1979; USGS and SCEC Scientists, 1994). The dam itself is 370.64 feet (113m) tall. This dam sustained significant damage during both earthquake events. The threshold value extracted from this study is presented in the following table:

Table 28: Threshold Values Suggested for Pacoima Concrete Gravity Dam

Damage State Level	Slight	Moderate	Extensive	Complete
PGA (g)	N/A	1.25	N/A	N/A

The post-earthquake damage state of the Koyna Dam subjected to the December 11, 1967, Koyna earthquake was evaluated by Chopra and Chakrabarti (1973). This structure is a concrete gravity dam and was constructed between 1954 and 1963. The longitudinal horizontal peak ground acceleration recorded during the Koyna earthquake was 0.63g. The response of the dam to the strong ground motion recorded during the earthquake was analyzed using the finite element method, and included the dynamic effects of the reservoir. The dam was in the epicentral region of the earthquake, and suffered notable structural damage. The authors emphasized that the most important structural damage to the dam was horizontal cracks on either the upstream or the downstream face or on both faces of several monoliths. Although the dam did not appear to be in danger of a major failure, the damage was serious enough to result in the lowering of the reservoir for inspection and repairs and required permanent strengthening. Considerations and criteria that had been employed in designing Koyna Dam were similar to those used in many parts of the world, including the United States. The PGA threshold value generated from the study is given in the following table:

Table 29: Threshold Values Suggested for Koyna Dam

Damage State Level	Slight	Moderate	Extensive	Complete
PGA (g)	N/A	0.63	N/A	N/A

Definition of Damage States for Dams and Levees

Four structural damage limit states are defined: slight, moderate, extensive, and complete. The damage state definitions used are based on recommendations from previous studies containing field survey damage data collected after earthquakes primarily. Descriptions of damage states for dams and levees are summarized below:

Slight Damage

- For earth dams, slight damage is defined as minor transverse or longitudinal surficial cracking in the area of the dam (i.e., upstream face, downstream face, crest, spillway vicinity)

- For concrete gravity dams, slight damage is defined as hairline cracks in the arc concrete structure
- For levees, slight damage is defined as minor permanent ground deformation at some locations as well as longitudinal and transverse cracking

Moderate Damage

- For earth dams, moderate damage is defined as small movement and settlement of the dam as well as small superficial cracks. There is no release of the reservoir in the moderate damage state
- For concrete gravity dams, moderate damage is defined as damage to the arc structure abutment, and horizontal cracks on either or both of the upstream or the downstream faces of the dam.
- For levees, moderate damage is defined as lateral spreading, longitudinal and transverse cracking, and deformations at some locations

Extensive Damage

- For earth dams, extensive damage is defined as relatively large movement and settlement, permanent liquefaction deformations, and large superficial cracking
- For concrete gravity dams, extensive damage is defined as damage to arc structure abutments and large cracking on either or both of the upstream or the downstream faces of the dam
- For levees, extensive damage is defined as considerable lateral spreading, large longitudinal and transverse cracking, and deformations

Complete Damage

- For earth dams, complete damage is defined as large settlement and movement, large superficial cracks, and the release of the reservoir without flood damage
- For concrete gravity dams, complete damage is defined as substantial damage to arc structure abutments, large and widespread horizontal and transverse cracks on either of both of the upstream or the downstream faces of the dam, leading to the release of water
- For levees, complete damage is defined as deep and large longitudinal and transverse cracks as well as large lateral spreading

Performance Threshold Values

Table 30: Threshold Values Suggested for Dams and Levees

Dams and Levees	Reference	Slight	Moderate	Extensive	Complete
Earth Dams	Tepel (1985)-1	0.41	N/A	N/A	N/A
	Tepel (1985)-2	0.63	N/A	N/A	N/A
	Tepel (1985)-3	1.29	N/A	N/A	N/A
	Davis and Bardet (1996)	N/A	0.56	N/A	N/A
	Rathje et al. (2006)	N/A	0.82	N/A	N/A
	Nusier and Alawneh (2006)	0.49	N/A	N/A	N/A
	Al-Homoud (1995)	0.17	N/A	N/A	N/A
Concrete Gravity and Arch Dams	Boulanger	N/A	N/A	1.25	N/A
	Trinufac and Hudson (1971)	N/A	1.25	N/A	N/A
	Chopra (1992)	N/A	1.25	N/A	N/A
	Behr et.al. (1998)	N/A	1.25	N/A	N/A
	Chopra and Chakrabarti (1973)	N/A	0.63	N/A	N/A
Levees	Rathje et al. (2006)	0.82	N/A	N/A	N/A
	Miller and Roycroft (2004)	0.33	N/A	N/A	N/A

Table 30 is designed to compare data collected from various studies presented previously. Reasonable approximate threshold values, which are defined as the median PGA values of the fragility relationships, are selected for damage states considered and are based on engineering judgment.

Suggested Threshold Values

Approximate threshold values for the earth dams, concrete gravity dams, and levees are based on detailed engineering judgment and are presented in the following table:

Table 31: Threshold Values Proposed for Dams and Levees

Dams & Levees	Slight	Moderate	Extensive	Complete
Earth Dams	0.50	0.63	1.25	N/A
Concrete Gravity and Arch Dams	0.63	1.25	N/A	N/A
Levees	0.33	N/A	N/A	N/A

Threshold Values for Hazardous Materials Facilities (Tanks)

Classification of Tanks

It has been observed in past earthquakes that steel and concrete storage tanks are two of the most common types of the hazardous materials storage tanks, and are also quite vulnerable to seismic activity. Broad classifications of these infrastructure components were employed based on the identification of common structural features. The storage tanks located in the region of interest are classified as:

- a. Steel storage tanks
 - i) Un-anchored steel storage tanks
 - ii) Anchored steel storage tanks
- b. Concrete storage tanks
 - i) Un-anchored concrete storage tanks
 - ii) Anchored concrete storage tanks
 - iii) Elevated concrete storage tanks
- c. Wood tanks

It has been observed in past earthquakes that storage tanks, especially metal cylindrical tanks, undergo considerable damage during strong ground motions. Figure 16 and Figure 17 show typical “elephant foot buckling” and deformation damage to steel storage tanks. It has been shown in previous research that a tank’s height-to-diameter (H/D) ratio, as well as the relative amount of stored contents (% fill level), have a considerable effect on the seismic performance of the tank (O’Rourke and So, 2000; Kilic and Ozdemir, 2007).



Figure 16: Elephant Foot Buckling of Tupras Refinery Cylindrical Tanks (left) and Deformation of Tanks in Kocaeli (right) After the 17 August 1999, Marmara Earthquake, Turkey



Figure 17: Damage at the OSB Amylum Factory by the 1995 Ceyhan, Turkey, Earthquake

Survey of Published Works

There is a wide variety of post-earthquake observational data available on the performance of tanks under seismic loading. The data and fragilities generated via field-survey after earthquakes are based on expert opinion, primarily. Previous research conducted on the vulnerability assessment of storage tanks have been briefly summarized.

Berahman and Behnamfar (2007) recently conducted a study on seismic fragilities of un-anchored, on-grade steel storage tanks (with fill level greater than 50%) based on historical data and the American Lifeline Alliance tanks database. Two hundred tank databases, which comprise 532 individual tanks, were considered in this study. The fragility curves developed in this study used PGA as the predictive parameter for damage to tanks. The fragility curves developed were compared to corresponding relationships currently available in the technical literature. The authors stated that the comparisons suggest that actual tank performance is better than that predicted in the literature. The threshold values suggested by the authors for the un-anchored, steel storage tanks are given in the following table:

Table 32: Threshold Values Suggested by Berahman and Behnamfar (2007) for Un-Anchored Steel Storage Tanks

Damage State Level	Slight	Moderate	Extensive	Complete
PGA (g)	0.60	0.87	1.07	N/A

Fragility curves for cylindrical, on-grade steel liquid storage tanks subjected to ground shaking hazard are presented in O'Rourke and So (2000). The fragility curves are based on the analysis of the reported performance of over 400 tanks in nine separate earthquake events. The amount of the ground shaking is quantified by the PGA at each specific site. The influence of tank height-to-diameter ratio, H/D, as well as the relative amount of stored contents, or % full, were investigated and found to have a significant affect on tank performance under seismic loading. New fragility curves were compared to corresponding relationships in the technical literature. The median fragility values, which consider the height-to-diameter ratio (H/D) and fill ratio (fullness), are delineated in the following table:

Table 33: Threshold Values Suggested by O'Rourke and So (2000) for Several Tanks

Tank Type	Slight	Moderate	Extensive	Complete
Un-anchored steel storage tanks (H/D<70%)	0.67	1.18	1.56	1.79
Un-anchored steel storage tanks (H/D≥70%)	0.45	0.69	0.89	1.07
Un-anchored steel storage tanks (%Full<50%)	0.64	N/A	N/A	N/A
Un-anchored steel storage tanks (%Full≥50%)	0.49	0.86	0.99	1.17
On-grade steel storage tanks (if base connection unknown)	0.70	1.10	1.29	1.35

In HAZUS (FEMA, 2008), several median fragility values were estimated using PGA as the ground shaking parameter. These values correspond to on-ground concrete (anchored and unanchored), on-ground steel (anchored and unanchored), elevated steel, and on-ground wood storage tanks. Anchored and unanchored conditions refer to positive connection, or a lack thereof, between the tank wall and the supporting concrete ring wall. Median PGA values related to each damage state are proposed as follows:

Table 34: Threshold Values Suggested in HAZUS for Several Types of Storage Tanks

Tank Type	Slight	Moderate	Extensive	Complete
Anchored concrete tanks	0.25	0.52	0.95	1.64
Un-anchored concrete tanks	0.18	0.42	0.70	1.04
Anchored steel tanks	0.30	0.70	1.25	1.60
Un-anchored steel tanks	0.15	0.35	0.68	0.95
Elevated steel tanks	0.15	0.55	1.15	1.50
Wood tanks	0.15	0.40	0.70	0.90
Buried concrete tanks	2.00	4.00	8.00	12.00

It is important to emphasize that the approximate threshold values defined in HAZUS do not consider the fill level and H/D ratios of tanks. It was shown in the previous studies, which were comprised of fragility relationships and field observations of damage to storage tanks after past earthquakes, that the fill level (% full) and H/D (height/diameter) ratio affect the response of the tanks considerably (O'Rourke and So, 2000; Kilic and

Ozdemir, 2007). These results indicate how effective the aforementioned characteristics are and encourage the consideration of these factors in the vulnerability assessment of storage tanks in order to reduce the potential loss in future devastating seismic events.

In the American Lifeline Alliance (2001a) study an inventory of 424 tanks, developed by Cooper (1997), was reviewed and for the most part found to be correct. In a few instances, the damage states for broken pipes were adjusted as follows: if damage to a pipe created only slight leaks or minor repairs such as damage to an overflow pipe, the damage state was considered slight (same as O'Rourke and So). However, if damage to a pipe led to complete loss of contents or complete breakage of the inlet-outlet line, then the damage state was considered extensive. In addition, it was stated that steel and concrete storage tanks supported above grade by columns or frames have failed due to the inadequacy of the support system under lateral seismic forces. This occurred in a steel/cement silo in Alaska in 1964 and a concrete tank in Izmit, Turkey, in 1999. Many elevated concrete water reservoirs failed or were severely damaged in the 1960 Chilean earthquake as well. Such failures most often led to complete loss of contents. The median PGA values generated from this research are given in the following table:

Table 35: Threshold Values Suggested in the American Lifeline Alliance (2001a) for Un-Anchored Steel Storage Tanks

Damage State Level	Slight	Moderate	Extensive	Complete
PGA (g)	0.15	0.63	1.08	N/A

In a study by Fabbrocino et al. (2005) empirical seismic fragility curves were defined both for building-like and non building-like industrial components. These components were matched with outcomes of a probabilistic seismic hazard analysis for a test site located in southern Italy. Once the seismic failure probabilities were quantified, consequence analyses were performed for those events which may result in a loss of containment following seismic activity. The median PGA values suggested by the authors are shown in Table 36.

Table 36: Threshold Values Suggested by Fabbrocino et al. (2005) for Several Tank Types

Tank Type	Slight	Moderate	Extensive	Complete
Anchored steel storage tanks (nearly full)	N/A	0.30	0.71	N/A
Anchored steel storage tanks (%Full \geq 50%)	N/A	1.25	3.72	N/A
Un-anchored steel storage tanks (nearly full)	N/A	0.15	0.68	N/A
Un-anchored steel storage tanks (%Full \geq 50%)	N/A	0.15	1.06	N/A

Field observations of damage to metal, cylindrical, liquid storage tanks during the August 17, 1999, ($M_w=7.4$) Marmara earthquake and analyses were performed to show the seismic behavior of such structures (Kilic and Ozdemir, 2007). The horizontal peak ground acceleration of Yarımca (YPT) EW record was 0.32g for this event. The authors emphasized that the earthquake caused significant structural damage to petrochemical containment tanks at the Tupras Refinery. The sloshing action of combustible liquid inside the tanks deformed the tank roofs and upper tank walls. Insufficient freeboard in fixed-roof tanks may have resulted in plate buckling at the roof level. The roof-shell junction ruptured

due to excessive joint stresses. In their analyses, the authors considered the tanks to be fully anchored to the base. The threshold values generated from the investigation are detailed in the following table:

Table 37: Threshold Values Suggested by Kilic and Ozdemir (2007) for Anchored Steel Tanks

Damage State Level	Slight	Moderate	Extensive	Complete
PGA (g)	N/A	0.32	N/A	N/A

Shinsaku (2003) stated that oil storage tanks at TUPRAS Refinery, close to the North Anatolian Fault in Turkey, suffered severe damage including large fires and sinking of floating roofs on oil storage tanks. This damage occurred because of liquid sloshing, which was generated by long-period strong ground motions. Fires continued for one week until liquids in tanks had burned off completely. In the ChiChi earthquake in Taiwan, damage such as buckling of floating roofs, rupturing of shell plates, buckling of shell-to-roof joints, and deformation of tank equipment was also caused by liquid sloshing, although the tank sites were located far from the epicenter. Also the peak ground accelerations were about 0.1g. The most severe damage was rupture of the lowest course shell plate, where the lower end of the guide pole was supported. Tank contents were released and subsequently spilled out inside a dike, and contaminated nearby soil. The threshold values generated by the investigation are as follows:

Table 38: Threshold Values Suggested by Shinsaku (2003) for Un-Anchored Steel Tanks

Damage State Level	Slight	Moderate	Extensive	Complete
PGA (g)	N/A	0.32	N/A	N/A

Damage to oil storage tanks and sloshing behavior during the earthquake are presented (Shinsaku et al., 2003). It was determined that the 2003 Tokachi-oki earthquake (M=8.0), which occurred on September 26th, east of Hokkaido in northern Japan. Overall, the extent of damage was not so large considering its magnitude. On the other hand, oil storage tanks in and around Tomakomai, a coastal city in southern Hokkaido, were severely damaged by liquid sloshing. In the Idmitsu Refinery, two fires broke out, six floating roofs sank, and thirty tanks suffered some amount of damage, such as overflow and splashing of oil, deformation of refinery components including; a rolling ladder, weather shield, guide pole, gauge pole and air foam dam, among others. The threshold values suggested in this study are presented in Table 39.

Table 39: Threshold Values Suggested by Shinsaku et al. (2003) for Un-Anchored Steel Storage Tanks

Damage State Level	Slight	Moderate	Extensive	Complete
PGA (g)	N/A	N/A	1.01	N/A

Jaiswal et al. (2007) asserted that liquid storage tanks generally possess lower energy-dissipating capacity than conventional buildings. During lateral seismic excitation, tanks are subjected to hydrodynamic forces. These two aspects are recognized by most seismic codes governing liquid storage tanks and, accordingly, provisions specify higher design seismic forces than buildings and require modeling of hydrodynamic forces during structural analyses. In addition, the authors emphasized that the review carried out revealed that there are significant differences among the codes governing seismic design forces for various types of tanks.

Definitions of Tanks Damage States

Four structural damage limit states (slight, moderate, extensive and complete) defined in HAZUS are considered in the damage evaluation of the storage tanks. The damage state definitions used are based on recommendations made by experts after field surveys and the qualitative descriptions of the damage states as provided by HAZUS primarily. Descriptions of tank damage states are summarized below:

Slight Damage

- For anchored tanks, slight damage is defined as minor anchor damage and stretched anchor bolts. With slight damage, the anchored tanks remain functional
- For unanchored tanks, slight damage is defined as elephant foot buckling of tanks with no leakage or loss of contents. With slight damage, the unanchored tanks remain functional
- For buried tanks, slight damage is defined as minor uplift (few inches) of the buried tanks or minor cracking of concrete walls.

Moderate Damage

- For anchored tanks, moderate damage is defined as elephant foot buckling of tanks with no leakage or loss of contents but considerable damage to tank occurs
- For unanchored tanks, moderate damage is defined as elephant foot buckling of tanks with partial loss of contents
- For buried tanks, moderate damage is defined as damage to roof supporting columns and considerable cracking of walls

Extensive Damage

- For anchored tanks, extensive damage is defined as elephant foot buckling of tanks with loss of contents. Inlet-outlet pipe breaks are also common in cases of extensive damage
- For unanchored tanks, extensive damage is defined as weld failure at the base of the tank with loss of contents, breaking of inlet-outlet pipes, and partial collapse of the roof system into the tank
- For buried tanks, extensive damage is defined as considerable uplift (more than a foot) of the tanks and rupture of the attached piping

Complete Damage

- For anchored tanks, complete damage is defined as weld failure at the base of the tank with loss of contents
- For unanchored tanks, complete damage is defined as tearing of the tank wall or implosion of the tank (with total loss of content)
- For buried tanks, complete damage is defined as considerable uplift (more than a foot) of the tanks and rupture of the attached piping

Performance Threshold Values

Several threshold values were developed for various damage states as described in HAZUS and are based on peak ground acceleration. These values correspond to on-ground concrete (anchored and unanchored), on-ground steel (anchored and unanchored), elevated steel, and on-ground wood tanks. For tanks, anchored and unanchored refers to connection between the steel or concrete tank wall and the supporting concrete ring wall.

Table 40: Threshold Values Suggested for Storage Tanks

Storage Tank Type	Reference	Slight	Moderate	Extensive	Complete
Unanchored steel tanks	Berahman et al. (2007)	0.60	0.87	1.07	N/A
	HAZUS (2003)	0.15	0.35	0.68	0.95
	ALA (2001a)	0.15	0.63	1.08	N/A
	Shinsaku (2003)	N/A	0.32	N/A	N/A
	Shinsaku et al. (2003)	N/A	N/A	1.01	N/A
Anchored steel tanks	HAZUS (1997)	0.30	0.70	1.25	1.60
	Kilic & Ozdemir(2007)	N/A	0.32	N/A	N/A
Anchored steel tanks (nearly full)	Fabbrocino et al. (2005)	N/A	0.30	0.71	N/A
Anchored steel tanks (Fill $\geq 50\%$)	Fabbrocino et al. (2005)	N/A	1.25	3.72	N/A
Unanchored steel tanks (H/D<70%)	O'Rourke & So (2000)	0.67	1.18	1.56	1.79
Unanchored steel tanks (H/D $\geq 70\%$)	O'Rourke & So (2000)	0.45	0.69	0.89	1.07
Unanchored steel tanks (Fill <50%)	O'Rourke & So (2000)	0.64	N/A	N/A	N/A
Unanchored steel tanks (Fill $\geq 50\%$)	O'Rourke & So (2000)	0.49	0.86	0.99	1.17
	Fabbrocino et al. (2005)	N/A	0.15	1.06	N/A
Unanchored steel tanks(nearly full)	Fabbrocino et al. (2005)	N/A	0.15	0.68	N/A
Elevated steel tanks	HAZUS (2003)	0.15	0.55	1.15	1.50
Unanchored concrete tanks	HAZUS (2003)	0.18	0.42	0.70	1.04
Anchored concrete tanks	HAZUS (2003)	0.25	0.52	0.95	1.64
Buried concrete tanks	HAZUS (2003)	2.00	4.00	8.00	12.00
Wood tanks	HAZUS (2003)	0.15	0.40	0.70	0.90

Suggested Threshold Values

Numerous previous studies have concluded that the fill level (% full) and H/D (height/diameter) ratio affect the response of the tanks considerably. However, in HAZUS, the fill level of the tanks (whether the tanks are full, nearly full, $\geq 50\%$ full, empty) as well as H/D (height/diameter) ratio of tanks are not taken into consideration. Therefore, in addition to the threshold values available in the HAZUS, the threshold values generated from previously conducted studies considering H/D (height/diameter) and fill level of tanks are proposed herein. The proposed threshold values can be seen in Table 41 and Table 42.

Table 41: Threshold Values Proposed for Storage Tanks

Tank Type	Slight	Moderate	Extensive	Complete
Unanchored steel tanks (H/D<70%)	0.67	1.18	1.56	1.79
Unanchored steel tanks (H/D $\geq 70\%$)	0.45	0.69	0.89	1.07
Unanchored steel tanks (Fill Level <50%)	0.64	N/A	N/A	N/A
Unanchored steel tanks (Fill Level $\geq 50\%$)	0.49	0.86	0.99	1.17
Unanchored steel tanks (nearly full)	N/A	0.15	0.68	N/A
Anchored steel tanks (Nearly Full)	N/A	0.30	1.25	N/A
Anchored steel tanks (Fill Level $\geq 50\%$)	N/A	0.71	3.72	N/A

**Table 42: Threshold Values Proposed for On-Grade Steel Storage Tanks
(If the Base Connection Type is Unknown)**

Damage State Level	Slight	Moderate	Extensive	Complete
PGA (g)	0.70	1.10	1.29	1.35

Conclusions

The research addresses rapid vulnerability assessment of critical infrastructure components, namely major river crossings, dams, levees, and hazardous materials storage tanks, located in the eight-state study region surrounding the New Madrid Seismic Zone in the Central US. Approximate threshold values have been determined for use in rapid earthquake damage assessment of the aforementioned infrastructure components. Using PGA as the ground shaking intensity parameter, approximate threshold values were developed for each subcategory of the various infrastructure components, corresponding to the four damage states described in HAZUS. The following conclusions are reached as a result of the literature review in this study:

- Continuous and simply supported truss bridges constitute nearly three quarters of the total MRCs inventory investigated
- Although it was common to classify MRCs simply based on their construction type and construction material, it should be emphasized that seismic vulnerability of the bridges greatly depends on the bridge type, materials, year of construction, site conditions, liquefaction, and mobility, among others
- The majority of the dams located in the eight states are categorized as earth dams, concrete gravity, and arch dams
- The proposed approximate threshold values generated from previous research are based on the records from post-earthquake surveys, predominantly, and they show that earth dams are more vulnerable than concrete gravity and arch dams
- The values of pass-fail peak ground accelerations presented in this study are ready for use in regional impact assessment in the Central US. The methodology is applicable to other situations where detailed analytical modeling approaches are not feasible
- Even though the comprehensive fragility analyses of such complex structural systems are time consuming, they are necessary in order to reduce the uncertainties and are based on basic engineering judgment. Fragility relationships based on analytical modeling provide more accurate vulnerability assessments than the threshold values proposed in this study. Further work on these analytical and bridge-specific fragilities will improve the damage characterizations that are based on the threshold values presented herein.

References

- Al-Homoud, A.S. (1995). Evaluation of Seismic Hazard, Local Site Effect, Liquefaction Potential, and Dynamic Performance of a World Example of an Embankment Dam Characterized by Very Complex and Unique Foundations Conditions: Karameh Dam in the Jordan Valley. *Bulletin of the International Association of Engineering Geology*. Paris. n 52, 9-32.
- American Lifeline Alliance (ALA) (2001a). Seismic Fragility Formulation for Water System: Part 1:Guideline. *ASCE*.
- API 650: Welded Storage Tanks for Oil Storage (2003). *American Petroleum Institute Standard*, Washington D.C.
- Behr, J., K. Hudnut, and N. King (1998). Monitoring Structural Deformation at Pacoima Dam, California Using Continuous GPS. *Proceedings of ION* (The Institute of Navigation) GPS.
- Berahman, F. and F. Behnamfar (2007). Seismic Fragility Curves for Un-Anchored On-Grade Steel Storage Tanks: Bayesian Approach. *Journal of Earthquake Engineering*. v 11, 166-192.
- Bessason B. and E. Haflidason (2004). Recorded and Numerical Strong Motion Response of a Base-Isolated Bridge. *Earthquake Spectra*. v 20, n 2, 309-331.
- Boulanger, R.W. and J.M. Duncan (n.d). "Geotechnical Engineering Photo Album." <http://cee.engr.ucdavis.edu/faculty/boulanger/geo_photo_album/GeoPhoto.html>
- Choi, E., R. DesRoshes, and B. Nielson (2004). Seismic Fragility of Typical Bridges in Moderate Seismic Zones. *Engineering Structures*. v 26, 187-199.
- Chopra, A.K. (1992). Earthquake Analysis, Design and Safety evaluation of Concrete Arch Dams. *Proceedings of the Tenth World Conference on Earthquake*. Spai., v 8, 6763.
- Chopra, A.K. and P. Chakrabarti (1973). The Koyna Earthquake and The Damage to Koyna Dam. *Bulletin of Seismological Society of America*. v 63, n 2, 381-392.
- Elnashai, A.S., B. Borzi, and S. Vlachos (2004). Deformation-based vulnerability functions for RC bridges. *Journal of Structural Engineering and Mechanics*. February.
- Elnashai, A.S., A. Mwafy, and O.S. Kwon (2006). Analytical Assessment of a Major Bridge in the New Madrid Seismic Zone. *Transportation Research Board of the National Academies*. Report No: A15.
- Elnashai, A.S., L.J. Cleveland, T. Jefferson, and J. Harrauld (2008). "Impact of Earthquakes on the Central USA", Report No.08-02, Mid-America Earthquake (MAE) Center, University of Illinois at Urbana-Champaign, Urbana, IL.

Fabbrocino, G., I. Ievoli, F. Orlando, and E. Salzano (2005). Quantitative Risk Analysis of Oil Storage Facilities in Seismic Areas. *Journal of Hazardous Materials*. V A123, 61-69.

Federal Emergency Management Agency [FEMA] (2005). "Federal Guidelines for Dam Safety, Earthquake Analyses and Design of Dams." May.

Federal Emergency Management Agency [FEMA] 549 (2006). "Hurricane Katrina in the Gulf Coast". Mitigation Assessment Team Report, Building Performance Observations, Recommendations, and Technical Guidance.

Federal Emergency Management Agency [FEMA] (2008). *HAZUS-MH MR3 Technical Manual*. Washington, D.C. FEMA.

Filiatrault, A., R. Tinawi, and B. Massicotte (1993). Damage To Cable-Stayed Bridge During 1988 Saguenay Earthquake, II: Dynamic Analysis. *Journal of Structural Engineering*. v119, n 5, 1450-1463.

HAZUS (1997). National Institute of Building Science. "Earthquake Loss Estimation Methodology," prepared by *Risk Management Solution*, Menlo Park, CA.

Hildenbrand, T.G., V.E. Langenheim, E. Schweig, P.H. Stauffer, and J.W. Hendley II, (1996). "Uncovering Hidden Hazards in the Mississippi Valley" <<http://quake.usgs.gov/prep/prepare/factsheets/HiddenHaz/>>.

Honda, R., S. Aoi, N. Morikawa, H. Sekiguchi, T. Kunugi, and H. Fujiwara (2005). Ground motion and rupture process of the 2004 Mid Niigata Prefecture earthquake obtained from strong motion data of K-NET and KiK-net. *Earth Planets Space*. v 57, 527-532.

Housner G.W. (1954). Earthquake Pressures on Fluid Containers. *8th Technical Report under Office of Naval Research*. California Institute of Technology, Pasadena, California. August.

Hwang, H., J.B. Jernigan, and Y. Lin (2000). Evaluation of Seismic Damage to Memphis Bridges and Highway Systems. *Journal of Bridge Engineering*. v 5, n 4, 322-330.

Jaiswal, O.R., C.R. Durgesh, and K.J. Sudhir (2007). Review of Seismic Codes on Liquid-Containing Tanks. *Earthquake Spectra*. v 23, n 1, 239-260.

Karim, K.R., and F. Yamazaki (2000). Comparison of Empirical and Analytical Fragility Curves for RC Bridge Piers in Japan. *8th Specialty Conference on Probabilistic Mechanics and Structural Reliability*. pp.1-6.

Karim, K.R., and F. Yamazaki (2001). Effect of Earthquake Ground Motions on Fragility Curves of Highway Bridge Piers Based on Numerical Simulation. *Journal of Earthquake Engineering and Structural Dynamics*. v 30, 1839-1856.

Luther, L. (2008). "Disaster Debris Removal After Hurricane Katrina: Status and Associated Issues". CRS Report for Congress, Congressional Research Service. <<http://ftp.fas.org/sgp/crs/misc/RL33477.pdf>>.

Miller E.A. and G.A. Roycroft (2004). Seismic Performance and Deformation of Levees: Four Case Studies. *Journal of Geotechnical and Geoenvironmental Engineering*. April. p. 344-354.

Missouri Department of Natural Resources [MDNR] (2008). Division of Geology and Land Sources Technical Bulletin <<http://www.dnr.mo.gov/geology/geosrv/geores/techbulletin1.htm>>.

Mississippi River Bridge Crossings (2009). <http://en.wikipedia.org/wiki/Mississippi_River#Bridge_crossings>.

Nielson, Bryant G. and R. DesRoshes (2007). Analytical Seismic Fragility Curves for Typical Bridges in the Central and Southeastern United States. *Earthquake Spectra*. v 23, n 3, 615-633.

Nusier, O.K. and A.S. Alawneh (2006). Kafrein Earth Dam Probabilistic Seismic Hazard Assessment. *Soil Mechanics and Foundation Engineering*. v 43, n 6, 211-215.

O'Rourke, M.J. and P. So (2000). Seismic Fragility Curves for On-Grade Steel Tanks. *Earthquake Spectra*. v 16, n 4, 801-814.

R. W. Boulanger's Career Award CMS-9502530, Virginia Tech through J. M. Duncan's University Distinguished Professorship and the Center for Geotechnical Practice and Research, the PEER Center, and the UC Davis Teaching Resources Center Project.

Ranf, R.T., M.O. Eberhard, and S. Malone (2007). Post-earthquake Prioritization of Bridge Inspections. *Earthquake Spectra*. v 23, n 1, 131-146.

Rathje, E.M., K. Kelson, S.A. Ashford, Y. Kawamata, I. Towhata, T. Kokusho, and J.P. Bardet (2006). Geotechnical Aspects of the 2004 Niigata Ken Chuetsu, Japan, Earthquake. *Earthquake Spectra*. v 22, n S1, S23-S46.

Kilic, S.A. and Z. Ozdemir (2007). Simulation of Sloshing Effects in Cylindrical Containers under Seismic Loading. 6. *LS-DYNA Anwenderforum*, Frankenthal 2007, Bauwesen.

Shinozuka, M., M.Q. Feng, J. Lee, and T. Naganuma (2000a). Statistical Analysis of Fragility Curves. *Journal of Engineering Mechanics*. v 126, n 12, 1224-1231.

Shinozuka, M., M.Q. Feng, H. Kim, and S. Kim (2000b). Nonlinear Static Procedure for Fragility Curve Development. *Journal of Engineering Mechanics*. v 126, n 12, 1287-1295.

Shinsaku, Z. (2003). Damage and Failure of Oil Storage Tanks due to the 1999 Kocaeli Earthquake in Turkey and Chi-Chi Earthquake in Taiwan. *Journal of High Pressure Institute of Japan*. v 41, n 2, 79-86. <<http://sciencelinks.jp/j-east/article/200311/000020031103A0275606.php>>.

Shinsaku, Z., M. Yamada, H. Nishi, M. Hirokawa, K. Hatayama, T. Yanagisawa, and R. Inoue (2003). "Damage of Oil Storage Tanks due to the 2003 Tokachi-oki Earthquake." <<http://www.fri.go.jp/>>.

Tepel, R.E. (1985). The Morgan Hill Earthquake of April 24, 1984-Effects on Facilities of the Santa Clara Valley Water District. *Earthquake Spectra*. v 1, n 3, 633-656.

Trifunac, M.D, and D.E. Hudson (1971). Analysis of The Pacoima Dam Accelerogram – San Fernando, California, Earthquake of 1971. *Bulletin of Seismological Society of America*. v 61, n 5, 1393-1141.

Wozniak, R.S, and W.W. Mitchell (1978). "Basis of Seismic Design Provisions for Welded Steel Oil Storage Tanks." American Petroleum Institute, 43rd Mid-year Meeting, Session on Advances in Storage Tank Design, Toronto, Canada.



Additional Bridge Data

There are 127 major river crossings located on five rivers (the Mississippi, Ohio, Missouri, Illinois, and Arkansas Rivers) within the eight states of interest in the Central US: Alabama, Arkansas, Illinois, Indiana, Kentucky, Mississippi, Missouri, and Tennessee.

This section gives brief information about each major river crossings considered. Most of the images and the brief summaries are provided from two sources:

- i) http://en.wikipedia.org/wiki/Mississippi_River#Bridge_crossings, and
- ii) <http://www.johnweeks.com/menu/hwy.html>.

1. Caruthersville Bridge

	
Carries	4 lanes of I-155 / US 412
Crosses	Mississippi River
Locale	Caruthersville, Missouri and Dyersburg, Tennessee
Design	Cantilever bridge
Longest span	920 feet (280 m) and 520 feet (158 m)
Total length	7,102 feet (2,165 m)
Width	78 feet (24 m)
Clearance below	99 feet (30 m)
Opening date	December 1, 1976
Coordinates	 36°06'54"N 89°36'47"W


The **Caruthersville Bridge** is a cantilever bridge carrying Interstate 155 and U.S. Route 412 across the Mississippi River between Caruthersville, Missouri and Dyersburg, Tennessee.

The Caruthersville Bridge on I-155 has 59 spans with a total length of 7,100 feet and was built in the early seventies across the Mississippi River between Missouri and Tennessee. The site is in the vicinity of the New Madrid central fault, at a distance of about 5 km from a presumed major fault. The superstructure consists of eleven units supported on a variety of elastomeric and steel bearings. The main river crossing is composed of two-span cantilever steel truss and ten-span steel girders, whilst approach spans are precast prestressed concrete girders. The substructure includes piers on deep caissons and bents on steel friction piles (Elnashai et al. 2006).

2. Harahan Bridge





Memphis&Arkansas Bridge (*left*), Frisco Bridge (*center*), Harahan Bridge (*right*)

Carries	Rail line
Crosses	Mississippi River
Locale	West Memphis, Arkansas and Memphis, Tennessee
Maintained by	Union Pacific Railroad
Design	Cantilevered through Truss bridge
Longest span	791 feet (241 m)
Total length	4,973 feet (1,516 m)
Clearance below	108 feet (33 m)
Opening date	July 14, 1916
Coordinates	 35°07′45″N 90°04′33″W﻿ / ﻿

The **Harahan Bridge** is a cantilevered through truss bridge carrying two rail lines across the Mississippi River between West Memphis, Arkansas and Memphis, Tennessee. The bridge also carried motor vehicles from 1917-1949, when the Memphis & Arkansas Bridge opened. The bridge is currently owned by Union Pacific Railroad.

3. Lyons-Fulton Bridge


	
Carries	2 lanes of Iowa Highway 136/IL-136
Crosses	Mississippi River
Locale	Clinton, Iowa and Fulton, Illinois
Design	Truss bridge
Opening date	January 1975
Coordinates	 41°51'53"N 90°10'23"W

The **Lyons-Fulton Bridge** (actually named the Mark N. Morris Bridge, but locally called the North Bridge) is a 2 lane automobile truss bridge across the Mississippi River in the United States. It connects the cities of Clinton, Iowa and Fulton, Illinois. (The town of Lyons, Iowa, was annexed to Clinton in 1895, but the north end of the city is still referred to as Lyons; hence the name Lyons-Fulton Bridge). The bridge is the terminus of both Iowa Highway 136 and Illinois Route 136.

The bridge was opened in January 1975, replacing an older span upstream that once carried the Lincoln Highway, U.S. Route 30. The older span, was originally built in 1891 with a wooden deck; this was replaced in 1933 with a metal grate to allow snow to melt through.

4. Quincy Bayview Bridge




Carries	2 lanes of Westbound US 24
Crosses	Mississippi River
Locale	West Quincy, Missouri Quincy, Illinois
Design	Cable-stayed bridge
Longest span	900 feet (274 m)
Total length	4,507 feet (1,374 m)
Width	27 feet (8 m)
Clearance below	63 feet (19 m)
Opening date	August 22, 1987
Coordinates	 39°56′00″N, 91°25′17″W

The **Bayview Bridge** is a cable-stayed bridge bringing westbound U.S. Highway 24 over the Mississippi River. It connects the cities of West Quincy, Missouri and Quincy, Illinois. Eastbound U.S. 24 is served by the older Quincy Memorial Bridge.

The bridge was built to alleviate traffic over the downstream Memorial Bridge. It was built prior to the extension of Interstate 72 west into Hannibal, Missouri. Traffic levels increased when the existing, downstream U.S. Highway 36 bridge over the Mississippi River was closed to make room for the new Interstate 72 bridge.

5. Cairo Mississippi River Bridge





Carries	2 lanes of US 60/US 62
Crosses	Mississippi River
Locale	Bird's Point, Missouri and Cairo, Illinois
Design	Cantilever bridge
Longest span	701 feet (214 m)
Total length	5,175 feet (1,577 m)
Clearance below	114 feet (35 m)
Opening date	1929
Coordinates	 36°58'43"N 89°08'52"W

The **Cairo Mississippi River Bridge** is a cantilever bridge carrying U.S. Route 60 and U.S. Route 62 across the Mississippi River between Bird's Point, Missouri and Cairo, Illinois.

Traveling downstream, the Cairo Mississippi River Bridge is the last bridge across the Mississippi River before the confluence of the Mississippi and Ohio Rivers.



6. Cairo I-57 Bridge

	
Carries	4 lanes of I-57
Crosses	Mississippi River
Locale	Charleston, Missouri and Cairo, Illinois
Design	Arch bridge
Longest span	821 feet (250 m)
Clearance below	107 feet (33 m)
Opening date	1978
Coordinates	 37°01'23"N 89°12'42"W

The **Cairo I-57 Bridge** is an arch bridge carrying Interstate 57 across the Mississippi River between Charleston, Missouri and Cairo, Illinois.

This bridge is the newest of the three major river bridges that cross the Mississippi and Ohio rivers at the little town of Cairo, Illinois.


7. Thebes Bridge

	
Carries	Union Pacific, previously the Missouri Pacific Railroad
Crosses	Mississippi River
Locale	Illmo, Missouri and Thebes, Illinois
Design	Continuous truss bridge
Longest span	651 feet (198 m)
Total length	3,959 feet (1,207 m)
Clearance below	104 feet (32 m)
Opening date	April 18, 1905
Coordinates	 37°13'00"N 89°28'01"W

The **Thebes Bridge** is a truss bridge carrying the Union Pacific Railroad (previously carried the Missouri Pacific and Southern Pacific, in a joint operation) across the Mississippi River between Illmo, Missouri and Thebes, Illinois.

8. Bill Emerson Memorial Bridge



Carries	4 lanes of MO 34/MO 74/IL 146
Crosses	Mississippi River
Locale	Cape Girardeau, Missouri and East Cape Girardeau, Illinois
Design	Cable-stayed bridge
Longest span	1,149 feet (350 m)
Total length	3,955 feet (1,205 m)
Width	94 feet (29 m)
Clearance below	60 feet (18 m)
Opening date	December 13, 2003
Coordinates	 37°17'43"N 89°30'57"W


The **Bill Emerson Memorial Bridge** is a cable-stayed bridge connecting Missouri's Route 34 and Route 74 with Illinois Route 146 across the Mississippi River between Cape Girardeau, Missouri and East Cape Girardeau, Illinois.

It was built just south of its predecessor, the Cape Girardeau Bridge, which was completed in 1928 and demolished in 2004. Prior to its destruction, it was documented for the Library of Congress Historic American Engineering Record Survey number HAER MO-84.

The bridge is named after Bill Emerson, a Missouri politician who served in the U.S. House of Representatives from 1981 until his death in 1996.

9. Chester Bridge





Carries	2 lanes of MO 51/IL 150
Crosses	Mississippi River
Locale	Perryville, Missouri and Chester, Illinois
Design	Truss bridge
Longest span	670 feet (204 m)
Total length	2,826 feet (861 m)
Width	22 feet (7 m)
Clearance below	104 feet (32 m)
Opening date	August 23, 1942
Coordinates	 37°54'11"N, 89°50'11"W

The **Chester Bridge** is a truss bridge connecting Missouri's Route 51 with Illinois Route 150 across the Mississippi River between Perryville, Missouri and Chester, Illinois. The Chester Bridge can be seen in the beginning of the 1967 film "In the Heat of the Night".

In the 1940's the main span was destroyed by a tornado. The current span was built to replace it on the original piers.


10. Crescent City Connection

	
Carries	8 lanes of BUS US 90 / I-910 2 reversible HOV lanes
Crosses	Mississippi River
Locale	New Orleans, Louisiana
Design	Twin steel truss cantilever bridges
Longest span	1,575 ft (480 m)
Total length	13,428 ft (4,093 m)
Width	52 ft (16 m) (eastbound) 92 ft (28 m) (westbound)
Clearance below	170 ft (52 m)
Opening date	April 1958 (eastbound) September 1988 (westbound)
Coordinates	 29°56'19"N, 90°03'27"W

The **Crescent City Connection**, abbreviated as **CCC**, (formerly the **Greater New Orleans Bridge**) refers to twin cantilever bridges that carry U.S. Route 90 Business over the Mississippi River in New Orleans, Louisiana. They are tied as the fifth-longest cantilever bridges in the world. Each span carries four general-use automobile lanes; additionally the westbound span has two reversible HOV lanes across the river. It is the most downstream bridge on the Mississippi River.

11. Hernando de Soto Bridge



Carries	6 lanes of I-40
Crosses	Mississippi River
Locale	West Memphis, Arkansas and Memphis, Tennessee
Design	Through arch bridge
Longest span	900 feet (274 m) each
Total length	19,535 feet (5,954 m)
Width	90 feet (27 m)
Clearance below	109 feet (33 m) (varies some due to river level)
Opening date	August 2, 1973
Coordinates	 35°09'10"N 90°03'50"W

The **Hernando de Soto Bridge** is a through arch bridge carrying Interstate 40 across the Mississippi River between West Memphis, Arkansas and Memphis, Tennessee. It is often called the "M Bridge" as the arches resemble the letter M. Memphians also call the bridge the "New Bridge", as it is newer than the Memphis & Arkansas Bridge (carrying Interstate 55) downstream.


The bridge is named for 16th century Spanish explorer Hernando de Soto who explored this stretch of the Mississippi River.

On August 27, 2007, an inspector discovered that a bridge pier on the approach bridge west of the river had settled overnight, and the bridge was subsequently closed to perform a precautionary inspection. The bridge was reopened later that day.

12. Frisco Bridge



Memphis&Arkansas Bridge (*left*), Frisco Bridge (*center*), Harahan Bridge (*right*)

Carries	1 BNSF Railway rail line
Crosses	Mississippi River
Locale	West Memphis, Arkansas and Memphis, Tennessee
Design	Cantilevered through Truss bridge
Longest span	791 feet (241 m)
Total length	4,887 feet (1,490 m)
Width	30 feet (9 m)
Clearance below	109 feet (33 m)
Opening date	May 12, 1892
Coordinates	 35°07'43"N, 90°04'35"W


The **Frisco Bridge**, previously known as the **Memphis Bridge**, is a cantilevered through truss bridge carrying a rail line across the Mississippi River between West Memphis, Arkansas and Memphis, Tennessee.

At the time of the Memphis Bridge construction, it was a significant technological challenge. No other bridges had ever been attempted on the Lower Mississippi River. Besides the difficulty of crossing this far south, it was required to provide at least 75 feet clearance, have a main span of more than 770 ft for the main river channel. It was also required to provide for vehicular and pedestrian traffic on the same level as the rail traffic. Construction began in 1888 and was completed May 12, 1892. In the end the project created a bridge that was the farthest south on the Mississippi River, featured the longest span in the United States. The bridge is listed as a Historic Civil Engineering Landmark.

13. Memphis & Arkansas Bridge





Memphis&Arkansas Bridge (*left*), Frisco Bridge (*center*), Harahan Bridge (*right*)

Carries	4 lanes of I-55/US 61/US 64/US 70/US 79
Crosses	Mississippi River
Locale	West Memphis, Arkansas and Memphis, Tennessee
Design	Cantilevered through Truss bridge
Longest span	770 feet (235 m)
Total length	5,222 feet (1,592 m)
Width	52 feet (16 m)
Clearance below	112 feet (34 m)
Opening date	December 17, 1949
Coordinates	 35°07'42"N, 90°04'36"W

The **Memphis & Arkansas Bridge** is a cantilevered through truss bridge carrying Interstate 55 across the Mississippi River between West Memphis, Arkansas and Memphis, Tennessee. It is referred as the "Old Bridge" to distinguish it from the "New Bridge", or Hernando de Soto Bridge, upstream.



The span is unusual among interstate bridges for the fact that it has a carriageway alongside the vehicular traffic lane that is capable of carrying both pedestrian and bicycle traffic. This area is positioned just outside the main steel support girders on the south side of the bridge and is accessible from the interstate right-of-way on the Arkansas side and a sidewalk access on the Memphis side.

14. Savanna-Sabula Bridge

	
Carries	2 lanes of U.S. Route 52/Iowa Highway 64/IL 64
Crosses	Mississippi River
Locale	Savanna, Illinois and Sabula, Iowa, River Mile 537.8
Design	Steel truss through deck
Total length	2,482 feet
Width	20 Feet, 2 lanes
Opening date	December 31, 1932
Coordinates	 42°06'16"N 90°09'38"W

The **Savanna-Sabula Bridge** is a truss bridge and causeway crossing the Mississippi River and connecting the city of Savanna, Illinois with the island city of Sabula, Iowa. The bridge carries U.S. Highway 52 over the river. It is also the terminus of both Iowa Highway 64 and Illinois Route 64.


15. Sabula Rail Bridge

	
Carries	Single railroad track
Crosses	Mississippi River
Locale	Sabula, Iowa and Savanna, Illinois
Design	Steel truss bridge with swing span
Coordinates	 42°03'51"N 90°09'58"W

The **Sabula Rail Bridge** is a swing bridge that carries a single rail line across the Mississippi River between the island town of Sabula, Iowa and Savanna, Illinois. Originally built for the Milwaukee Railroad, the bridge is operational and is currently owned by the Iowa, Chicago and Eastern Railroad.

16. Huey P. Long Bridge



Carries	4 lanes of US 90 2 tracks of the NOPB
Crosses	Mississippi River
Locale	Jefferson Parish, Louisiana
Design	Cantilever truss bridge
Longest span	790 feet (241 m)
Total length	8,076 feet (2,462 m) (road) 22,996 feet (7,009 m) (rail)
Clearance below	153 feet (47 m)
Opening date	December 1935
Coordinates	 29°56'39"N, 90°10'08"W

The **Huey P. Long Bridge** in Jefferson Parish, Louisiana, is a cantilevered steel through truss bridge that carries a two-track railroad line over the Mississippi River.

Opened in December 1935 to replace the Walnut Street Ferry Bridge. The bridge was the first Mississippi River span built in Louisiana and the 29th along the length of the river.


The widest clear span is 790 feet (240 m) long and sits 135 feet (41 m) above the water. There are three navigation channels below the bridge, the widest being 750 feet (230 m). The distinctive rail structure is 22,996 feet (7,009 m) long and extends as a rail viaduct well into the city. The highway structure is 8,076 feet (2,462 m) long with extremely steep grades on both sides. Each roadway deck is a precarious 18 feet (5.5 m) wide, with 2 9-foot lanes, but because of the railroad component, is unusually flat for a bridge of this height. Normally, bridges this high have a hump to accommodate the height but this bridge is flat to accommodate rail traffic.

The bridge is the longest railroad bridge in the U.S.

17. New Chain of Rocks Bridge



New bridge in foreground, old bridge background


Carries	4 lanes of I-270
Crosses	Mississippi River
Locale	St. Louis, Missouri
Opening date	September 2, 1966
Coordinates	 38°45'53"N 90°10'25"W

The New Chain of Rocks Bridge is a pair of bridges across the Mississippi River on the north edge of St. Louis, Missouri. It was constructed in 1966 to bypass the Chain of Rocks Bridge immediately to the south. It originally carried traffic for Bypass US 66 and currently carries traffic for Interstate 270. The bridge opened to traffic on September 2, 1966.

The original Chain of Rocks Bridge was a narrow bridge with a 22 degree bend midway over the river. Reportedly, two tractor-trailers could not pass each other on that bridge. The Illinois Department of Transportation marks Historic Route 66 over the New Chain of Rocks Bridge, but it is only considered a way to make the route continuous.

18. Chain of Rocks Bridge



Carries	Pedestrians and bicycles
Crosses	Mississippi River
Locale	St. Louis, Missouri
Maintained by	Trailnet
Design	Cantilever through-truss
Total length	5,353 feet (1,632 m)
Width	24 feet (7 m)
Opening date	1929
Coordinates	 38°45′38″N, 90°10′35″W



The **Chain of Rocks Bridge** spans the Mississippi River on the north edge of St. Louis, Missouri. The eastern end of the bridge is on Chouteau Island, (part of Madison, Illinois), while the western end is on the Missouri shoreline.

The Bridge was the route used by U.S. Route 66 to cross over the Mississippi. Its most notable feature is a 22-degree bend occurring at the middle of the crossing, necessary for navigation on the river. Originally a motor route, it now carries walking and biking trails over the river.

The bridge's name comes from a rock-ledged reach of river literally described as a chain of rocks, stretching for seven miles (11 km) immediately to the north of the city of St. Louis.

The bridge was built in 1929. In the late 1930s, Bypass US 66 was designated over this bridge and around the northern and western parts of St. Louis to avoid the downtown area (City US 66 continued to cross the Mississippi River over the MacArthur Bridge). In 1967, the New Chain of Rocks Bridge was built immediately to the bridge's north in order to carry I-270; the Chain of Rocks Bridge was subsequently closed in 1967.



19. Clark Bridge

	
Carries	4 lanes of US 67
Crosses	Mississippi River
Locale	West Alton, Missouri and Alton, Illinois
Design	Cable-stayed bridge
Longest span	756 feet (230 m)
Total length	4,620 feet (1,408 m)
Opening date	January 1994
Coordinates	 38°52'56"N, 90°10'44"W

The **Clark Bridge** (sometimes referred to as the **Superbridge** as the result of its construction being the subject of a documentary aired by Nova) is a cable-stayed bridge across the Mississippi River between West Alton, Missouri and Alton, Illinois.

The bridge was built in 1994 and carries U.S. Route 67 across the river. It is the northernmost river crossing in the St. Louis metropolitan area. The new Clark Bridge replaces the *old Clark Bridge*, a truss bridge built in 1928, also named after explorer William Clark. The bridge carries four lanes of divided highway traffic, as well as two bike lanes, whereas the old bridge only carried two lanes (similar to the upstream Champ Clark Bridge).

20. Martin Luther King Bridge

	
Carries	4 lanes of Image:MO-799.svg Route 799
Crosses	Mississippi River
Locale	St. Louis, Missouri and East St. Louis, Illinois
Design	Cantilever truss bridge
Longest span	962 feet (293 m)
Total length	4,009 feet (1,222 m)
Width	40 feet (12 m)
Vertical clearance	19.4 feet (6 m)
Clearance below	98 feet (30 m)
Opening date	1951
Coordinates	 38°37'52"N 90°10'46"W


The **Martin Luther King Bridge** (formerly known as the **Veterans Bridge**) in St. Louis is a cantilever truss bridge of about 4000 feet in total length across the Mississippi River, connecting St. Louis with East St. Louis, Illinois. The bridge serves as traffic relief connecting the concurrent freeways of Interstate 55, Interstate 70, Interstate 64, and U.S. Route 40 with the downtown streets of St. Louis.

The bridge was built in 1951 as the **Veterans' Memorial Bridge** to relieve congestion on the MacArthur Bridge to the south.

Eventually, ownership was transferred dually to the Missouri and Illinois Departments of Transportation and the bridge was renamed after Martin Luther King, Jr. In the spring of 1989, the rebuilt bridge was reopened.

21. Eads Bridge



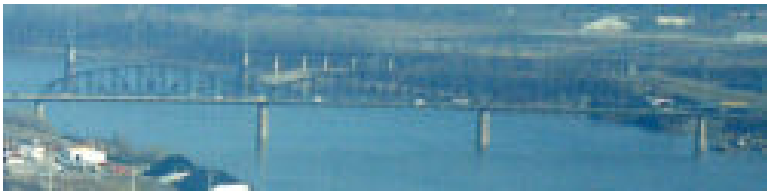

Carries	4 highway lanes 2 MetroLink tracks
Crosses	Mississippi River
Locale	St. Louis, Missouri and East St. Louis, Illinois
Design	Arch bridge
Longest span	520 feet (158 m)
Total length	6,442 feet (1,964 m)
Width	46 feet (14 m)
Clearance below	88 feet (27 m)
Opening date	1874
Coordinates	 38°37'45"N 90°10'47"W

The **Eads Bridge** is a combined road and railway bridge over the Mississippi River at St. Louis, connecting St. Louis and East St. Louis, Illinois.

When completed in 1874, the Eads Bridge was the longest arch bridge in the world, with an overall length of 6,442 feet (1,964 m). The ribbed steel arch spans were considered daring, as was the use of steel as a primary structural material: it was the first such use of true steel in a major bridge project.

The Eads Bridge was also the first bridge to be built using cantilever support methods exclusively, and one of the first to make use of pneumatic caissons. The particular physical difficulties of the site stimulated interesting solutions to construction problems. The deep caissons used for pier and abutment construction signalled a new chapter in civil engineering. The triple span, tubular metallic arch construction was supported by two shore abutments and two mid-river piers. The Eads Bridge is still in use.



22. McKinley Bridge

	
Carries	1 dedicated service lane, 2 lanes of traffic, and 1 dedicated pedestrian/bicycle lane
Crosses	Mississippi River
Locale	St. Louis, Missouri and Venice, Illinois
Design	Steel truss bridge
Longest span	3 519 feet (158 m) spans
Total length	6,313 feet (1,924 m)
Clearance below	90 feet (27 m)
Opening date	November 10, 1910 November 17, 2007 (pedestrian reopening) December 17, 2007 (full reopening)
Coordinates	 38°39'54"N 90°10'58"W

The **McKinley Bridge** is a steel truss bridge across the Mississippi River. It connects northern portions of the city of St. Louis, Missouri with Venice, Illinois. It opened in 1910 and was taken out of service on October 30, 2001. The bridge was reopened for pedestrian and bicyclists on a November 17, 2007. Since December 2007, McKinley has been open to vehicular traffic as well. The bridge carried both railroad and vehicular traffic across the Mississippi River for decades. By 1978, the railroad line over the span was closed, and an additional set of lanes were opened for vehicles in the inner roadway.

Rehabilitation began in 2004. The Bridge reopened to pedestrians and bicycles on November 17, 2007. The bridge was fully reopened to traffic on December 17, 2007.



23. Poplar Street Bridge

	
Official name	Bernard F. Dickmann Bridge
Carries	8 lanes of I-55/I-64/I-70/US 40
Crosses	Mississippi River
Locale	St. Louis, Missouri and East St. Louis, Illinois
Design	Steel girder bridge
Longest span	600 feet (183 m)
Total length	2,164 feet (660 m)
Width	104 feet (32 m)
Clearance below	92 feet (28 m)
Opening date	1967
Coordinates	 38°37'05"N 90°10'59"W

The **Poplar Street Bridge**, officially the **Bernard F. Dickmann Bridge**, completed in 1967, is a 647-foot (197 m) long (197m) deck girder bridge across the Mississippi River between St. Louis, Missouri and East St. Louis, Illinois. The bridge arrives on the Missouri shore line just south of the Gateway Arch.

Interstate 55, Interstate 64, Interstate 70, and U.S. Route 40 cross the Mississippi on the Poplar Street bridge. It is crossed by approximately 120,000 vehicles daily, making it possibly the most heavily used bridge on the river.

24. MacArthur Bridge

	
Carries	Terminal Railroad Association of St. Louis, Union Pacific
Crosses	Mississippi River
Locale	St. Louis, Missouri and East St. Louis, Illinois
Design	Truss bridge
Longest span	677 feet (206 m)
Total length	18,261 feet (5,566 m)
Clearance below	108 feet (33 m)
Opening date	1917
Destruction date	To auto traffic 1981
Coordinates	 38°36'53"N 90°11'01"W

The MacArthur Bridge over the Mississippi River between St. Louis, Missouri and East St. Louis, Illinois is a 647 foot (197 m) long truss bridge. Construction on the bridge began in 1909 by the city of St. Louis to break the monopoly the Terminal Railroad Association of St. Louis had on the area's railroad traffic at the time. However, money ran out before the bridge approaches could be finished and the bridge did not open until 1917, and even then only to automobile traffic. Railroad traffic would not make use of the bridge's lower deck until 1928.


Initially, the bridge was called the "St. Louis Municipal Bridge" and known as the "Free Bridge."

The MacArthur Bridge was one of several bridges in St. Louis which carried U.S. Highway 66 until the completion of the nearby Poplar Street Bridge. At one time, U.S. Highway 460 crossed the bridge, terminating on the west side of the bridge. The bridge is now in use only by railroads.

25. Gateway Bridge




Copyright © 2008 John A. Weeks III

Carries	2 lanes of U.S. Route 30
Crosses	Mississippi River
Locale	Clinton, Iowa and Fulton, Illinois
Design	Suspension bridge
Opening date	June 1956
Coordinates	 41°50'16"N 90°11'02"W

The **Gateway Bridge** (locally called the **South Bridge**) is a suspension bridge over the Mississippi River in Clinton, Iowa, USA. It carries U.S. Route 30 from Iowa into Illinois just south of Fulton, Illinois. The bridge itself is two travel lanes wide. The Gateway Bridge was closed in March 2006 for repainting and reconstruction of U.S. Route 30 on the Illinois side of the river, and reopened in November 2006. Traffic on U.S. Route 30 intending to cross the river was detoured north to the Lyons-Fulton Bridge.

26. Merchants Bridge




Carries	Rail line
Crosses	Mississippi River
Locale	St. Louis, Missouri
Design	Steel truss bridge
Opening date	1889
Coordinates	 38°40'29"N 90°11'10"W

The **Merchants Bridge** is a rail bridge crossing the Mississippi River in St. Louis, Missouri owned by the Terminal Railroad Association of St. Louis. It opened in May 1889 and crossed the river three miles north of Eads Bridge.

The bridge was originally built by the St. Louis Merchants Exchange after it lost control of the Eads Bridge it had built to the Terminal Railroad. The Exchange feared a Terminal Railroad monopoly on the bridges but it would eventually lost control of the Merchants Bridge also.

27. Jefferson Barracks Bridge





Carries	6 lanes of I-255/US 50
Crosses	Mississippi River
Locale	St. Louis, Missouri and Columbia, Illinois
Design	Two tied arch bridges
Longest span	910 feet (277 m)
Total length	3,998 feet (1,219 m)
Clearance below	88 feet (27 m)
Opening date	September 30, 1983 (westbound) 1992 (eastbound)
Coordinates	 38°29'14"N 90°16'38"W

The **Jefferson Barracks Bridge**, often called the **J.B. Bridge**, is a pair of bridges that span the Mississippi River on the south side of St. Louis, Missouri. Both bridges are 909-foot (277 m) long steel arch bridges. The first bridge was built in 1983, the south bridge opened in 1992. A delay occurred during the construction of the second bridge when a crane dropped a section of it into the river and it had to be rebuilt.

They replaced the former steel truss bridge built in 1941 that originally carried U.S. Highway 50. It carries traffic for Interstate 255 (part of the St. Louis beltway) and U.S. Highway 50.

28. Fred Schwengel Memorial Bridge



	
Carries	4 lanes of I-80
Crosses	Mississippi River
Locale	Le Claire, Iowa and Rapids City, Illinois
Total length	3,483 feet (1,062 m)
Width	66 feet (20 m)
Opening date	October 27, 1966
Coordinates	 41°34'49"N 90°21'54"W

The **Fred Schwengel Memorial Bridge** is a 4-lane steel girder bridge that carries Interstate 80 across the Mississippi River between Le Claire, Iowa and Rapids City, Illinois.

The bridge opened October 27, 1966 and overlooks the Iowa and Illinois Welcome centers, as well as Rapids City, Illinois and LeClaire, Iowa.



The bridge is named for Fred Schwengel, a former U.S. Representative from Davenport, Iowa and one of the driving forces behind the Interstate Highway Act.

29. I-74 Bridge

	
Carries	4 lanes of I-74/U.S. Route 6
Crosses	Mississippi River
Locale	Bettendorf, Iowa and Moline, Illinois
Design	Twin suspension bridges
Total length	3,372 feet (1,028 m)
Width	27 feet (8 m)
Opening date	November 1935 (northbound) December 1959 (southbound)
Coordinates	 41°31'12"N, 90°30'48"W

Originally known as the **Iowa-Illinois Memorial Bridge**, today it is more commonly referred to as the **I-74 Bridge**. The bridge crosses the Mississippi River and connects Bettendorf, Iowa and Moline, Illinois. It is located near the geographic center of the Quad Cities. The first span opened in 1935 as a toll bridge. In 1959 an identical twin span was added to satisfy increased traffic. The twin spans were upgraded to carry interstate traffic in the mid-1970's.



30. Rock Island Government Bridge

	
Carries	2 lanes of roadway 1 rail line
Crosses	Mississippi River
Locale	Davenport, Iowa and Rock Island, Illinois
Designer	Ralph Modjeski ^[1]
Design	two riveted Pratt trusses five riveted Baltimore trusses one pin-connected Baltimore swing truss
Material	steel
Total length	1,608 feet (490 m)
Width	27 feet (8 m)
Opening date	1896
Coordinates	 41°31'09"N 90°34'01"W

The **Rock Island Government Bridge**, or Arsenal Bridge, spans the Mississippi River connecting Rock Island, Illinois and Davenport, Iowa. The current structure, the fourth in a succession at this location, includes a swing section to accommodate traffic navigating the locks. The first bridge, constructed in the early 1850s and located around 1500 feet upstream of the present, was the first bridge to ever span the Mississippi River. All that remains of the first bridge are two piers on opposite sides of the river.

The current Government Bridge is the fourth crossing of the Mississippi in this vicinity, having been built in 1896 on the same location and using the same piers as the 1872 structure.

31. Rock Island Centennial Bridge



	
Carries	4 lanes of US 67
Crosses	Mississippi River
Locale	Davenport, Iowa and Rock Island, Illinois
Design	Steel arch bridge
Total length	4,447 feet (1,355 m) ^[1]
Clearance below	66 feet (20 m)
Opening date	July 12, 1940 ^[3]
Coordinates	 41°30′54″N, 90°34′54″W

The **Centennial Bridge**, or Rock Island Centennial Bridge, connects Rock Island, Illinois and Davenport, Iowa. The bridge is 3,850 feet (1,173 m) long and stands 170 feet (52 m) above water level. Construction of the bridge began in 1938 and it opened on July 12, 1940.

It was originally going to be named the "Galbraith Bridge", after Rock Island's mayor at the time, Robert Galbraith. He suggested it be named the Centennial Bridge, in commemoration of the city of Rock Island's centennial.

The five arches of the bridge are a symbol often used to represent the Quad Cities.

32. Helena Bridge


	
Carries	2 lanes of US 49
Crosses	Mississippi River
Locale	Helena-West Helena, Arkansas and Lula, Mississippi
Design	Cantilever bridge
Longest span	804 feet (245 m)
Total length	5,204 feet (1,586 m)
Width	28 feet (9 m)
Clearance below	119 feet (36 m)
Opening date	July 27, 1961
Coordinates	 34°29'48"N 90°35'17"W

The **Helena Bridge** is a cantilever bridge carrying US 49 across the Mississippi River between Helena-West Helena, Arkansas and Lula, Mississippi.

The main cantilever span was modeled on the similar Benjamin G. Humphreys Bridge which had been built downstream by Arkansas & Mississippi roughly two decades earlier. However, the river navigation issues that led to the pending replacement of the Humphreys Bridge with the Greenville Bridge do not apply to the Helena Bridge, as the river curve here is far less severe than the one just upstream from the Humphreys Bridge.



33. I-280 Bridge



Carries	4 lanes of I-280
Crosses	Mississippi River
Locale	Davenport, Iowa and Rock Island, Illinois
Design	Tied arch Bridge
Total length	4,194 feet (1,278 m)
Width	82 feet, 4 lanes
Opening date	October 25, 1973
Coordinates	 41°28'45"N 90°37'56"W

The **I-280 Bridge** carries Interstate 280 across the Mississippi River between Davenport, Iowa and Rock Island, Illinois.

34. Dubuque-Wisconsin Bridge


	
Carries	4 lanes of U.S. Route 61/U.S. Route 151
Crosses	Mississippi River
Locale	Dubuque, Iowa, with Grant County, Wisconsin
Design	Tied arch bridge
Longest span	670 feet (204 m)
Total length	2,951 feet (899 m)
Clearance below	65 feet (20 m)
Opening date	August 21, 1982
Coordinates	 42°30'56"N 90°38'08"W

The **Dubuque-Wisconsin Bridge** is a steel tied arch bridge connecting Dubuque, Iowa, with still largely rural Grant County, Wisconsin. It is an automobile bridge that traverses the Mississippi River. It is one of two automobile bridges in the Dubuque area. A railroad bridge is between them. The Julien Dubuque Bridge - the other automobile bridge - is located about three miles (5 km) south.

The bridge is a four lane, limited access bridge. It is part of the US Highway 61/151 route. This bridge replaced the older Eagle Point Bridge that previously served as the connection between Dubuque and Wisconsin.

35. Julien Dubuque Bridge



Carries	2 lanes of U.S. Route 20 1 pedestrian walkway
Crosses	Mississippi River
Locale	Dubuque, Iowa, and East Dubuque, Illinois
Design	Continuous steel arch truss bridge
Longest span	845 feet (258 m)
Total length	5,760 feet (1,756 m)
Width	29 feet (9 m)
Clearance below	64 feet (20 m)
Opening date	1943
Coordinates	 42°29'30"N 90°39'22"W


The **Julien Dubuque Bridge** traverses the Mississippi River. It joins the cities of Dubuque, Iowa, and East Dubuque, Illinois. The bridge is part of the U.S. Highway 20 route. It is one of two automobile bridges over the Mississippi in the area (the Dubuque-Wisconsin Bridge three miles (5 km) north links Dubuque with Wisconsin), and is listed in the National Register of Historic Places. In 1942, the first parts of the bridge were begun. In 1943, the bridge was completed.

In the early 1990s, the bridge underwent an extensive renovation. The deck was completely replaced, and a new walkway was installed on the bridge.

On June 9, 2008 the bridge was struck by a number of runaway barges. On June 10th the Iowa Department of Transportation inspected the bridge and determined that it was safe and they had reopened the bridge to traffic.

36. Old Vicksburg Bridge




Carries	1 Kansas City Southern rail line, one service lane
Crosses	Mississippi River
Locale	Delta, Louisiana and Vicksburg, Mississippi
Design	Cantilever bridge
Longest span	825 feet (251 m)
Total length	8,546 feet (2,605 m)
Clearance below	116 feet (35 m)
Opening date	May 1, 1930
Coordinates	 32°18'52"N 90°54'17"W

The **Old Vicksburg Bridge** is a cantilever bridge carrying one rail line across the Mississippi River between Delta, Louisiana and Vicksburg, Mississippi. Until 1998, the bridge was open to motor vehicles and carried US 80 across the Mississippi River, though one road lane runs through the bridge for inspection by workers.

37. Vicksburg Bridge




Carries	4 lanes of I-20/US 80
Crosses	Mississippi River
Locale	Delta, Louisiana and Vicksburg, Mississippi
Design	Cantilever bridge
Longest span	870 feet (265 m)
Total length	12,974 feet (3,954 m)
Width	60 feet (18 m)
Clearance below	116 feet (35 m)
Opening date	February 14, 1973
Coordinates	 32°18'55"N 90°54'30"W

The **Vicksburg Bridge** is a cantilever bridge carrying Interstate 20 and US 80 across the Mississippi River between Delta, Louisiana and Vicksburg, Mississippi. Next to it is the Old Vicksburg Bridge.

38. Sunshine Bridge




Carries	4 lanes of LA 70
Crosses	Mississippi River
Locale	Sorrento, Louisiana and Donaldsonville, Louisiana
Design	Cantilever bridge
Longest span	825 feet (251 m)
Total length	8,236 feet (2,510 m)
Width	4 lanes
Clearance below	170 feet (52 m)
Opening date	August 1964
Coordinates	 30°05'53"N 90°54'44"W

The **Sunshine Bridge** is a cantilever bridge over the Mississippi River in St. James Parish, Louisiana. Completed in 1963, it carries LA 70, which connects Donaldsonville on the west bank of Ascension Parish with Sorrento on the east bank of Saint James Parish as well as with Gonzales on the east bank of Ascension Parish. The approach roads on the east and west banks begin in Ascension Parish before crossing into St. James Parish.

At time of construction it was the only bridge across the Mississippi between New Orleans and Baton Rouge.



39. Norbert F. Beckey Bridge



Carries	2 lanes of Iowa Highway 92 and IL 92
Crosses	Mississippi River
Locale	Muscatine, Iowa and Illinois
Total length	3,018 feet (920 m)
Opening date	December 2, 1972
Coordinates	 41°25'21"N, 91°02'01"W

The **Norbert F. Beckey Bridge**, or Beckey Bridge for short, carries Iowa Highway 92 and Illinois Route 92 across the Mississippi River between Muscatine, Iowa and Rock Island County, Illinois. Completed in December 1972, it replaced the Muscatine High Bridge which stood from 1891-1973. A pillar from the old High Bridge still stands at Riverside Park in Muscatine.


40. Louisiana Rail Bridge

	
Carries	Single track rail line
Crosses	Mississippi River
Locale	Louisiana, Missouri and Illinois
Coordinates	 39°26'43"N 91°02'01"W

The **Louisiana Railroad Bridge** carries a single track rail line across the Mississippi River between Louisiana, Missouri and Pike County, Illinois. It is currently owned by the Kansas City Southern Railway. This bridge was opened for service in 1873.

41. Champ Clark Bridge





Carries	2 lanes of US 54
Crosses	Mississippi River
Locale	Louisiana, Missouri and Illinois
Design	Truss bridge
Longest span	418 feet (127 m)
Total length	2,286 feet (697 m)
Width	20 feet (6 m)
Opening date	1928
Coordinates	 39°27'24"N 91°02'52"W

The **Champ Clark Bridge** is a five-span truss bridge over the Mississippi River connecting Louisiana, Missouri with the state of Illinois. It carries U.S. Route 54 northeast to Pittsfield, Illinois, where U.S. 54 terminates.

The bridge is narrow, allowing for two lanes of traffic on a 20 feet (6 m) deck. It was built in 1928. The bridge, originally painted silver, was repainted deep green in 1983, and repaired in 1999. In 2005, the Missouri Department of Transportation again rehabbed and repainted the bridge, replacing the green color of the bridge with gray. The bridge is 2,286.4 feet (697 m) in length. The span over the main channel of the Mississippi River is 418.5 feet (128 m) in length.



42. Burlington Rail Bridge

	
Carries	Double track rail line
Crosses	Mississippi River
Locale	Burlington, Iowa and Gulf Port, Illinois
Design	6 truss spans and one swing-span
Opening date	1893
Coordinates	 40°47'55"N 91°05'31"W

The **Burlington Bridge** carries a double tracked rail lines across the Mississippi River between Burlington, Iowa, and Gulf Port, Illinois. The bridge is currently owned by BNSF Railway as part of its Chicago to Denver mainline. It is somewhat controversial in that its swing-span only allows one barge to pass at a time.

The original bridge at this location was constructed in 1868. It was reconstructed in 1893 in its current form.

43. Great River Bridge

	
Carries	4 lanes of US 34
Crosses	Mississippi River
Locale	Burlington, Iowa and Gulf Port, Illinois
Design	Cable-stayed bridge
Longest span	660 feet (201 m)
Total length	1,245 feet (379 m)
Width	27 feet (8 m)
Clearance below	60 feet (18 m)
Opening date	October 4, 1993
Coordinates	 40°48'43"N, 91°05'44"W


The **Great River Bridge** is an asymmetrical, one-tower cable-stayed bridge over the Mississippi River. It carries U.S. Highway 34 from Burlington, Iowa to the town of Gulf Port, Illinois.

Construction began in 1989, but work on the main tower did not begin until April 1990. The main tower is 370 feet (113 m) in height from the top of the tower to the riverbed. During the Great Flood of 1993, construction continued despite record crests on the Mississippi below.

The Great River Bridge replaced the MacArthur Bridge, an aging two-lane toll steel bridge built in 1917. The new bridge is five lanes wide (two westbound, three eastbound) and provides a safer crossing across the Mississippi River than the old bridge.

44. Greenville Bridge




Carries	4 lanes of US 82 and US 278
Crosses	Mississippi River
Locale	Lake Village, Arkansas and Greenville, Mississippi
Design	Cable-stayed bridge
Longest span	1,378 feet (420 m)
Total length	13,560 feet (4,133 m)
Width	80 ft.
Clearance below	122 feet (37 m)
Opening date	Fall 2009
Coordinates	 33°17'14"N 91°09'15"W

The **Greenville Bridge** is a cable-stayed bridge crossing the Mississippi River between the U.S. states of Arkansas and Mississippi.

The main span of the bridge was completed April 17, 2006, but has yet to open to traffic. When the approach roads are finished in early 2009, the bridge will carry US 82 (and, until the Charles W. Dean Bridge is built, US 278) across the river between Lake Village, Arkansas and Greenville, Mississippi.

45. Benjamin G. Humphreys Bridge





Carries	2 lanes of US 82 and US 278
Crosses	Mississippi River
Locale	Lake Village, Arkansas and Greenville, Mississippi
Design	Cantilever bridge
Longest span	840 feet (256 m)
Total length	9,957 feet (3,035 m)
Width	24 feet (7 m)
Clearance below	130 feet (40 m)
Opening date	October 4, 1940
Destruction date	Fall 2009
Coordinates	 33°17'37"N 91°09'34"W

The **Benjamin G. Humphreys Bridge** is a two lane cantilever bridge carrying US 82 and US 278 across the Mississippi River between Lake Village, Arkansas and Greenville, Mississippi. The bridge is named for Benjamin G. Humphreys II, a former United States Congressman from Greenville. A new bridge, the Greenville Bridge, is being built as a replacement slightly downriver. This is because the bridge is a navigation hazard for vehicles on the bridge as well as barges going underneath the bridge.

On October 4, 1940, the Bridge was officially opened to traffic.

Until the Charles W. Dean Bridge is constructed, US 278 will cross the Mississippi River at Greenville.


46. Horace Wilkinson Bridge

	
Carries	6 lanes of I-10
Crosses	Mississippi River
Locale	Baton Rouge, Louisiana
Design	Cantilever bridge
Longest span	1,235 feet (376 m)
Total length	4,550 feet (1,387 m) (superstructure) 14,150 feet (4,313 m) (overall)
Width	80 feet (24 m)
Clearance below	175 feet (53 m)
Opening date	April 10, 1968
Coordinates	 30°26'22"N 91°11'47"

The **Horace Wilkinson Bridge** is a cantilever bridge carrying Interstate 10 across the Mississippi River from Port Allen in West Baton Rouge Parish to Baton Rouge, Louisiana. This is the only point where Interstate 10 crosses the Mississippi River in Louisiana. Around the Baton Rouge Metropolitan Area, the bridge is more commonly known as the "New Bridge" because it is the youngest of the two bridges that cross the river at Baton Rouge. The structure begins at the Louisiana Highway 1 exit south of Port Allen. After the interstate crosses the superstructure, it remains an elevated viaduct up to the Dalrymple Drive exit to Louisiana State University. Locally it is notorious for daily traffic snags due to the high volume of vehicles using the bridge and the style of entrances from Highway 1 on the west bank, and from St. Ferdinand Street in downtown on the east bank.

47. Black Hawk Bridge




Carries	2 lanes of IA 9 and WI 82
Crosses	Upper Mississippi River
Locale	Lansing, Iowa and Crawford County, Wisconsin, River Mile 663.4
Design	Melvin B. Stone
Total length	1,653 feet (504 m)
Width	21 feet (6 m), 2 Lanes
Clearance below	68 feet (21 m)
Opening date	June 17, 1931
Coordinates	 43°21'55"N, 91°12'54"W

The **Black Hawk Bridge** spans the Mississippi River, joining the town of Lansing, in Allamakee County, Iowa, to rural Crawford County, Wisconsin. It is the northernmost Mississippi River bridge in Iowa. It carries Iowa Highway 9 and Wisconsin Highway 82.

This riveted cantilever through truss bridge (other examples) has one of the more unusual designs of any Mississippi River bridge. Construction started in 1929 and was completed in 1931.

48. Fort Madison Toll Bridge




Carries	2 lanes of IA 2 and IL 9 and rail lines
Crosses	Mississippi River
Locale	Fort Madison, Iowa and Niota, Illinois
Opening date	July 1928
Coordinates	 40°37'37"N 91°17'45"W

The **Fort Madison Toll Bridge** (also known as the **Santa Fe Swing Span Bridge** for the old Santa Fe rail line) is a tolled, swinging truss bridge over the Mississippi River that connects Fort Madison, Iowa and unincorporated Niota, Illinois. Rail traffic occupies the lower deck of the bridge, while two lanes of road traffic occupy the upper deck. It is widely considered the longest double-deck swing-span bridge in the world.

Completed in 1927, it replaced an inadequate combination single-track / roadway bridge completed in 1887. The main river crossing consists of four 270-foot (82 m) through truss spans and a swing span made of two equal arms, 266 feet (81 m) long.

49. John James Audubon Bridge



Carries	4 lanes of LA 10
Crosses	Mississippi River
Locale	Pointe Coupee Parish, Louisiana, West Feliciana Parish, Louisiana
Design	Cable-stayed bridge
Longest span	1,583 feet (482 m)
Total length	12,883 feet (3,927 m)
Width	64 feet (20 m)
Clearance below	65 feet (20 m)
Opening date	Approx. 2010
Coordinates	 30°43'39"N 91°21'18"W

The **John James Audubon Bridge** project is a new Mississippi River crossing between Pointe Coupee and West Feliciana parishes in south central Louisiana.

The bridge--proposed to be the longest cable-stayed bridge in North America when complete--will replace an existing ferry between the communities of New Roads and St. Francisville.

The bridge will also serve as the only bridge structure on the Mississippi River between Natchez, Mississippi and Baton Rouge, Louisiana (approximately 90 river miles).


The Audubon Bridge project will include:

A 2.44-mile (3.93 km) four-lane elevated bridge structure with two 11-foot (3.4 m) travel lanes in each direction with 8-foot (2.4 m) outside shoulders and 2-foot (0.61 m) inside shoulders

The John James Audubon Bridge project is expected to be complete by summer 2010.

50. Mark Twain Memorial Bridge



Carries	4 lanes of I-72 and US 36
Crosses	Mississippi River
Locale	Hannibal, Missouri
Longest span	640 feet (195 m)
Total length	4,491 feet (1,369 m)
Width	86 feet (26 m)
Opening date	September 16, 2000
Coordinates	 39°43'13"N 91°21'30"W

The **Mark Twain Memorial Bridge** is the name for two bridges over the Mississippi River at Hannibal, Missouri. The current bridge, north of the original site, was finished in 2000; the original bridge, built in 1936, was demolished. The bridge currently carries traffic for Interstate 72 and U.S. Highway 36.


The original bridge (also called the Mark Twain Memorial Bridge) was opened in 1936. It originally carried only US 36, but with the extension of Interstate 72 west across Missouri, a new bridge was needed and was built to the north of the original bridge.

The current bridge opened to traffic on September 16, 2000. As part of the construction project, U.S. 36 was rerouted further north, eliminating a dangerous sharp curve that had been on the Missouri approach. Prior to the rerouting, the old bridge ran through downtown Hannibal, just north of Hill Street.

51. Wabash Bridge (w/ vertical lift)



The Wabash Bridge looking southeast

Carries	1 track of Norfolk Southern
Crosses	Mississippi River
Locale	Hannibal, Missouri and Illinois
Design	5 Truss spans with Vertical lift over main channel
Longest span	409 feet (125 m)
Coordinates	 39°43'27"N 91°21'44"W


The **Wabash Bridge** carries rail lines across the Mississippi River between Hannibal, Missouri and Illinois.

It has been a vertical lift bridge since 1994, but it was originally constructed as a swing span. The vertical lift span was relocated from a bridge over the Tennessee River at Florence, Alabama to increase the width of the navigational channel. During a three day outage, the previous span was removed and the replacement span was installed to minimize impact to traffic. Originally constructed for the Wabash Railroad.

A 250-foot truss span was struck by the towboat and collapsed into the river on May 3, 1982. The bridge span was repaired.

52. Keokuk Rail Bridge





Carries	Double deck single track railway and highway bridge
Crosses	Mississippi River
Locale	Keokuk, Iowa and Hamilton, Illinois
Design	Swing bridge
Opening date	1916
Coordinates	 40°23'28"N 91°22'24"W

The **Keokuk Bridge**, also known as the Keokuk & Hamilton Bridge, carries a double deck single track railway and highway bridge across the Mississippi River between Keokuk, Iowa and Hamilton, Illinois. Designed and constructed 1915–1916 on the piers of its predecessor that was constructed in 1869–1871.

Following the completion of the Keokuk-Hamilton Bridge, the upper deck of this bridge, on the Keokuk side, was converted to an observation deck to view the nearby lock and dam and is no longer used for road traffic, but is still used for rail traffic.

53. Keokuk-Hamilton Bridge


	
Carries	4 lanes of US 136
Crosses	Mississippi River
Locale	Keokuk, Iowa and Hamilton, Illinois
Design	Steel girder bridge
Opening date	November 1985
Coordinates	 40°23'25"N 91°22'24"W

The **Keokuk-Hamilton** bridge is a steel girder, 4-lane bridge from Keokuk, Iowa to Hamilton, Illinois. It carries U.S. Route 136 across the Mississippi River.

The Keokuk-Hamilton Bridge was built in 1985, taking over automobile traffic from the Keokuk Rail Bridge (though the latter bridge still carries rail traffic).

54. Natchez-Vidalia Bridge




Carries	4 lanes of US 65/US 84/US 425
Crosses	Mississippi River
Locale	Vidalia, Louisiana and Natchez, Mississippi
Design	Twin Cantilever bridges
Longest span	3 848 feet (258 m) spans per bridge
Total length	4,205 feet (1,282 m) (westbound) 4,202 feet (1,281 m) (eastbound)
Width	24 feet (7 m) (westbound) 42 feet (13 m) (eastbound)
Clearance below	125 feet (38 m)
Opening date	October 1940 (westbound) July 1988 (eastbound)
Coordinates	 31°33'33"N 91°25'09"W

The **Natchez-Vidalia Bridge** are two twin cantilever bridges carrying US Routes 65, 84 and 425 across the Mississippi River between Vidalia, Louisiana and Natchez, Mississippi.

55. Quincy Memorial Bridge




Carries	2 lanes of Eastbound US 24
Crosses	Mississippi River
Locale	West Quincy, Missouri and Quincy, Illinois
Design	Truss bridge
Longest span	627 feet (191 m)
Total length	3,510 feet (1,070 m)
Width	27 feet (8 m)
Clearance below	63 feet (19 m)
Opening date	1928
Coordinates	 39°55'53"N 91°25'14"W

The **Quincy Memorial Bridge** is a truss bridge over the Mississippi River in Quincy, Illinois. It brings eastbound U.S. Highway 24 into the city of Quincy from Missouri. It was built in 1928 and remains structurally sound.

In 1986, to serve additional traffic volumes crossing the Mississippi River into Quincy, the Illinois Department of Transportation constructed the Bayview Bridge just to the north of the Memorial Bridge. Westbound traffic was then routed onto the Bayview Bridge, while eastbound traffic was routed onto the Memorial Bridge.

56. Bayview Bridge



Carries	2 lanes of Westbound US 24
Crosses	Mississippi River
Locale	West Quincy, Missouri Quincy, Illinois
Design	Cable-stayed bridge
Longest span	900 feet (274 m)
Total length	4,507 feet (1,374 m)
Width	27 feet (8 m)
Clearance below	63 feet (19 m)
Opening date	August 22, 1987
Coordinates	 39°56'00"N 91°25'17"W


The **Bayview Bridge** is a cable-stayed bridge bringing westbound U.S. Highway 24 over the Mississippi River. It connects the cities of West Quincy, Missouri and Quincy, Illinois. Eastbound U.S. 24 is served by the older Quincy Memorial Bridge.

The bridge was built to alleviate traffic over the downstream Memorial Bridge. It was built prior to the extension of Interstate 72 west into Hannibal, Missouri. Traffic levels increased when the existing, downstream U.S. Highway 36 bridge over the Mississippi River was closed to make room for the new Interstate 72 bridge.

57. Quincy Rail Bridge



Copyright © 2008 John A. Weeks III

Crosses	Mississippi River
Locale	West Quincy, Missouri and Quincy, Illinois
Design	Vertical lift span over main channel
Coordinates	 39°56'30"N 91°25'51"W


The **Quincy Rail Bridge** carries rail lines across the Mississippi River between West Quincy, Missouri and Quincy, Illinois, USA. Originally constructed for the Chicago, Burlington and Quincy Railroad which is now BNSF Railway.

From the 1950s until 1971 it served the Kansas City Zephyr and American Royal Zephyr daily passenger trains between Chicago and Kansas City. It served Amtrak's Illinois Zephyr from Chicago to West Quincy, MO from 1971 to 1993.

Since the Great Flood of 1993 Amtrak *Illinois Zephyr* and *Carl Sandburg* service terminates at the Quincy station. This Mississippi river crossing does serve as a backup route should the Fort Madison Toll Bridge crossing be unavailable.

58. Moline-Arsenal Bridge




Carries	2 Lanes, Rodman Avenue
Crosses	Mississippi River
Locale	River Mile 485.7, Moline, Illinois
Design	Steel girder, concrete deck.
Longest span	230 feet
Total length	1,344 feet
Width	42 feet
Clearance below	28 feet
Opening date	April 1982.
Coordinates	 41°30'37"N 90°31'07"W

This bridge is one of three highway bridges serving the Rock Island Arsenal. Prior to 9/11, one could simply drive across the bridge and tour the Arsenal. Today, security is high, and one has to have a need to enter the island. There is an Army museum, National River Visitors Center, Lock and Dam #15 overlook, National Cemetery, and a historical driving tour, all of which are good reasons to take a tour of the island.

This is a very historic river crossing. The first structure here was a dam built in 1837. It was used by pedestrians, and was wide enough for wagons to cross. That dam survived until 1868. A wooden bridge was built by the City of Moline in 1860, but it was destroyed by ice in 1867. An iron bridge was built in 1873, and was replaced by a concrete arch bridge in 1932. That bridge was built with substandard concrete, and it gradually crumbled under its own weight. It was closed in 1981, and replaced with the current modern steel girder bridge.

59. Crescent Rail Bridge




Carries	Burlington Northern Santa Fe Railroad.
Crosses	Mississippi River
Locale	Davenport, Iowa and Rock Island, Illinois
Design	Steel Truss Through Deck w/Swing Span
Longest span	442 ft swing span
Total length	2,383 ft
Width	1 track
Clearance below	26 ft
Opening date	1899
Coordinates	 41°30'42"N 90°35'41"W

The **Crescent Rail Bridge** carries rail lines across the Mississippi River between Davenport, Iowa and Rock Island, Illinois. The bridge and the Illinois track are owned by BNSF, and the Iowa side is a Canadian Pacific line.

Bridge is called the Crescent Bridge due to its curved shape. The hump back bridge sections and the swing span form a straight line. But the three smaller flat top bridge sections form an arc to allow the bridge to meet up with the railroad that runs parallel to the river on the Illinois side without that railroad taking up a lot of space by making a big loop.

60. Double Chain Bridge



Carries	I-270
Crosses	Mississippi River
Locale	River Mile 190.8, St. Louis, Missouri
Design	Steel Truss Through Deck, Twin Spans
Longest span	480 feet
Total length	1,990 feet
Width	30 feet
Clearance below	82 feet
Opening date	1967
Coordinates	 38°45'56"N 90°08'07"W

There are four bridges as part of the Chain of Rocks crossing, two on the new I-270 alignment, and two on the old US-66 alignment. This bridge, or rather, pair of twin spans, is on the new I-270 alignment, and they cross the Chain Of Rocks Canal.


The reason for two bridges on each alignment is that the highways have two waterways to cross, the Mississippi River main channel, and the Chain Of Rocks Canal.

Since the canal carries riverboat traffic, these bridges have to be very high above the water. There could also be no piers in the navigation channel, so the main span had to be relatively long. The solution was to build a pair of massive steel truss bridges.

These bridges are often called the Double Chain Bridge in that there are two spans, and they cross the Chain Of Rocks Canal. They are the first of the big metal monster bridges that you find as you head south on the Mississippi River.

61. Single Chain Bridge





Carries	2 lanes, Old Chain Of Rocks Road, US-66
Crosses	Mississippi River
Locale	River Mile 190.5, St. Louis, Missouri
Design	Steel Truss Through Deck
Longest span	463 feet
Total length	2,368 feet
Width	26 feet
Clearance below	82 feet
Opening date	1949, (Rebuilt 1999)
Coordinates	 38°45'43"N 90°08'18"W

There are four bridges as part of the Chain of Rocks crossing, two on the new I-270 alignment, and two on the old US-66 alignment. This bridge is on the old US-66 alignment, and it crosses the Chain of Rocks Canal. The old Chain of Rocks Bridge was built in 1929. When the canal was dug in 1949, a bridge had to be built in this spot to provide access to the Illinois side of the Chain Of Rocks Bridge.

While this crossing is lightly used today, it still has to be high enough and long enough to allow riverboat traffic to pass without being a navigation hazard. The solution was to build a steel truss bridge to stand up to the long span, and a pair of trusses handling the approaches at either end of the bridge.

This bridge is called the Single Chain Bridge given that there is only one structure in the bridge, as opposed to the Double Chain Bridge just upstream, which has two bridges in parallel. The Chain of Rocks Bridge was abandoned in 1970, so the Single Chain Bridge was largely ignored. It deteriorated to the point where it required major renovation in 1999. Today, it looks like a brand new bridge.


62. Grand Tower Pipeline Bridge

	
Carries	Natural gas
Crosses	Mississippi River
Locale	Grand Tower, Illinois
Maintained by	Natural Gas Pipeline Company of America
Design	Suspension bridge
Longest span	2,161.5 feet (659 m)
Opening date	1955
Coordinates	 37°38'31"N 89°31'03"W

The **Grand Tower Pipeline Bridge** is a suspension bridge carrying a natural gas pipeline across the Mississippi River near Grand Tower, Illinois.

63. A. W. Willis. Jr. Bridge




Carries	4 lanes of Auction Road
Crosses	Mississippi River
Locale	River Mile 737.1, Memphis, Tennessee
Design	Steel Girder
Total length	1,405 feet
Width	57 feet (8 m)
Opening date	1987
Coordinates	 35°09'30"N 90°03'11"W

Prior to 1987, the only access to Mud Island was via the monorail and pedestrian bridge that was built in 1982. The city desired to develop the north end of Mud Island, so an automobile bridge was built. It is an extension of Auction Road, and it is named after A. W. Willis Jr., a famous black attorney who practiced in Memphis for many years. Once this bridge was opened to traffic, developers started to build housing on Mud Island. This area has become a neighborhood that attracts younger upscale residents, partly due to the land prices being very high compared to the rest of Memphis.

This bridge does not cross the main channel of the Mississippi River. Rather, it crosses a back channel named Wolf Harbor.

64. Memphis Suspension Railway





Carries	1 lane
Crosses	Mississippi River
Locale	Memphis, Tennessee
Design	Suspended monorail bridge
Total length	1,700 feet
Opening date	1982
Coordinates	

The **Memphis Suspension Railway** or **Mud Island Monorail** is a suspended monorail that connects the city center of Memphis with the entertainment park on Mud Island.

The system consists of two suspended cars constructed in Switzerland, delivered in summer 1981. The 1,700 ft (518 m) long bridge opened to pedestrians on June 29, 1981; however, the suspended monorail would not be operational until July 1982. The cars are driven by a 3,500 ft (1,067 m) long, external cable instead of by internal motors. The two cars simultaneously shuttle back and forth on parallel tracks between the Front Street Terminal on the downtown side and the Mud Island Terminal. Each car has a maximum capacity of 180 passengers and travels at a speed of 7 mph (11.3 km/h).

At the time of its construction, both the U.S. Coast Guard stated that the proposed bridge would have to have the same clearance as the Hernando de Soto Bridge, as it was deemed it was spanning a commercially used public waterway. This resulted in the bridge being constructed at its current elevation.


65. Cairo Ohio River Bridge

	
Carries	2 lanes of US 51/US 60/US 62
Crosses	Ohio River
Locale	Wickliffe, Kentucky and Cairo, Illinois
Design	Cantilever bridge
Longest span	243 84 meters (800 feet)
Total length	1,787.26 meters {5,863.7 feet)
Width	6.10 meters (20 feet)
Vertical clearance	5.97 meters (19.6 feet)
Opening date	1937
Coordinates	 36°59'39"N 89°08'45"W

The **Cairo Ohio River Bridge** is a cantilever bridge carrying US 51, US 60 and US 62 across the Ohio River between and Wickliffe, Kentucky and Cairo, Illinois. Of all the Ohio River crossings, it is the furthest downstream – the Mississippi River can be seen while crossing the bridge and looking westward.

66. Cairo Rail Bridge




Carries	Single track of Canadian National Railway (formerly Illinois Central Railroad)
Crosses	Ohio River
Locale	Wickliffe, Kentucky and Cairo, Illinois
Design	Simple truss bridge, with steel trestle approaches
Longest span	518.5 feet (158 m)
Total length	20,461 feet (6,236.5 m) (including approaches)
Opening date	October 29, 1889, rebuilt in 1951
Coordinates	 37°01'23"N 89°10'32"W

Cairo Rail Bridge is the name of two bridges crossing the Ohio River near Cairo, Illinois. The first was an 1889 George S. Morison through truss and deck truss bridge replaced in 1951. The second and current bridge is a through truss bridge that reused many of the original bridge piers. As of 2007, trains like the City of New Orleans travel over the Ohio River supported by the same piers whose construction began in 1887.

The first train crossed the bridge from Illinois to Kentucky on October 29, 1889. Work continued until it was turned over to the railroad on March 1, 1890. In order to comply with regulations meant to allow steam boat travel on the Ohio, the bridge was required to be 53 feet (16.2 m) above the river's high water mark. This resulted in the structure extending nearly 250 feet (76.2 m) from the bottom of the deepest foundation to the top of the highest iron work. Cairo bridge's two 518.5 feet (158 m) main spans were the longest pin-connected Whipple truss spans ever built. At the time, the bridge was the largest and most expensive ever undertaken in the United States. At 10,580 feet (3,224.8 m), it was the longest metallic structure in the world. Its total length was 20,461 feet (6,236.5 m) including wooden approach trestles. Its construction completed the first rail link between Chicago and New Orleans and revolutionized north-south rail travel along the Mississippi River.

67. Metropolis Bridge



Carries	Single track of Canadian National Railway (formerly Chicago, Burlington and Quincy Railroad)
Crosses	Ohio River
Locale	Metropolis, Illinois and McCracken County, Kentucky
Design	Simple truss bridge, with steel trestle approaches
Longest span	708 feet (215.798 m)
Total length	6,424 feet (1958.035 m) (including approaches)
Opening date	1917
Coordinates	 37°08'41"N 88°44'31"W



The **Metropolis Bridge** is a railroad bridge which spans the Ohio River at Metropolis, Illinois. Originally built for the Chicago, Burlington and Quincy Railroad, construction began in 1914.

The bridge consists of the following: (from north to south)

- Deck plate-girder approach spans
- One riveted, 9-panel Parker through truss
- Five pin-connected, Pennsylvania through trusses
- One pin-connected, 8-panel Pratt deck truss
- Deck plate-girder approach spans

Total length of the bridge is 6,424 feet (1958.035 meters).


68. Interstate 24 Bridge

	
Carries	I-24
Crosses	Ohio River
Locale	Metropolis, Illinois and Paducah, Kentucky
Design	Continuous box and plate girder bridge & two-span tied arch bridge
Total length	5,623.4 feet
Opening date	1973
Coordinates	 37°08'00"N 88°41'13"W

The **Interstate 24 Bridge** may refer to one of two distinct bridges on Interstate 24. The Interstate 24 Bridge is a two-span tied arch bridge that carries I-24 across the Ohio River. Built in 1973, it is 5,623.4 feet (1,714.0 m) in length. The bridge is one of two that connects the Metropolis, Illinois area with Paducah, Kentucky.

69. Irvin S. Cobb Bridge




Carries	2 lanes of US 45
Crosses	Ohio River
Locale	Paducah, Kentucky and Brookport, Illinois
Design	Truss bridge
Longest span	711.0 feet (216.7 m)
Total length	5,385.8 feet (1,641.6 m)
Width	19.7 feet (6.0 m)
Vertical clearance	14.1 feet (4.3 m)
Completion date	1929
Coordinates	 37°06'53"N 88°37'45"W

The **Irvin S. Cobb Bridge** (also known as the **Brookport Bridge**) is a ten-span, narrow two-lane truss bridge that carries U.S. Route 45 across the Ohio River in the U.S. states of Illinois and Kentucky. It runs from Paducah, Kentucky north to Brookport, Illinois.

The bridge is named after Irvin S. Cobb, an author and journalist who was born in Paducah.

70. Shawneetown Bridge




Carries	
Crosses	Ohio River
Locale	Old Shawneetown, Illinois
Design	Cantileverd truss bridge
Longest span	825.1 ft
Total length	3,200.2 ft
Width	23.9 ft
Vertical clearance	19 ft
Completion date	1955
Coordinates	 37°41'28"N 88°07'53"W

The **Shawneetown Bridge** is a cantilever truss bridge carrying Kentucky Route 56 and Illinois Route 13 across the Ohio River. The bridge connects Old Shawneetown, Illinois to rural Union County, Kentucky.

71. Henderson Bridge



Carries	Railroad
Crosses	Ohio River
Locale	Henderson, Kentucky
Design	Truss bridge
Coordinates	 37°50′45″N 87°35′47″W

The **Henderson Bridge** is an active railroad bridge located at Henderson, Kentucky. It is a five spans truss bridge crossing the Ohio River just North of the Henderson boat ramp and downtown area.

72. Bi-State Vietnam Gold Star Bridges




Carries	US 41
Crosses	Ohio River
Locale	Henderson, Kentucky and Evansville, Indiana
Design	Cantilever truss bridges
Longest span	720 feet
Total length	5,395 feet
Vertical clearance	100 ft (30m)
Completion date	1932 (northbound) 1966 (southbound)
Coordinates	 37°54'15"N 87°33'02"W

The **Bi-State Vietnam Gold Star Bridges**, also known as the **Twin Bridges**, connect Henderson, Kentucky and Evansville, Indiana along U.S. 41, one mile (1.6 km) south of the terminus of I-164. The northbound bridge opened to traffic on July 4, 1932 and the southbound bridge opened in December 1966. The main span of the bridges is 720 feet (220 m).

The northbound span of the Bi-State Vietnam Gold Star Bridges was the second of three bridges built in Henderson County in 1932. It was originally named the **John James Audubon Bridge**, or **Audubon Memorial Bridge**. Both of the Bi-State Vietnam Gold Star Bridges are 5,395-foot (1,644 m) long cantilever bridges. The northbound bridge stands 100 feet (30 m) over the Ohio River with a main span of 732 feet (223 m), with the steel gridwork extending 100 feet (30 m) above the driving surface. The southbound span has a main span of 600 feet (180 m).

73. Glover Cary Bridge



Carries	US 431
Crosses	Ohio River
Locale	Owensboro, Kentucky and Spencer County, Indiana
Design	Continuous truss bridge
Completion date	1940
Coordinates	 37°46'45"N 87°06'33"W


Local residents call the **Glover H. Cary Bridge** the "Blue Bridge" because of its color. It is a continuous truss bridge that spans the Ohio River between Owensboro, Kentucky and Spencer County, Indiana. It was named for the late U.S. Congressman Glover H. Cary (1885-1936), and opened to traffic in September 1940.

At first, the bridge connected Kentucky Highway 75 to Indiana Highway 75; in 1954, Kentucky 75 was redesignated U.S. Highway 431 and Indiana 75 became U.S. Highway 231.

In the fall of 2002, when the William H. Natcher Bridge was completed, U.S. 231 was rerouted onto that bridge and the former U.S. highway became the southern leg of an extended State Road 161.

74. William H. Natcher Bridge



Carries	U.S. Highway 231
Crosses	Ohio River, Indiana State Road 66
Locale	Owensboro, Kentucky to Rockport, Indiana
Design	Cable stayed bridge
Total length	4,505 feet (1,373 m)
Width	67 feet (20 m)
Opening date	October 21, 2002
Coordinates	 37°54′04″N 87°02′02″W

The **William H. Natcher Bridge** is a cable-stayed bridge that carries U.S. Highway 231 over the Ohio River. The bridge connects Owensboro, Kentucky to Rockport, Indiana and opened on October 21, 2002.

The William H. Natcher Bridge is 4,505 feet (1,373 m) in length (including its approaches) and 67 feet (20 m) wide. It is supported by cables connected to two identical diamond-shaped towers, each 374 feet (114 m) tall. At the time of its construction, it was the United States' longest cable-supported bridge over an inland waterway.

75. Bob Cummings - Lincoln Trail Bridge



Carries	Road traffic
Crosses	Ohio River
Locale	Indiana-Kentucky State Line
Design	Arch bridge with suspended deck
Longest span	824.6 feet (251.3 m)
Total length	2,708.3 feet (825.5 m)
Width	27.8 feet (8.5 m)
Opening date	1966


The **Bob Cummings - Lincoln Trail Bridge** crosses the Ohio River and connects the towns of Cannelton, Indiana and Hawesville, Kentucky. Indiana State Road 237 becomes Kentucky Route 69 upon entering Hawesville.

Construction began in June 1964 and the bridge opened on December 21, 1966. The steel arch bridge with its suspended deck was a toll facility until the state of Indiana lifted the tolls in the 1990s.

In 2006, the bridge was resurfaced with concrete that many drivers find to be rougher than the previous surface.

76. Matthew E. Welsh Bridge



Carries	KY 79/ IN 135
Crosses	Ohio River
Locale	Brandenburg, Kentucky and Mauckport, Indiana
Design	Continuous truss bridge
Longest span	725 ft
Total length	3098 ft
Completion date	November 19, 1966
Coordinates	 38°01'02"N 86°11'49"W


Matthew E. Welsh Bridge is a two-lane, single-deck continuous truss bridge^[1] on the Ohio River. The bridge connects Kentucky Route 79 and Indiana State Road 135, as well as the communities of Brandenburg, Kentucky and Mauckport, Indiana.

It is 3098 feet long and was built by the State of Indiana. The truss portion of the bridge is continuous across two 725-foot spans. Construction of the bridge began in August 1964 and the bridge was opened to traffic on November 19, 1966.

Although 90% of the Bridge is within the Commonwealth of Kentucky, the bridge is owned and maintained by the State of Indiana.

77. Lewis Bridge




Carries	4 lanes of US-67
Crosses	Missouri River
Locale	St. Louis County and St. Charles County in Missouri
Design	Deck girder bridge
Opening date	1979
Coordinates	 38°50'38"N 90°14'03"W

The **Lewis Bridge** is a bridge carrying U.S. Route 67 across the Missouri River between St. Louis County and St. Charles County, Missouri. It replaced an earlier narrow, 2-lane through truss bridge of the same name that ran adjacent to the Bellefontaine Bridge.



78. Bellefontaine Bridge



Crosses	Missouri River
Locale	St. Louis County and St. Charles County, Missouri
Design	Four-span truss bridge
Longest span	440 foot
Total length	1760 foot
Completion date	December 27, 1893
Coordinates	 38°50'37"N 90°14'11"W

The **Bellefontaine Bridge** is a four-span truss BNSF railroad bridge over the Missouri River between St. Charles County, Missouri and St. Louis County, Missouri. It has four 440 foot spans. Construction started on July 4, 1892 and it opened on December 27, 1893.



79. Discovery Bridge

	
Carries	6 lanes of Route 370
Crosses	Missouri River
Locale	St. Louis County and St. Charles County in Missouri
Design	Truss bridge
Longest span	190.5 m (625 ft)
Total length	1,053 m (3,455 ft)
Width	16.8 m (55 ft)
Opening date	1993
Coordinates	 38°47'53"N 90°28'01"W

The **Discovery Bridge** are two twin truss bridges carrying Route 370 across the Missouri River between St. Louis County and St. Charles County, Missouri.



The shoulder on both sides is designated a bicycle (and pedestrian) path. Separate bicycle/pedestrian access ramps are available immediately on both sides of the bridge. This provides a connection to traffic to and from the Katy Trail, which passes under the bridge.

80. Wabash Bridge (St. Charles, Missouri)

	
Carries	Railroad
Crosses	Missouri River
Locale	St. Louis County and St. Charles County in Missouri
Design	Truss bridge
Coordinates	 38°47'51"N 90°28'02"W

The **Wabash Bridge** carries a railroad from St. Louis County to the city of St. Charles. It is positioned next to the Discovery Bridge. It is used by the freight trains of Norfolk Southern Railway.

81. Blanchette Memorial Bridge


	
Carries	10 lanes of Interstate 70
Crosses	Missouri River
Locale	St. Louis County and St. Charles County in Missouri
Design	Cantilever
Longest span	146.3 m (480 ft)
Total length	1,244 m (4,083 ft)
Width	WB: 18.3 m (60 ft) EB: 20.7 m (68 ft)
Opening date	WB: 1958 EB: 1978
Coordinates	 38°45'54"N 90°28'55"W

The **Blanchette Memorial Bridge** are two twin cantilever bridges carrying Interstate 70 across the Missouri River between St. Louis County and St. Charles County, Missouri, opened in 1959. Handling an average of 165,000 vehicle transits per day, it is the area's busiest bridge. Construction of the first interstate highway project under provisions of the Federal Aid Highway Act of 1956 started west of the bridge's present location. A sign commemorating the site of the nation's first interstate project stands next to Interstate 70 just east of the Missouri Route 94/First Capitol Drive overpass.

The bridge is named for French Canadian fur trader and hunter Louis Blanchette, who founded St. Charles as a post along the Missouri River; the village was the first European settlement along this waterway.

82. Veterans Memorial Bridge





Carries	MO-364 Route 364
Crosses	Missouri River
Locale	St. Louis County and St. Charles County, Missouri
Design	Twin Tied Arch Bridges
Longest span	617 ft
Total length	3,238 ft
Width	83 ft 4 traffic lanes
Opening date	1999
Coordinates	 38°44'13"N 90°31'20"W

The **Veterans Memorial Bridge** is a twin steel through tied arch, suspended concrete deck bridge over the Missouri River connecting St. Louis County and St. Charles County, Missouri via Route 364. Steel Through Arch,

It was built and opened in 1999. It is 83 feet wide and 3,238 feet long. The longest span length is 617 feet.



83. Daniel Boone Bridge

	
Carries	7 lanes (4 EB, 3 WB) of I-64/US 40/US 61
Crosses	Missouri River
Locale	St. Louis County and St. Charles County in Missouri
Design	Twin Cantilever bridges
Opening date	1935 (westbound span) 1988 (eastbound span)
Coordinates	 38°41'17"N 90°39'47"W

The **Daniel Boone Bridge** are two twin cantilever bridges carrying Interstate 64, U.S. Route 40 and U.S. Route 61 across the Missouri River between St. Louis County and St. Charles County, Missouri.

On December 10, 2004, the Missouri Highways and Transportation Commission approved the design location of a third span, to be built upstream (to the west) of the two current spans. This new span will carry eastbound traffic, while the the current eastbound span will carry westbound traffic and the current westbound span will carry westbound outer road traffic.

84. Washington Bridge

	
Carries	Route 47
Crosses	Missouri River
Locale	Washington, Missouri
Design	Cantilevered truss bridge
Longest span	474.6 ft
Total length	2,561.3 ft
Width	22 ft
Clearance below	14.6 ft
Opening date	1934
Coordinates	 38°33'27"N 90°59'54"W


The **Washington Bridge** is a cantilevered truss bridge over the Missouri River at Washington, Missouri over which Route 47 passes between Franklin County, Missouri and Warren County, Missouri.

The bridge was built in 1934. Its main span is 474.6 feet and it has a total length of 2,561.3 feet and a deck width of 22 feet. Its vertical clearance is 14.6 feet. The bridge carries one lane of automobile traffic in each direction.

The Missouri Department of Transportation shut down the bridge on 11 August 2007, claiming to have discovered problems during regularly scheduled inspections. As the bridge is similar to the I-35W bridge which collapsed in Minnesota, locals have speculated that the inspection and closure were related to this incident. The nearest open crossing over the Missouri river is approximately sixty miles from the closed bridge. The bridge was reopened on 12 August 2007.

85. Christopher S. Bond Bridge (Hermann)





Carries	Route 364
Crosses	Missouri River
Locale	Hermann, Missouri
Design	Truss bridge
Total length	2247 ft
Width	55ft
Opening date	July 23, 2007
Coordinates	 38°42'34"N 90°26'20"W

The **Christopher S. Bond Bridge** is a highway bridge crossing the Missouri River at Hermann, Missouri. The bridge was opened to vehicle traffic on July 23, 2007, replacing an adjacent span opened in 1930.

Construction on the bridge continues as a portion of the south end of old bridge needs to be removed to allow completion of the south approach. The 8-foot pedway will not be open until the bridge construction is finished.

The bridge is 2,247 feet long. The total width of the bridge is 55 feet, 4 inches, consisting of two 12-foot driving lanes, two 10-foot shoulders, and an 8-foot bicycle/pedestrian lane.

86. Jefferson City Bridge

	
Carries	US 54/ US 63
Crosses	Missouri River
Locale	Jefferson City, Missouri
Design	2 compression arch suspended-deck bridge
Longest span	639.9 feet (southbound) 595.6 feet (northbound)
Total length	3,093 feet (southbound) 3,124.2 feet (northbound)
Width	37.7 feet (southbound) 46.9 feet (northbound)
Opening date	1955 (southbound) 1991 (northbound)
Coordinates	 38°35'15"N 92°10'42"W

The **Jefferson City Bridge** are two compression arch suspended-deck bridge bridges over the Missouri River at Jefferson City, Missouri over which U.S. Highway 54 and U.S. Highway 63 pass between Cole County, Missouri and Callaway County, Missouri.


The southbound bridge opened in August 1955. Its main span is 639.9 feet and has a total length of 3,093 feet and a deck width of 37.7 feet and vertical clearance of 37.7 feet.

The northbound bridge opened in 1991. Its main span is 595.6 feet with a total length of 3,124.2 feet. The deck width is 46.9 feet and it has vertical clearance of 16.1 feet.

The northbound bridge has a marked bicycle and pedestrian lane in the shoulder. It is used in both directions by users of the Katy Trail State Park. A city-maintained extension of the Katy (formerly a railroad spur) connects the North Jefferson trailhead to near the first exit north of the bridge.

87. Rocheport Interstate 70 Bridge




Carries	Interstate 70
Crosses	Missouri River
Locale	Cooper County and Boone County , MO
Design	Cantilevered truss bridge
Longest span	550.7 ft
Total length	3,017.2 ft
Width	60.3 ft
Opening date	1960
Coordinates	 38°57'35"N 92°32'41"W

The **Rocheport Interstate 70 Bridge** is a four-lane Cantilevered through truss bridge over the Missouri River on Interstate 70 between Cooper County, Missouri and Boone County, Missouri at Rocheport, Missouri.

The bridge was built in 1960 and rehabilitated in 1993. Its main span is 550.7 feet and has a total length of 3,017.2 feet. Its deck width is 60.3 feet and vertical clearance is 20 feet.

88. Boonslick Bridge




Carries	US 40, Route 5 and Route 87
Crosses	Missouri River
Locale	Boonville, Missouri
Design	Girder bridges
Opening date	1995
Coordinates	 38°58'51"N 92°44'45"W

The **Boonslick Bridge** is a series of girder bridges on U.S. Route 40, Route 5 and Route 87 across the Missouri River between Cooper County, Missouri and Howard County, Missouri at Boonville, Missouri.

The bridge also has a segregated pedestrian and bicycle path. The bridge which opened in 1995 replaced a six-span truss bridge built in 1924 that was 19 feet (5.8 m) wide. The earlier bridge was 2,100 feet (640 m) long with a 584-foot (178 m) approach in Cooper County and 500-foot (150 m) approach in Howard County. Three of its spans were 420 feet (130 m) and three were 280 feet (85 m).

89. Glasgow Bridge



Carries	Route 240
Crosses	Missouri River
Locale	Glasgow, Missouri
Design	five-span through truss
Longest span	343.7 ft
Total length	2,243.5 ft
Width	20.3 ft
Clearance below	14.8 ft
Opening date	1925
Coordinates	 39°13'21"N 92°51'00"W

The **Glasgow Bridge** is five-span through truss bridge over the Missouri River on Route 240 between Howard County, Missouri and Saline County, Missouri at Glasgow, Missouri.


Glasgow Bridge from southwest along with rail bridge upstream from it. The bridge is single lane now with a stop light on either side.

It was built in 1925 and rehabilitated in 1986. Its main span is 343.7 feet and its total length is 2,243.5 feet. It has a deck width of 20.3 feet and vertical clearance of 14.8 feet.

A project to replace the trusses with a new superstructure began on August 4, 2008.

90. Glasgow Railroad Bridge




Crosses	Missouri River
Locale	Glasgow, Missouri
Design	four-span through truss
Opening date	1878
Coordinates	 39°13'22"N 92°51'03"W

The **Glasgow Railroad Bridge** is four-span through truss bridge over the Missouri River belonging to the Kansas City Southern railroad between Howard County, Missouri and Saline County, Missouri.

It was originally built in 1878-79 by Gen. William Sooy Smith for the Chicago and Alton railroad as a five-span Whipple through truss and described as the world's first all-steel bridge. In 1900 it was rebuilt with Parker truss spans. It was damaged in the Great Flood of 1993.

91. Hardin-Joe Page Bridge




Carries	2 lanes on IL-16, IL-100
Crosses	Illinois River
Locale	Hardin Illinois
Design	Truss bridge
Longest span	308.7 ft
Total length	2,150 ft
Width	22 ft
Clearance below	26 ft
Opening date	July 23, 1931
Coordinates	 39°09'36.23"N 90°36'48.61"W

The Joe Page Bridge is located in the small town of Hardin, Illinois. Many sources state that this is the longest bridge in Illinois, and the lift span of 308 foot 9 inches is the longest lift span in the world. While there may be some category of bridge where it is (or was) the longest in the world, both the Arthur Kill and Cape Cod Canal bridges have longer lift spans at 558 feet and 544 feet long, respectively.

The bridge consists of a series of Pennsylvania through truss spans that reach from high ground on the west side of the river to the levee on the east side of the river. The trusses include 6 that are fixed in size, the larger lift span, and then a somewhat shorter fixed truss between the lift span and the western shore. It is rare to have a lift bridge for vehicle traffic since cars can climb slopes that a train would find impossible to climb. In the case of the Illinois River, the first two automobile bridges, the Joe Page Bridge and the Florence Bridge just upstream are both automobile lift bridges. This 1931 era bridge was rehabilitated between March 2003 and December 2004.

92. Florence Bridge



Carries	2 lanes IL-100, IL-106
Crosses	Illinois River
Locale	Florence, Illinois
Design	Truss bridge
Longest span	217 ft
Total length	3,178 ft
Width	23 ft
Clearance below	27 ft
Opening date	1929 (Reconstructed 2004)
Coordinates	 39°37'57.30"N 90°36'26.36"W


The **Florence Bridge** was installed as part of the US highway system. It carried US-36 until the new Valley City Eagle Bridges were built as part of the I-72 project in 1988. US-36 is now multiplexed on I-72 in western Illinois. Given that I-72 is only a few miles to the north, the Florence bridge is very lightly used.

The bridge consists of 4 Parker style through truss spans, the main lift span, and then 4 more Parker style through truss spans. There is a lengthy causeway on the east end of the crossing, and a very short fill on the west end.

The Florence bridge was refurbished in 1981, and refurbished again in 2004. In the 2004 project, the deck was replaced, the bridge was sandblasted and painted, the lift cables were replaced, a new operators house was built, and electrical work was performed.

93. Valley City Eagle Bridges



Carries	I-72 US 36, 2 lanes per span
Crosses	Illinois River
Locale	Valley City, Illinois
Design	Post Tensioned Cast-In-Place Concrete Box Girder
Longest span	616 ft
Total length	3,329 ft (Eastbound) 3,203 ft (Westbound)
Width	39 ft
Clearance below	72 ft
Opening date	1988
Coordinates	 39°41'13.34"N 90°38'28.43"W

The two spans of the **Valley City Eagle Bridges** were built in 1988, but the highway itself was not fully finished until 1991. Prior to that time, US-36 was routed across the Florence Bridge a few miles south of the I-72 river crossing.


The bridges are anchored to the flat river plain on the east side of the Illinois River, and land high in the bluffs on the west side of the river, gaining about 80 feet in altitude as part of the river crossing.

The expressway runs from Decatur in the middle of Illinois west to Hannibal, Missouri. The highway required two major bridges. The bridge over the Mississippi River is called the Mark Twain Bridge, and it opened in 2000. The other is the Valley City Eagle Bridges, twin spans over the Illinois River.

The bridges were built with two relatively new construction techniques. First, the bridges were cast in place using a moving concrete form. Workers would cast one section of the bridge in place, then move the forms ahead a few feet and cast the next section.

94. Meredosia Bridge




Carries	IL 104
Crosses	Illinois River
Locale	Meredosia, Illinois
Design	Steel Truss Through Deck
Longest span	568 ft
Total length	2,232 ft
Width	24 ft, 2 lanes
Clearance below	72 ft
Opening date	1936, Reconstructed 1984
Coordinates	 40°00'54.67"N 90°26'48.70"W

This 1936 era big metal monster crosses the Illinois River on the west side of the small town of Meredosia. The **Meredosia Bridge** bridge replaced an earlier wagon bridge. A railroad bridge once crossed the river a few hundred feet downstream from the highway bridge. The Meredosia bridge was reconstructed in 1984. A group of bad floor beams were discovered and fixed in the 1990s.

The bridge was quickly inspected and pronounced to be safe following the I-35W bridge collapse in August, 2007. Despite the bridge being safe, it has a very low sufficiency rating and is eligible for federal funds for replacement.

95. Beardstown Bridge




Carries	US-67, IL-100
Crosses	Illinois River
Locale	Beardstown, Illinois
Design	Truss bridge
Longest span	540 ft
Total length	3,624 ft
Width	28 ft
Clearance below	68 ft
Opening date	1955, (Reconstructed 1985)
Coordinates	 40°00'54.67"N 90°26'48.70"W

A steel toll bridge was built by the city and opened in 1898. That bridge produced revenue for the city until 1955, when a new highway bridge was built in the mid-1950s to give highway US-67 a bypass route around the downtown area.

The **Beardstown Bridge** is one massive bridge, something that would only be expected on the lower Mississippi or other similarly large river. The main bridge is a through truss span about 1,365 feet long, with a 540 foot main span for navigation traffic. It rises nearly 70 feet above the water to the low steel line. To the north, there is a second through truss bridge about 710 feet long. A 1,000 foot long trestle crosses a backwater slough to the north, and a 500 foot steel deck truss bridge spans a creek on the south end. The overall river crossing is 2/3 of a mile.

96. Scott W. Lucas Bridge




Carries	US 136 IL 78 IL 97
Crosses	Illinois River
Locale	Havana, Illinois
Design	Steel Truss Through Deck
Longest span	420 ft
Total length	1727 ft
Width	29 ft, 2 lanes
Clearance below	70 ft
Opening date	1936, Reconstructed 1998
Coordinates	 40°17'38.92"N 90°04'08.24"W

The **Scott Wike Lucas Bridge** (Havana Bridge) carries US-136 and two state highways across a narrow spot in the Illinois River. The bridge consists of a single large steel truss. Since the bridge has to be high enough to allow boats to travel under the main span, yet the bridge does not have any side spans, the resulting bridge approaches are relatively steep. The bridge is very much like a highway roller-coaster. The effect would be much more pronounced if the speed limit was higher than the posted 35 miles per hour.

97. Pekin Bridge



Carries	IL 9
Crosses	Illinois River
Locale	Pekin, Illinois
Design	Cotnuous Steel Girder bridge
Longest span	550 ft
Total length	2,634 ft
Width	23 ft
Clearence below	27 ft
Opening date	May 1 1982
Coordinates	 40°34'25.07"N 89°39'15.43"W

The **Pekin Bridge** is 9 span bridge over the Illinois River with 1,320in. It has 3 span steel box girder river section and the approaches are steel plate girders.

The Bridges' orthotropic roadway deck has longitudinal and transverse welds.